2015

Developing Co-current and Counter-current Spray Drying Computational Fluid Dynamics (CFD) Simulation Studies to Predict the Quality of Microencapsulated Fish Oil with Egg White Hydrolysates Powders

Kevin Estuardo Mis Solval
Louisiana State University and Agricultural and Mechanical College

DEVELOPING CO-CURRENT AND COUNTER-CURRENT SPRAY DRYING COMPUTATIONAL FLUID DYNAMICS (CFD) SIMULATION STUDIES TO PREDICT THE QUALITY OF MICROENCAPSULATED FISH OIL WITH EGG WHITE HYDROLYSATES POWDERS

A Dissertation

Submitted to the Graduate Faculty of the
Louisiana State University and
Agricultural and Mechanical College
in partial fulfillment of the
requirements for the degree of
Doctor of Philosophy

in

The Interdepartmental Program in
Engineering Science

by
Kevin Estuardo Mis Solval
B.S., Escuela Agrícola Panamerica, El Zamorano, 2008
M.S., Louisiana State University, 2011
May 2015

Dedicated to

GOD

ACKNOWLEDGEMENTS

My special and sincere gratitude goes to Dr. William B. Richardson, Chancellor of the Louisiana State University (LSU) Agricultural Center (AgCenter) who financially supported my education at LSU. Without his support, my time at LSU would not have been possible.

Also, I would like to express my deepest gratitude to my major professor and dear friend Dr. Subramaniam Sathivel for his support and guidance in every little matter throughout the entire time that I have been at LSU; his advice has helped to become a better person and professional.

I want to thank my committee members, Dr. Joan M. King, Dr. J. David Bankston, Dr. Marybeth Lima, Dr. Louis J. Thibodeaux, and Dr. Kenneth Fasching-Varner for their valuable time to serve on my committee, and for their unconditional help and advice on the conduction of this project. Thank you so much! Special thanks go to the staff of the LSU-AgCenter Biotechnology Lab for this help in the SDS-PAGE and amino acid analysis. My studies and research at LSU would not have been the same, without the charm and joy of my Zamorano friends: M. Moncada, F. Vaca, A. Soto-Vaca, J. Charal, J. Marenco, A. Castro, K. Carabante, D. Torrico, L. Alfaro and lab mates in the Food Engineering group: A. Chotiko, J. Lee, J. Zhang, L. Espinoza, A. Chouljenko, V. Reyes, F. Bonilla, C. Galindo, and C. Gurdian. Special thanks to my wife Deborah Xavier-Mis for her unconditional love and support. Nothing would be completed without showing my gratitude and love to those ones who brought me to this world, my beloved parents Luis Mis Morales and Maria Solval; who altogether with my brother Alvaro Luis and my sister Maria Jose have encouraged and supported me with their love during my life. Especial thanks to all the people in the departments of Biological and Agricultural Engineering, Food Science, and Engineering Science at LSU for their help and support. And those ones I did not mention above, but who assisted in the countless hours spent in this project; thank you!

TABLE OF CONTENTS

LIST OF TABLES

LIST OF FIGURES

ABSTRACT

Eggs are an excellent source of high quality protein containing all essential amino acids (EAA) including leucine. Food-grade protein hydrolysates can enhance the growth of lactic acid bacteria (LAB). Thermal degradation of bioactives normally occurs during microencapsulation by spray drying. Spray drying modeling using computational tools is essential to engineer new food powders and to minimize and thermal degradation of bioactives.

The first chapter of this work discusses the optimization of an enzymatic process in terms of reaction temperature, pH, enzyme:substrate ratio, and reaction time using a response surface methodology (RSM) to produce food-grade protein hydrolysates from egg whites (EWH). Resulting EWH produced with proteases from *Aspergillus oryzae* contained all EAA and showed high antioxidant activity.

The EWH were evaluated as a nitrogen source in MRS media for the growth of *L. plantarum, L. acidophilus,* and *L. reuteri*. MRS containing EWH had similar performance to that of conventional MRS and produced higher cell yields and better quality of biomass than MRS containing dried egg white proteins.

Three-dimensional computational fluid dynamics (CFD) simulations were performed to study the effect of co-current and counter-current spray drying configurations on the quality of microencapsulated fish oil with EWH powders in the last section of this work. Also, the separation of powder particles from drying air at the spray dryer's cyclone separator was evaluated using CFD.

CFD models predicted the drying air flow pattern, particle histories including temperature, residence times (RT), moisture content and particle size of the microencapsulated powders. Predicted moisture content of powders was lower than measured values; however, the predicted

mean particle sizes were similar to the measured values. Lower lipid oxidation and microstructure degradation was observed in emulsions dried at 130°C inlet air temperature at feeding rates of 1.0 Kg/h and under counter-current spray drying conditions. The 3D-CFD model predicted lower RT (s) for emulsions dried in counter-current compared to co-current spray drying configurations.

The study demonstrated that EWH can be enzymatically produced and can be used as an effective nitrogen source in MRS media. Also, 3D-CFD spray drying modeling can be effectively used to study the moisture evaporation and to predict the final quality of spray dried powders.

CHAPTER 1- LITERATURE REVIEW

1.1 Dietary Protein

Dietary protein is needed for the survival of both humans and animals. The main proteins' role is to supply adequate amounts of amino acids required by the human body. Moreover, the nutritional quality of dietary proteins is given by their amino acid composition, ratios of essential amino acids, susceptibility to hydrolysis during digestion, source and the effects of processing (Friedman, 1996).

It has been recognized that dietary protein is highly important in athletes and a key nutritional component in the athlete's success. Intakes of high quality protein and amino acids is essential (especially in resistance and team sport athletes) for adequate performance (Tipton & Wolfe, 2004). According to Maughan, Depiesse and Geyer (2007), many athletes consume protein supplements to improve muscle growth and to promote muscle recovery after exercise.

The recommended daily allowance (RDA) for protein in the USA is 0.8 to 0.9 g/kg body weight/day; however, strength athletes may have a 50 – 100% higher RDA protein intake (Tarnopolsky, 2000).

Usually, conventional foods with a high protein content also contain high amounts of fat which can create an unbalanced diet for elite athletes (Maughan, Depiesse & Geyer, 2007). Hence, protein supplements may offer the advantage of providing the protein needs to athletes without altering their dietary fat intakes and without major changes in their diet.

Most of the protein supplements available on the market are derived from milk proteins including whey and casein powder, whey protein concentrate and isolate. The protein content of these products range from 11 to more than 90%, with a lactose content ranging from 0.5 to more than 75%, and milk fat content ranging from 0.5 to 10% (Hoffman & Falvo, 2004). Products

containing proteins extracted from milk may not be suitable for lactose-intolerant individuals due to their significant lactose content. Eggs are another source of high quality protein. Proteins from egg white may be better than whey proteins because egg proteins contain all of the EAA and most importantly it is a lactose-free high quality protein source. Proteins derived from soy may contain anti-nutritional factors such as trypsin inhibitors, lecithins, and tannins (Salgado, Montagne, Freire, Ferreira, Teixeira, Bento et al., 2002).

1.1.1 Table eggs as a source of high quality protein

Table eggs are an excellent source of high-quality protein, vitamins and minerals. An average large egg provides around 6.25 g of high-quality protein, 5 g of fat and 200 mg of cholesterol, which is mainly located in the yolk (Weggemans, Zock & Katan, 2001). Moreover, table eggs contain all nine essential amino acids (EAA) including histidine, isoleucine, leucine, lysine, methionine, phenylalanine, threonine, tryptophan and valine. Usually, the egg protein pattern is used as a standard of comparison for measuring the protein quality of other foods because it is very similar to the pattern needed by the human body (AEB, 1999). According to Surai and Sparks (2001), no other single food in the World is consumed by so many people in such a variety of ways. Due to their unique nutritional properties, eggs have been used as leavening, thickening, binding, and emulsifying agents in many foods (Surai & Sparks, 2001).

Egg white is composed mainly of water and proteins, being ovalbumin, ovotransferrin, ovomucoid, lysozyme and ovoinhibitor the most abundant (Stevens, 1991). Many of the egg white proteins are globular glycoproteins and have a specific binding site for vitamins and minerals. Lysozyme is the only egg white protein with catalytic activity; meanwhile, ovomucoid and ovoinhibitor have a protease inhibitory activity. Ovotransferrin is normally bonded with Iron and ovalbumin may be a source of amino acids for the egg (Stevens, 1991). Additionally, eggs

are excellent source of leucine. Despite all of the nutritional benefits of eggs; there is a significant barrier to increasing egg consumption in western countries due to their association with blood cholesterol levels (Surai & Sparks, 2001).

1.1.2 Branched chain amino acids (BCAAs)

Due to their molecular structure, leucine, isoleucine and valine are identified as branched chain amino acids (BCAAs). Several studies have indicated that BCAAs function as nutritional signaling molecules that control skeletal muscle anabolism; being leucine unique in this regard (Anthony, Anthony, Kimball & Jefferson, 2001; Anthony, Anthony, Kimball, Vary & Jefferson, 2000). Moreover, it has been reported that leucine contributes to muscles' ability to use energy and aids in post-exercise muscle recovery. Also, a diet rich in leucine could be advantageous to men and women undergoing resistance exercise due to the complementary effect between leucine and glucose utilization by muscles (Layman & Rodriguez, 2009). Anthony, Anthony, Kimball, Vary and Jefferson (2000) have reported that higher concentrations of plasma insulin and leucine have increased skeletal protein synthesis in food-deprived rats. Intake of carbohydrates results in an increased skeletal muscle glycogen synthesis after exercise; these responses increase plasma insulin (Anthony, Anthony & Layman, 1999). Hence, diets containing carbohydrates and leucine can promote higher rates of skeletal muscle synthesis after exercise (Anthony, Anthony, Kimball & Jefferson, 2001). A detailed signaling mechanisms in the stimulation of protein synthesis initiated by leucine is described by Anthony, Anthony, Kimball and Jefferson (2001).

1.1.3 Protein hydrolysates

Recently, modification of food proteins by enzymatic means has become popular (Pokora, Eckert, Zambrowicz, Bobak, Szołtysik, Dąbrowska et al., 2013). Enzymatic hydrolysis of food

proteins are carried out under mild conditions of pH (6-8) and temperature (40 – 60 °C) which minimize side reactions. Functionality improvements have been observed in enzymatic-modified proteins such as solubility, gelling, fat- and water holding capacity, emulsion stability and foaming capacity (Panyam & Kilara, 1996). Uses of protein hydrolysates include geriatric products, high-energy supplements, weight-control and therapeutic or enteric diets (Clemente, 2000). The use of protein hydrolysates in post-exercise food supplements have been one the main reasons of the popularity of food protein hydrolysates in the last years.

According to Clemente (2000), protein hydrolysates can be also produced by acid and alkaline hydrolysis; however, these methods are more difficult to control and yield products with reduced nutritional characteristics because chemicals can destroy L-form amino acids, produce D-form amino acids and can induce the formation of toxic substances like lysino-alanine.

The most popular commercial hydrolysates are derived of cow's milk protein are due to their large availability and moderate cost. Some individuals may show allergic reactions to cow's milk proteins. Commercial protein hydrolysates from cow's milk protein may not be suitable for lactose-intolerant consumers because they may contain high amounts of lactose (Hoffman & Falvo, 2004). These are two of the main drawbacks of using cow's milk proteins to produce protein hydrolysates. Production of plant-base protein hydrolysates have also been reported (Clemente, 2000); however, these hydrolysates contain low levels of EAA.

Bitterness associated with protein hydrolysates is one of major drawbacks of the use of these types of products in food. Clemente (2000) have reported that the bitter flavor of some peptides is attributed to their hydrophobic amino acid content. Several post-hydrolysis processes have been successfully incorporated in the production of protein hydrolysates; these processes focus on reducing bitterness of the hydrolysates by controlling the molecular size of the peptides

(Clemente, 2000). In this context, ultrafiltration technology has been an efficient process to remove residual high-molecular weight peptides and proteins (Clemente & Chambers, 2000).

According to Manninen (2009), protein hydrolysates containing di- and tripeptides are better than whole proteins and free amino acids on skeletal muscle anabolism . Furthermore, protein hydrolysates containing di- and tripeptides from whey, egg, and casein are more rapidly absorbed than those protein hydrolysates containing longer peptides (Grimble, Guilera Sarda, Sessay, Marrett, Kapadia, Bowling et al., 1994; Grimble, Rees, Keohane, Cartwright, Desreumaux & Silk, 1987; Raimundo, Grimble, Rees, Hunjan & Silk, 1988).

In a clinical study carried out by van Loon, Saris, Verhagen and Wagenmakers (2000), the effect of protein hydrolysates from whey, pea and wheat proteins combined with carbohydrates on plasma insulin was investigated. They reported that protein hydrolysates produced higher plasma amino acid response compared to intact protein after 2-h of ingestion; this is a result of a better insulin secretion. Moreover, wheat protein hydrolysates showed better results than the other types of protein hydrolysates tested. The researchers also found that protein hydrolysates are better than intact proteins because they show higher solubility in water.

One of the most complete studies to evaluate the efficacy of protein hydrolysates has been reported by Koopman, Crombach, Gijsen, Walrand, Fauquant, Kies et al. (2009); they reported that a 35 g dose of rapidly absorbed casein hydrolysates is about 30% more effective in stimulating skeletal muscle protein synthesis than intact casein when measured over a 6-h period. Supplements containing protein hydrolysates, insulin and carbohydrates increase insulin secretion compared to supplements containing only carbohydrates. Therefore, a higher deposition of post-exercise muscle mass may occur (Manninen, 2009).

Certain egg white-derived peptides also play a role in controlling the development of hypertension and also have shown antioxidant properties (Davalos, Miguel, Bartolome & Lopez-Fandino, 2004; Miguel, López-Fandiño, Ramos & Aleixandre, 2005; Miguel, Recio, Gómez-Ruiz, Ramos & López-Fandiño, 2004). According to Park, Jung, Nam, Shahidi and Kim (2001), the use of protein hydrolysates with antioxidant activities may be advantageous in functional foods because they also provide other desired functional properties.

Nevertheless, there is no scientific evidence either on the efficacy of egg white protein hydrolysates on skeletal muscle protein synthesis following exercise or their efficiency as wall material in microencapsulation of bioactives. Up to date, commercial protein hydrolysates products from egg white proteins have not been identified.

1.1.3.1 Protein hydrolysates in culture media for lactic acid fermentation

Lactic Acid Bacteria (LAB) are an economically important group of bacteria that has a long and safe history of applications in the production of food and beverages (Zhang, Ren, Zhao, Zhao, Xu & Zhao, 2011). LAB produces an acidification of the raw material due to the production of lactic acid (mainly); even more, this changes result in an enhancement of the shelf life, texture, and sensory attributes of the product (Ummadi & Curic-Bawden, 2010). The use of LAB in food products have increased in recent years due to the positive effects of LAB in maintaining a healthy human microbial gastrointestinal balance; which may be beneficial for the overall human health (Gomes, Malcata & Klaver, 1998). Among the most important genus of LAB are the lactococci, lactobacilli, streptococci, and pediococci. Each species of LAB has its own nutritional requirements (energy, carbon and nitrogen sources) which must be optimized to produce active and vigorous LAB starter cultures (Ummadi & Curic-Bawden, 2010). So, the

selection of the right raw ingredients and the design of the optimum fermentation media is unquestionably the most important step in the production of concentrated LAB starter cultures. The source and type of amino acids in the fermentation media is a key factor for the viability of LAB (Zhang, Ren, Zhao, Zhao, Xu & Zhao, 2011). Normally, industrial fermentations utilize a broad spectrum of raw materials and unidentified additives such as peptones, protein hydrolysates, yeasts extracts, growth factor; etc. Hence, it is important to study the effect of identified protein hydrolysates on the growth of lactic acid cultures (Zhang, Ren, Zhao, Zhao, Xu & Zhao, 2011).

1.1.3.1.1 Starter cultures

According to Ummadi and Curic-Bawden (2010), commercial starter cultures contain a single or multiple strains which are commonly commercialized as frozen or free dried cultures. Commercial productions of starter cultures are not only optimized to obtain high biomass quantity (cell yield) but also high biomass quality. Cell wall composition of LAB is one of the most important factors to determine biomass quality; this factor determines the survival rate of cell during downstream processing. Moreover, cell wall composition is species-dependent and greatly affected by the fermentation media, growth conditions, and physiological status of cells at the time of harvesting. So, production process of LAB must be optimized for each LAB strain based on the organism, growth requirements and final application of the culture.

1.1.3.1.2 Fermentation media

In accordance with Meli, Lazzi, Neviani and Gatti (2014), fermentation media for LAB have to provide the nutritional requirements of each LAB species/strain such as essential amino acids; peptides; vitamins, mineral; nucleic acid bases and growth factors. Furthermore, fermentation media should be formulated with readily available, inexpensive, and reproducible quality raw

materials. Most of the fermentation media are formulated to contain sugars as a source of energy and carbon; proteins as a nitrogen source; vitamins and minerals (Ummadi & Curic-Bawden, 2010).

1.1.3.1.3 Energy and carbon sources

It is been reported that LAB are homofermentative organisms that are unable to utilize a functional tricarboxylic (TCA) cycle to generate energy; instead, LAB generates energy via the glycolytic (Embden-Meyerhoff-Parnas-EMP) pathway; where two moles of ATP are produced per mole of hexose consumed (Konings, Poolman, Driessen & Maloney, 1989). LAB does not produce any energy storage compound like glycogen, polyphosphate, and poly-β-hydroxybutyrate; hence, fermentation media must supply enough energy to support anabolic process and cell growth (Ummadi & Curic-Bawden, 2010). Lactose and glucose are the preferred energy and carbon sources for industrial LAB fermentations; nevertheless, if the cell wall components (teichoic acid and peptidglycans) and RNA precursos (purine and pyrimidine bases) are not provided in the fermentation medium in enough amounts; a small fraction of sugars will be used for these purposes; so, it is important to supply adequate amounts of nitrogen and growth factors.

1.1.3.1.4 Nitrogen requirements

According to Meli, Lazzi, Neviani and Gatti (2014), nitrogen is essential for growth of starter LAB cultures. Normally, amino acids provide the nitrogen require for bacteria growth. The capability to synthesize amino acids is limited in LAB; therefore, exogenous sources of amino acids and peptides are critical for their growth (Ummadi & Curic-Bawden, 2010). Bacteria cells have to translocate available proteins, peptides and/or free amino acids from the fermentation media as building blocks for production of new proteins and enzymes. Furthermore,

protein hydrolysis is a necessary step that the bacteria cell needs to carry out in order to handle large proteins and peptides by the uptake system. Some LAB are equipped with uptake systems that can secrete extracellular proteases; which can break down proteins into peptides and amino acids; making them available for translocation; however, this is an energy consuming process for the cell (Juillard, Guillot, Le Bars & Gripon, 1998).

1.1.3.1.5 Protein hydrolysates as a nitrogen source and growth factors

Fermentation media containing protein hydrolysates is a more economical option in terms of cell energy expenditure. Protein hydrolysates are predigested proteins and their size and amino acid composition greatly affect the growth rate and biomass yield of the organism (Castro & Sato, 2014). Several studies have reported the use of protein hydrolysates on the growth of LAB (Castro & Sato, 2014; Gomes, Malcata & Klaver, 1998; Zhang, Ren, Zhao, Zhao, Xu & Zhao, 2011). Moreover, biological activities have been attributed to protein hydrolysates that have an effect on the growth stimulation of probiotic bacteria. According to Liu, Kong, Xiong and Xia (2010), these biological properties in protein hydrolysates are due to (1) a reduction of the molecular weight of the protein and to (2) an increase in the concentration of free amino and carboxyl groups, which enhances their solubility in water.

1.2 Sport Supplements

The performance and health of athletes are tremendously impacted by their diet. It has been reported that balance diets help athletes to make the most of their potential by providing the right amounts of energy and nutrients (Maughan, Depiesse & Geyer, 2007). Nevertheless, elite athletes require huge amounts of readily available nutrients and energy which are not easily supplied by conventional foods. So, balance diets often require the use of food supplements and

conventional foods to meet energy and nutrients requirements of athletes (Terjung, Clarkson, Eichner, Greenhaff, Hespel, Israel et al., 2000).

According to the Dietary Supplement Health and Education Act reported in Young and Bass (1995), a dietary supplement is a product taken orally that contains a "dietary ingredient" intended to supplement the diet. Vitamins, minerals, herbs, amino acids, enzymes, organ tissues, glandular and metabolites are considered "dietary ingredients". Sport supplements are food supplements that are consumed by individuals involved in any kind of sport activity.

Froiland, Koszewski, Hingst and Kopecky (2004) have reported that eighty-nine percent of college athletes consume at least one type of nutritional supplements. Energy drinks, vitamins, and proteins are among the most popular nutritional supplements among college athletes. Furthermore, it has been reported that around 48.3% of college athletes consume protein supplements. Protein powders (combination of several types of proteins) are the most popular supplement (21.7%) followed by whey proteins (12.6%), especial combination of amino acids (11.6%), and weight gainers (10.6%). Meanwhile 6.3% of college athletes consume soy proteins.

1.3 Omega-3 fish oil and exercise

According to Simopoulos (2007), excessive radical formation in the form of superoxide radical (O_2-) in the lipid bilayers of muscle mitochondria and trauma during high-intensity exercise produces an inflammatory state that is aggravated by a high ratio of ω-6 to ω-3 polyunsaturated fatty acids (PUFA) which ranges from 10:1 to 20:1 in Western diets. Positive effects on human health have been attributed to the consumption of ω-3 PUFA (Riediger, Othman, Suh & Moghadasian, 2009). Alpha linolenic acid (ALA) (C18:3), eicosapentaenoic acid (EPA) (C20:5) and docosahexaenoic acid (DHA) (C22:6) are the main ω-3 PUFA (Clandinin, Jumpsen & Suh, 1994). Omega-3 fatty acids (EPA and DHA in particular) may reduce

proinflammatory cytokines while raising anti-inflammatory markers (Ferrucci, Cherubini, Bandinelli, Bartali, Corsi, Lauretani et al., 2006). Moreover, ω-3 PUFA prevent hyperglycemia and increases oxygen delivery to the heart muscle due to a decrease in blood viscosity (Simopoulos, 2007). Furthermore, ω-3 PUFA have shown neuroprotective mechanisms in athletes and soldiers (Lewis & Bailes, 2011). In a study conducted in rats by Peoples and McLennan (2010), it was reported that dietary fish oil reduces skeletal muscle oxygen consumption, provides fatigue resistance and improves contractile recovery in the animals' hind limb.

Despite this potentially beneficial modulation of the inflammation process, relatively few studies have examined the efficacy of dietary ω-3 PUFA on delayed onset muscle soreness and its recovery. Phillips, Childs, Dreon, Phinney and Leeuwenburgh (2003) provided a supplement containing DHA along with flavonoids, quercetin, and tocopherol to subjects after performing 30 eccentric elbow flexions at 80% effort to elicit muscle damage and inflammation. On the third day following exercise, plasma concentrations of IL-6 and CRP were reduced. However, no attempt was made to assess the effect of this apparent reduction in inflammation response on muscle function recovery. In addition it was not possible to attribute the effects to any one of the ingredients of the supplement. Lenn et al. (Lenn, Uhl, Mattacola, Boissonneault, Yates, Ibrahim et al., 2002) hypothesized that 1.8 g/day of dietary ω-3 in the form of fish oil would reduce muscle damage after eccentric elbow flexion exercise and promote faster recovery of muscle strength after the exercise. They found no significant effect of the fish oil on markers of damage (rise in CPK) or in recovery of muscle strength for 7 days after the exercise. Type 2 error is, however, possible as there were only 5 subjects in the fish oil group and muscle strength was

only slightly impaired by the exercise protocol, leaving open the possibility that the magnitude of damage and inflammatory response were insufficient to detect a possible effect of the fish oil.

1.4 Omega-3 PUFA and cancer cachexia

Preston, Fearon, Robertson, East and Calman (1987) describe cancer cachexia as a condition of selective depletion of skeletal muscle protein reserves (muscle mass). Dietary eicosapentaenoic acid (EPA) has significantly reduced the loss of body weight and suppressed protein catabolism in soleus muscles in mice with cancer cachexia condition (Whitehouse, Smith, Drake & Tisdale, 2001). Moreover, the rate of weight loss in pancreatic cancer patients has been reduced by dietary EPA (Wigmore, Ross, Stuart Falconer, Plester, Tisdale, Carter et al., 1996). According to Barber, Ross, Voss, Tisdale and Fearon (1999) pancreatic cancer patients under a diet of EPA combined with a nutritional supplement have shown a significant weight gain (2.5 kg after 7 weeks). These results may indicate that a diet rich in EPA may be useful for patients with cancer cachexia. Furthermore, (Colomer, Moreno-Nogueira, García-Luna, García-Peris, García-de-Lorenzo, Zarazaga et al., 2007) have suggested that dietary ω-3 PUFA (EPA and DHA) in a doses higher than 1.5 g/day for an extended period of time to patients with advanced cancer may be associated with an improvement in their clinical, biological (including cachexia) and quality of life parameters.

1.5 Omega-3 PUFA fortified eggs

Due to the high nutritional value of eggs and ω-3 PUFA's benefits; attempts to combine both products in a single form has been reported. For example, Ferrier, Caston, Leeson, Squires, Weaver and Holub (1995) produced a ω-3 PUFA fortified eggs through the manipulation of the hens' diets. As a result, ω-3 PUFA fortified eggs contain up to three times the amount of ω-3 PUFA present in conventional eggs. However, a conventional egg is not a rich source of ω-3

PUFA; therefore, even a three-fold increase is considered small, if it is compared to the recommended daily intake for ω-3 PUFA by the governments of Canada, Scandinavia, and Britain, which is between 1000 and 2000 mg/d. In The United States a recommended daily intake for ω-3 PUFA has not been given yet (Kassis, Drake, Beamer, Matak & Jaczynski, 2010). The DHA content of a ω-3 fortified egg is approximately 150 mg/egg (Surai & Sparks, 2001). The incorporation of flaxseed into the hen's diet has reduced the total saturated FA and increased the PUFA levels in eggs without affecting their cholesterol levels (Arantes da Silva, Naiverti Elias, Aricetti, Sakamoto, Murakami, Marques Gomes et al., 2009). Incorporation of fish meal into hen's diet has also been reported in order to increase the amount of ω-3 PUFA in eggs; however, a 'fishy' flavor in the resulting eggs has been reported (Surai & Sparks, 2001). This tremendously affects the acceptability of a ω-3 PUFA enriched eggs by the consumer.

1.6 Microencapsulation technology

According to Champagne and Fustier (2007), microencapsulation is a method in which small quantities of solid, liquid or gaseous materials are packed into a wall matrix to form microcapsules which can control the release of the encapsulated compounds. Furthermore, microencapsulation can also help to overcome the main problems of food fortification with ω-3 PUFA which is the unpleasant "fishy" flavor of fish oil and the oxidation of polyunsaturated fatty acids that has negative influence on food acceptability (Kolanowski, 1999).

Due to the direct effect of the wall material on microencapsulation efficiency, microencapsulation stability, and protection efficiency of the microencapsulated compound, the selection of the wall material is very important in the microencapsulation process (Pérez-Alonso, Báez-González, Beristain, Vernon-Carter & Vizcarra-Mendoza, 2003). So, the wall material should have a low viscosity at high concentrations and be highly soluble in water and

(Reineccius, 1988). Carbohydrates, especially glucose and sucrose and polysaccharides like starch, maltodextrins, pectin, alginate and chitosan have been successfully used as wall materials (Risch, 1995). However, carbohydrates cannot be used in wall systems without the presence of a surface-active constituent because they generally have no emulsifying properties (Bangs & Reineccius, 1988). The incorporation of carbohydrates in a wall matrix has been shown to improve the drying properties of the wall by enhancing the formation of a dry crust around the droplets of the microencapsulated compound. However, high concentrations of low molecular weight sugars may not be suitable for spray drying due to caramelization and the formation of sticky powders (Bayram, Bayram & Tekin, 2005).

On the other hand, proteins have the ability to assemble at interfaces because of their amphiphilic nature. It has been proven that proteins are good wall materials for flavor compounds because of their high binding activity with flavors (Landy, Druaux & Voilley, 1995). Whey proteins have been reported to be an effective wall material for microencapsulation of anhydrous milkfat or volatiles. The combination of whey protein with lactose significantly limits the diffusion of core material through the wall thereby leading to high microencapsulation efficiency (Moreau & Rosenberg, 1993). Sodium caseinate is also an effective wall material for microencapsulation of oils. It has strong amphiphilic characteristics and high diffusivity, which provides a better distribution around the enclosed oil surface (Hogan, McNamee, O'Riordan & O'Sullivan, 2001). Maltodextrin, and highly branched cyclic dextrin (HBCD) in combination with sodium caseinate and whey protein isolate have been used as wall materials for the microencapsulation of fish oil. The combination of maltodextrin or HBCD with sodium caseinate have improved the oxidative stability of encapsulated fish oil (Kagami, Sugimura, Fujishima, Matsuda, Kometani & Matsumura, 2003). Microencapsulation by spray drying has significantly

reduced the bitterness and hygroscopicity of casein hydrolysates (Favaro-Trindade, Santana, Monterrey-Quintero, Trindade & Netto, 2010; Mendanha, Molina Ortiz, Favaro-Trindade, Mauri, Monterrey-Quintero & Thomazini, 2009). Currently, there is a lack of scientific literature regarding lipid compounds microencapsulated in wall systems containing egg proteins/ egg protein hydrolysates; however, it is believed that egg proteins may be good encapsulating agents due to their emulsifying properties (Mine, 1995).

1.7 Spray drying

Spray drying is a cost-effective processing technique of transforming a liquid feed into a low-moisture content powder by spraying the liquid feed into a hot drying medium. In accordance with Anandharamakrishnan, Rielly and Stapley (2007), the process is divided in four stages: (1) atomization of feed into a drying chamber, (2) contact between sprayed liquid feed droplets and the drying air (3) moisture evaporation and (4) separation of dried powder from drying air (Fig. 1.1).

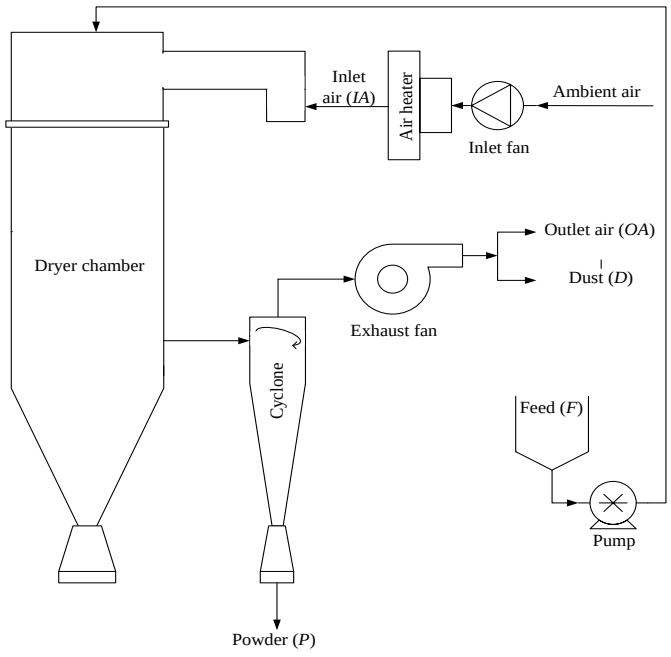

Fig. 1.1 - Schematic representation of a spray drying system

1.7.1 Atomization of liquid feed

It is a procedure to transform the liquid feed material into a large number of small droplets; this process is critical in spray drying because it increases the surface area of the liquid feed and defines the particle size of the final product. The most common atomizers are: (1) pressure nozzles, (2) two-fluid nozzles, and (3) centrifugal nozzles (Gharsallaoui, Roudaut, Chambin, Voilley & Saurel, 2007).

1.7.2 Feed droplets – drying air contact

In this stage, the feed droplets interact with the drying hot air inside the spraying chamber. Depending on the dryer design, the flow of the droplets can be co-current or counter-current to drying air flow (Fig. 1.2). In a co-current drying configuration, the feed droplets and drying air flow in the same direction (Fig. 1.2.a). Meanwhile, in a counter-current drying configuration, the flow of the feed droplets is opposite to the flow of the drying air (Fig. 1.2.b). According to Anandharamakrishnan (2013), co-current configuration is more suitable for the drying of heat-sensitive materials because of a rapid spray evaporation and shorter residence time.

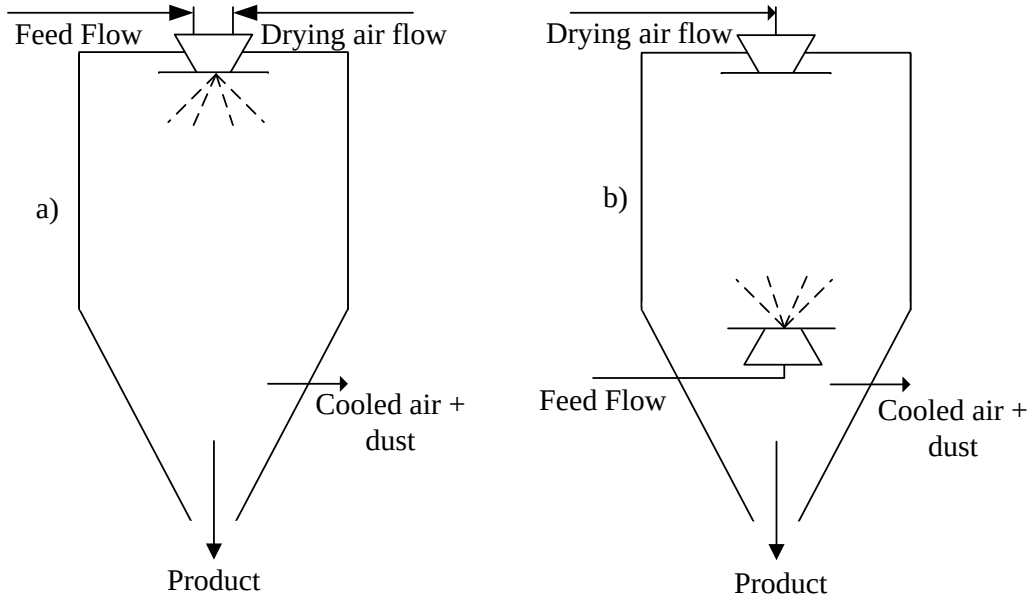

Fig. 1.2 – Spray drying configuration: a) co-current; b) counter-current conditions.

1.7.3 Moisture evaporation

Moisture evaporation takes place when the feed droplets come in contact with the drying air. Higher surface of area of the feed droplets results in higher evaporation rates, which keeps the temperature of the feed droplets at the wet-bulb temperature (Anandharamakrishnan, 2013). According to Gharsallaoui, Roudaut, Chambin, Voilley and Saurel (2007), during the moisture evaporation phase, three processes can be distinguished (Fig. 1.3). The three droplet-drying stages are as follows; (1), an excess of moisture forms a liquid envelope at the droplet surface, and the drying rate is similar to pure liquid water, liquid evaporation results in the shrinkage of the droplet diameter. At certain point, the excess of moisture is evaporated and the droplet turns into a wet particle; (2), at this point, the hindered drying begins, two regions of the wet particle can be clearly identified: a layer of dry porous crust and an internal wet core. Drying rate is controlled by the rate of moisture diffusion from the wet particle core through the crust pores toward the particle outer surface which results in particle shrinkage; and (3), the particle diameter remains unchanged and particle moisture content decreases to a minimal possible value (equilibrium moisture content that cannot be removed by drying). After the drying period, different physical phenomena can occur to the dried particles such as expansion, collapse, disintegration and irregular shape (Mezhericher, Levy & Borde, 2012).

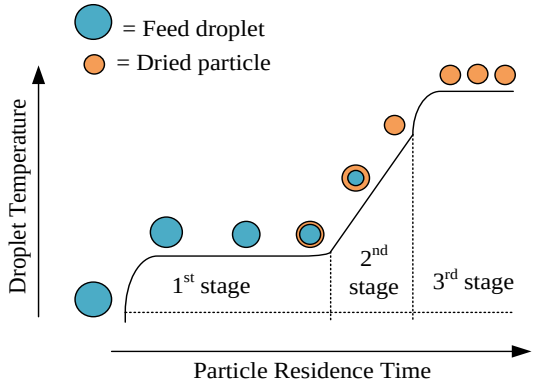

Fig. 1.3 – Schematic representation of the droplet temperature curve during spray drying.

1.7.4 Separation of dried powders

The dried feed powder is normally separated from the drying air by different means such as screw conveyors, pneumatic systems with a cyclone separator, bag filters and electrostatic precipitators (Fellows, 2009). Cyclones are often used in stage since they reduce product losses to the atmosphere. According to Schuck (2002), thermal effectiveness and residence time can be increased by using multi-stage spray-dryers which can minimize thermal degradation of heat sensitive materials.

1.7.5 Microencapsulation of fish oil by spray drying

According to Kolanowski (1999), microencapsulation is a process that transforms fish oil into powder by surrounded the tiny fish oil droplets with a wall material resulting in small granules that have powder like flow characteristics. This process delays the oxidation of ω-3 fish oil that results in the unpleasant "fishy" flavor. One of the most common and low-cost microencapsulation processing technologies is spray drying which can be 30 to 50 times cheaper than freeze-drying (Desobry, Netto & Labuza, 1997).

1.7.6 Processing challenges in spray drying

Prediction of the quality of the final product is extremely difficult and usually one of the drawbacks associated with spray drying (Kieviet, 1997). Parameters like moisture content, thermal degradation of bioactives, aroma retention, stickiness, shape and size of the particles are normally associated with product quality. Product quality is highly linked with the spray drying processing conditions (temperature, humidity, etc.). (Kieviet & Kerkhof, 1995; Paris, Ross Jr, Dastur & Morris, 1971). Furthermore, many biological products like protein, enzymes, antioxidants, vitamins and bacteria are prone to thermal degradation during spray drying processing due to their exposure to high drying temperatures (Kuriakose &

Anandharamakrishnan, 2010). Thermal degradation of heat sensitive materials can be minimized by reducing particle residence time at higher temperatures (Bimbenet, Bonazzi & Dumoulin, 2002). Several approaches to predict the final quality of spray dried powders have been reported in the literature (Birchal, Huang, Mujumdar & Passos, 2006); however, most of these attempts are based on experimental calculations of drying kinetics of discrete droplets immersed into a current of hot air. Predicting the quality of spray dried powders is a challenging task due to the complexity of the process.

Computational methods like computational fluid dynamics (CFD) have allowed the improvement on device design and somehow predict the final quality of the spray dried powders; nevertheless, predicting the quality of spray dried powders by using only computational means is complicated due to the number of parameters that intervene during the process such as droplet evaporation, collision, breakups, agglomeration, heat and mass exchange between the droplets and drying medium and so on (Gharsallaoui, Roudaut, Chambin, Voilley & Saurel, 2007). Therefore, the combination of computational approaches with lab experiments is a more feasible and practical approach for predicting the final quality of spray dried food powders.

1.8 Computational fluid dynamics (CFD)

According to Kuriakose and Anandharamakrishnan (2010), computational fluid dynamics (CFD) is a powerful computational simulation tool that has been utilized in basic and applied research and has attracted the interest of the food processing sector in recent years. CFD is a numerical technique for solving governing equations of fluid flow inside a geometry. CFD uses powerful computers combined with applied mathematics to model fluid flow processes (Scott & Richardson, 1997). Fluid flow can be defined using the Navier-Stokes transport equations which are derived by considering mass, momentum and energy balances in an element of fluid that

results in a set of partial differential equations (Bird, Stewart & Lightfoot, 2007). A detailed explanation of the theory of CFD modeling is given by Anandharamakrishnan (2013).

1.8.1 Continuity or conservation of mass equation

The conservation of mass equation describes the rate of change of density at a fixed point resulting from the divergence in the mass velocity vector ρv. The continuity or conservation of mass equation is the unsteady, three-dimensional and simplified case of a constant density fluid (incompressible fluid) is described by Equation 1.1.

$$\nabla . v = 0 \tag{1.1}$$

Where, ∇ has the dimension of reciprocal length given by Equation 1.2.

$$\nabla = \frac{\partial}{\partial x} i + \frac{\partial}{\partial y} j + \frac{\partial}{\partial z} k \tag{1.2}$$

1.8.2 Momentum equation

The principles of the conservation of momentum is an application of Newton's second law of motion (F=m a) to an element of fluid. The equation states that a small volume of element moving with the fluid is accelerated due to the force acting upon it (Equation 1.3).

$$\rho_g \frac{Dv}{Dt} = -\nabla p + \nabla . \underline{\underline{\tau}} + \rho_g \underline{g} \tag{1.3}$$

Convection terms are described on the left size of Equation 1.3, meanwhile on the right hand side are the pressure gradient (p), density of drying air (ρ_g), source terms of gravitational force ($\underline{g}$) and stress tensor ($\underline{\underline{\tau}}$) which is responsible for diffusion of momentum.

1.8.3 Energy equation

The energy equation applies the first law of thermodynamics that states that energy is conserved. The energy equation is solved in CFD solver ANSYS FLUENT® as follows (Equation 1.4):

$$\frac{\partial}{\partial t}(\rho E) + \nabla\left[\underline{v}(\rho E + p)\right] = \nabla.\left[k_{eff}\nabla T - \sum_j h_j \underline{J}_j + (\underline{\underline{\tau}} \,.\, \underline{v})\right] \quad (1.4)$$

Where, E is the thermal (internal) energy, k_{eff} is the effective conductivity (k_{ta}+$k_{t,}$ where k_{ta} is thermal conductivity and k_t is turbulent thermal conductivity). T is the temperature, $\underline{\underline{\tau}}$ is the stress tensor, $\underline{J}_j$ is the diffusion flux of species j, and h_j is the enthalpy of species j. The three terms on the right-hand side of Equation 1.4 indicates energy transfer due to conduction, species diffusion and viscous dissipation, respectively. In the case of spray drying, CFD can be used to predict the drying air flow pattern and food particle histories such as temperature, velocity, and residence time within the drying chamber. These parameters are extremely difficult and expensive to be measured in large-scale spray dryers. The study of the effect of chamber design on drying behavior of food materials can also be done using CFD. Even more, CFD is a useful tool to scale-up spray chambers from pilot to full industrial scale (Mezhericher, Levy & Borde, 2009).

1.8.4 CFD analysis

To conduct a CFD analysis, it is necessary to have a good understanding of the problem to express it mathematically in the CFD solver; then the CFD solver will express the stated problem in more understandable scientific terms. Finally, the computer will conduct the operations commanded by the CFD solver (Xia & Sun, 2002). According to Tu, Yeoh and Liu (2007) to solve a CFD problem requires of three steps: pre-processing, processing, and post-processing. The CFD pre-processing stage includes problem thinking, geometry and meshing generation. It is very important to consider the physics of the problem during problem thinking. The geometry of the flow region is created (computational domain for the CFD calculation) in 2D or 3D depending of the problem setup. This could be accomplished with the help of a CAD modeling software such as Autodesk Inventor. Afterwards, the mesh for the computational domain can be generated; which is basically the division of the computational domain into a number of smaller,

non-overlapping subdomains in order to solve the flow physics of the CFD problem. The set of these new cells are called *mesh* and each of these cells contains the equations for the conservation of mass, momentum and energy which are solved numerically to describe the flow properties such as velocity, pressure, and temperature and other variables of the fluid being study. Once the mesh has been generated, the fluid properties of fluid are defined. Then, the specific boundary conditions can be set according to the CFD problem (Xia & Sun, 2002). Processing is the second step in solving a CFD problem which involves the use of a CFD solver to get a numerical solution. Several commercial CFD solvers are available including ANSYS FLUENT®, ANSYS CFX ®, COMSOL, FLOW3D, etc. However, ANSYS FLUENT®, and ANSYS CFX® are the most popular CFD solvers (Tu, Yeoh & Liu, 2007). Setting a CFD solver for a computational solution requires the following steps: Initiation, solution control, monitoring solution, CFD calculation and checking for convergence. This is a very intensive process that requires powerful computers to solve many thousands of equations; therefore, it can be a time-consuming procedure (Xia & Sun, 2002). Post-processing is used to evaluate the results generated by the CFD solver. This step is basically how the generated results are presented and visualized. Generally, the results of the solved problem can be analyzed both numerically and graphically (Xia & Sun, 2002). Post-processing tools of CFD software are invaluable design instruments to effectively report the computational results. In general, the computational results can be presented in 2D graphs or 3D representations using x-y plots, vector plots, contour plots, streamlines, and animations (Anandharamakrishnan, 2013).

1.8.5 Study of spray drying processing using computational fluid dynamics

Several approaches to predict the final quality of spray dried powders have been reported in the literature (Birchal, Huang, Mujumdar & Passos, 2006); however, most of these attempts are

based on experimental calculations of drying kinetics of discrete droplets immersed into a current of hot air. Moreover, simple mass transport phenomena assumptions that occur in the drying chamber are applied and the physical phenomena that takes place at the cyclone is normally neglected. This may result in inaccurate predictions of the spray drying process because thermal degradation of the dried product may also occur at the cyclone. Furthermore, experimental spray drying studies involve difficulties due to the complexity in measuring and describing the flow, heat, and mass transfer mechanism within the drying chamber (Birchal, Huang, Mujumdar & Passos, 2006).

1.8.6 Reference frames in CFD

Reference frame is a coordinate system used to characterize and determine the position and orientation of an object at different times. In fluid mechanics, several reference frames are utilized (Aris, 1990). Commonly, the Eulerian-Eulerian and Eulerian-Lagrangian modelling frames are used in spray drying modelling by CFD. In the case of Eulerian-Eulerian frame, two continuous phases are assuming (one for the droplets and one for the drying air). So, each computational cell has a fraction for the drying air and the droplets phases. Also, it contains the all of the CFD equations are written in such a way that the fractions of drying air and droplets sum to unity (Kuriakose & Anandharamakrishnan, 2010). According to Jakobsen, Sannæs, Grevskott and Svendsen (1997), this method requires less computational demands and a set of equations to model turbulence is fairly simple. This approach is more suitable to model the drying of droplets with a narrow range of particle sizes.

On the other hand, the Eulerian-Lagrangian frame models the drying air phase using the standard Eulerian approach; meanwhile the droplets are represented by a number of discrete computational “particles”. This methodology requires less computational needs than the

Eulerian-Eulerian methods for a large range of particle sizes (Nijdam, Guo, Fletcher & Langrish, 2006). Also, the Eulerian-Lagrangian approach provides more details about the behavior and particle residence times; therefore, approximates mass and heat transfer more accurately. For spray drying modeling a Eulerian-Lagrangian reference frame is more suitable (Kuriakose & Anandharamakrishnan, 2010).

1.8.7 Air flow patterns

In accordance with Kuriakose and Anandharamakrishnan (2010), particle behavior in spray drying operations depends on the drying air flow pattern. Additionally, the presence of air flow instabilities needs to be considered to study the drying behavior of droplets inside the spray chamber; therefore, the effect of turbulence inside the drying chamber must be taken into account.

1.8.8 Turbulence models

Southwell and Langrish (2000) have reported the presence of significant flow instabilities inside a pilot-scale spray dryer. These instabilities are large scale drifting of droplets if the inlet flow is not swirled or regular precession if there is inlet swirl. Therefore, it is important to carry out three-dimensional spray drying simulations to account for all of the drying air flow instabilities inside the dryer chamber (Fletcher, Guo, Harvie, Langrish, Nijdam & Williams, 2006).

Several turbulence models have been proposed to describe the air flow patter inside a spray dryer; however, the standard k- ε (k – turbulence kinetic energy and ε - turbulence dissipation rate) is the widely used because it can be applied over a range of turbulent flows due to its robustness and reasonable accuracy (Kuriakose & Anandharamakrishnan, 2010). The

mechanisms that affect the kinetic energy are focused in the standard *k*- ε model. The transport of the turbulent kinetic energy *k* and its dissipation rate ε is given as follow:

$$\frac{\partial}{\partial_t}(\rho k) + \nabla.\left(\rho k \underline{v}\right) = \nabla.\left[(\mu + \frac{\mu_t}{\sigma_k})\nabla k\right] + G_k - \rho\varepsilon \qquad (1.5)$$

and

$$\frac{\partial}{\partial_t}(\rho \varepsilon) + \nabla.\left(\rho \varepsilon \underline{v}\right) = \nabla.\left[(\mu + \frac{\mu_t}{\sigma_\varepsilon})\nabla \varepsilon\right] + C_{1\varepsilon}\frac{\varepsilon}{k}(G_k) - C_{2\varepsilon}\rho\frac{\varepsilon^2}{k} \qquad (1.6)$$

Where ρ, $\underline{v}$, and μ are the density, velocity, and viscosity of the drying air; respectively. G_k is the generation of kinetic energy due to the mean velocity gradients; σ_k and σ_ε are the turbulent Prandtl numbers for *k* and ε, respectively. $C_{1\varepsilon}$, $C_{2\varepsilon}$, and C_μ are constants; μ_t is the turbulent (eddy) viscosity given by Equation 1.7.

$$\mu_t = \rho C_\mu \frac{k^2}{\varepsilon} \qquad (1.7)$$

1.8.9 Particle histories

Designing and modeling spray drying operations requires a deep understanding of particles histories such as velocity, temperature, residence time and impact position (Kuriakose & Anandharamakrishnan, 2010). Also, the quality of the dried powder depends of these particle histories which can be simulated using CFD.

1.8.10 Drying air-particle interaction

According to Kuriakose and Anandharamakrishnan (2010), the first challenge in spray drying modelling is the coupling of the mass, momentum and energy equations between the drying air and the droplets. The mass transfer phenomena from droplets to the drying air are coupling by evaporation; momentum exchange via drag and energy coupling by heat transfer. It is important to consider heat transfer from the drying air to the droplets by convection which decreases the drying air temperature; therefore, affecting its viscosity and density. Changes in viscosity and

density of the drying air may result in changes on its flow (Crowe, Sharma & Stock, 1977). As discussed previously, the Eulerian-Lagrangian reference frame provides good approximations for particle residence time with a large range of particle sizes. Using this approach, the drying air phase is considered the continuous phase (Eulerian approach) and is described by first solving the drying air flow filed assuming no droplets are present; afterwards, droplet trajectories and other particle histories are calculated (Crowe, Sharma & Stock, 1977). Then, the mass, momentum and energy terms for each cell in the flow field are determined. Moreover, the source terms are evaluated from the droplet equation and are integrated over the time required to cross the length of the trajectory inside each control volume. The results are multiplied by the number flow rate of drops associated with this trajectory. Finally, the drying air flow field is solved again; but this time incorporating the new source terms and then new droplet trajectories and particles histories are calculated. This approach provides the effect of the droplets on the drying air velocity and temperature fields (Kuriakose & Anandharamakrishnan, 2010).

Using the Eulerian-Lagrangian reference frame in CFD simulations the particle trajectories are obtained by solving the force balance equation (Equation 1.8).

$$\frac{\mathrm{d}\underline{u_p}}{\mathrm{d}t} = \frac{18\mu}{\rho_p d_p}\frac{C_D Re}{24}\left(\underline{v} - \underline{u_p}\right) + \underline{g}\left[\frac{\rho_p - \rho_g}{\rho_p}\right] \tag{1.8}$$

Where, $\underline{v}$ is the fluid phase velocity, $\underline{u_p}$ is the particle velocity, ρ_g is the density of the drying air and ρ_p is the density of the particle.

Also, the particle force balance (motion equation) includes discrete phase inertia, aerodynamic drag and gravity. The slip Reynolds umber (*Re)* and the drag coefficient (C_D) are determined by Equations 1.9 and 1.10, respectively:

$$Re = \frac{\rho_g d_p |\underline{u_p} - \underline{v}|}{\mu} \tag{1.9}$$

$$C_D = a_1 + \frac{a_2}{Re} + \frac{a_3}{Re^2} \quad (1.10)$$

Where, d_p is the particle diameter, and a_1, a_2 and a_3 are constants that apply to smooth spherical particles over several ranges of Reynolds number (*Re*) given by (Morsi & Alexander, 1972).

Particle velocity relative to drying air velocity is used in calculation of trajectories (Eq. 1.8). The heat and mass transfer between the particles and the hot drying air is derived following the motion of the particles given by Equation 1.11.

$$m_p c_p \frac{\mathrm{d}T_p}{\mathrm{d}t} = hA_p\left(T_g - T_p\right) + \frac{\mathrm{d}m_p}{\mathrm{d}t} h_{fg} \quad (1.11)$$

Where, m_p is the mass of the particle, c_p is the particle heat capacity, T_p is the particle temperature, h_{fg} is the latent heat, A_p is the surface area of the particle and *h* is the heat transfer coefficient.

The heat transfer coefficient (*h*) is obtained from the Ranz-Marshall equation (Eq. 1.12).

$$Nu = \frac{hd_p}{k_{ta}} = 2 + 0.6(Re_d)^{\frac{1}{2}}(Pr)^{1/3} \quad (1.12)$$

Where, Prandtl number (*Pr*) is defined as follows (Eq. 1.13).

$$Pr = \frac{c_p \mu}{k_{ta}} \quad (1.13)$$

Where, d_p is the particle diameter, k_{ta} is the thermal conductivity of the fluid, μ is the molecular viscosity of the drying air.

Equation 1.14 describes the rate of mass transfer (for evaporation).

$$\frac{\mathrm{d}m_p}{\mathrm{d}t} = -k_c A_p (Y_s - Y_g) \quad (1.14)$$

Where, Y_s* is the saturation humidity, Y_g is the drying air humidity and k_c is the mass transfer coefficient which is obtained from Sherwood number (Eq. 1.15).

$$Sh = \frac{k_c d_p}{D_{i,m}} = 2 + 0.6(Re_d)^{1/2}(Sc)^{1/3} \quad (1.15)$$

Where, $D_{i,m}$ is the diffusion coefficient of water vapor in the drying air phase and *Sc* is the Schmidt number, defined by Equation 1.16 as follows:

$$Sc = \frac{\mu}{\rho_g D_{i,m}} \quad (1.16)$$

Specific values for vapor pressure, density, specific heat and diffusion coefficients can be obtained from Incropera, Dewitt, Bergman and Lavine (2011).

The boiling rate model (Equation 1.17) is used when the temperature of the droplets reaches the boiling point and while the mass of the droplets exceeds the non-volatile fraction (Kuo, 1986).

$$\frac{\mathrm{d}(d_p)}{\mathrm{d}t} = \frac{4k_{ta}}{\rho_p c_g d_p}\left(1 + 0.23\sqrt{Re}\right) ln\left[1 + \frac{c_g(T_g - T_p)}{h_{fg}}\right] \quad (1.17)$$

Where, k_{ta} is the thermal conductivity of the drying air and c_g is the heat capacity of the drying air.

1.8.11 Particle temperature

Kuriakose and Anandharamakrishnan (2010) have reported that particle temperature is critical for heat sensitive products during spray drying. Even more, thermal degradation of bio-compounds is affected by the residence time and temperature of the particles. According to Crowe, Sharma and Stock (1977) smaller particles have higher temperatures than larger particles. This due to the ratio of surface area to volume which is higher in smaller particles compared to that of larger particles. Particle temperature distribution during spray drying has been studied by Anandharamakrishnan, Gimbun, Stapley and Rielly (2010). They reported that droplet temperatures can be almost as high as the drying air temperature. Furthermore, drying air

temperatures at the core of the drying chamber are lower than those at the region close to the dryer chamber wall due to the cooling effect of evaporation.

1.8.12 Particle residence time distribution (RT)

Particle residence time (RT) during spray dying is another parameter that has a tremendous effect on the final quality of the spray dried powders. In accordance with Kuriakose and Anandharamakrishnan (2010), solubility and bulk density of the spray dried powders are affected by their RT. Conventionally, RT is divided in primary and secondary residence times. The primary RT account for the time taken by the feed droplets from leaving the nozzle to impact on the wall or leave at the outlet. Meanwhile, secondary RT is the time taken for a particle to slide along the wall from the impact position to the exit. Kieviet (1997) have reported that larger particles have longer RT's compared to smaller particles during spray drying of maltodextrin solution in a co-current spray drying configuration. Measuring the RT during spray drying is extremely challenging and a complicated task; therefore, CFD simulation methods have been effectively used to predict the RT of spray dried particles (Ducept, Sionneau & Vasseur, 2002). Moreover, different particle trajectories has been observed during spray drying (Huang, Kumar & Mujumdar, 2003). Anandharamakrishnan, Gimbun, Stapley and Rielly (2010) have observed that a bent outlet pipe inside the drying chamber can increase the drying air and particle recirculation; this will increase the RT of the dried powders which leads to higher protein denaturation rates. However, this work did not include the suction effect given by an outlet fan that may prevent drying air recirculation inside the drying chamber.

Up to date, scientific literature about the production and the effect of food grade egg white protein hydrolysates on the growth of LAB is limited. Scientific information about the production of microencapsulated ω-3 fish oil with food grade egg white protein hydrolysates is

also limited. Moreover, the use of computational tools to predict the performance of a spray dryer and the quality of spray dried food powders is also partial because these methods are relatively new to the food industry; therefore, leaving a great opportunity to explore this field.

1.9 References

AEB. (1999). Eggcyclopedia - The incredible edible egg. Park Ridge, IL: American Egg Board.

Anandharamakrishnan, C. (2013). Computational Fluid Dynamics Applications in Food Processing: Springer.

Anandharamakrishnan, C., Gimbun, J., Stapley, A., & Rielly, C. D. (2010). A study of particle histories during spray drying using computational fluid dynamic simulations. *Drying Technology*, 28(5), 566-576.

Anandharamakrishnan, C., Rielly, C., & Stapley, A. (2007). Effects of process variables on the denaturation of whey proteins during spray drying. *Drying Technology*, 25(5), 799-807.

Anthony, J. C., Anthony, T. G., Kimball, S. R., & Jefferson, L. S. (2001). Signaling pathways involved in translational control of protein synthesis in skeletal muscle by leucine. *The Journal of nutrition*, 131(3), 856S-860S.

Anthony, J. C., Anthony, T. G., Kimball, S. R., Vary, T. C., & Jefferson, L. S. (2000). Orally administered leucine stimulates protein synthesis in skeletal muscle of postabsorptive rats in association with increased eIF4F formation. *The Journal of nutrition*, 130(2), 139-145.

Anthony, J. C., Anthony, T. G., & Layman, D. K. (1999). Leucine supplementation enhances skeletal muscle recovery in rats following exercise. *The Journal of nutrition*, 129(6), 1102-1106.

Arantes da Silva, W., Naiverti Elias, A. H., Aricetti, J. A., Sakamoto, M. I., Murakami, A. E., Marques Gomes, S. T., Visentainer, J. V., Evelázio de Souza, N., & Matsushita, M. (2009). Quail egg yolk (*Coturnix coturnix japonica*) enriched with omega-3 fatty acids. *LWT-Food Science and Technology*, 42(2), 660-663.

Aris, R. (1990). Vectors, Tensors and the Basic Equations of Fluid Mechanics: Dover Publications.

Bangs, W. E., & Reineccius, G. A. (1988). Corn starch derivatives: possible wall materials for spray-dried flavor manufacture. In Risch, S., & Reineccius, G. Flavor encapsulation. ACS Symposium Series pp. 12-28): ACS Publications.

Barber, M., Ross, J., Voss, A., Tisdale, M., & Fearon, K. (1999). The effect of an oral nutritional supplement enriched with fish oil on weight-loss in patients with pancreatic cancer. *British Journal of Cancer*, 81(1), 80.

Bayram, Ö. A., Bayram, M., & Tekin, A. R. (2005). Spray drying of sumac flavour using sodium chloride, sucrose, glucose and starch as carriers. *Journal of food engineering*, 69(2), 253-260.

Bimbenet, J., Bonazzi, C., & Dumoulin, E. (2002). Drying of foodstuffs. *Drying 2002*, 64-80.

Birchal, V., Huang, L., Mujumdar, A., & Passos, M. (2006). Spray dryers: modeling and simulation. *Drying Technology*, 24(3), 359-371.

Bird, R. B., Stewart, W. E., & Lightfoot, E. N. (2007). Transport phenomena: John Wiley & Sons.

Castro, R. J. S. d., & Sato, H. H. (2014). Functional properties and growth promotion of bifidobacteria and lactic acid bacteria strains by protein hydrolysates using a statistical mixture design. *Food Bioscience*.

Champagne, C. P., & Fustier, P. (2007). Microencapsulation for the improved delivery of bioactive compounds into foods. *Current opinion in biotechnology*, 18(2), 184-190.

Clandinin, M. T., Jumpsen, J., & Suh, M. (1994). Relationship between fatty acid accretion, membrane composition, and biologic functions. *The Journal of Pediatrics*, 125(5, Part 2), S25-S32.

Clemente, A. (2000). Enzymatic protein hydrolysates in human nutrition. *Trends in Food Science & Technology*, 11(7), 254-262.

Clemente, A., & Chambers, S. J. (2000). Development and Production of Hypoallergenic Protein Hydrolysates for Use in Infant Formulas. Food Allergy and Intolerance pp. 175 - 190).

Colomer, R., Moreno-Nogueira, J. M., García-Luna, P. P., García-Peris, P., García-de-Lorenzo, A., Zarazaga, A., Quecedo, L., del Llano, J., Usán, L., & Casimiro, C. (2007). N-3 fatty acids, cancer and cachexia: a systematic review of the literature. *British Journal of Nutrition*, 97(05), 823-831.

Crowe, C. T., Sharma, M., & Stock, D. E. (1977). The particle-source-in cell (PSI-CELL) model for gas-droplet flows. *Journal of Fluids Engineering*, 99(2), 325-332.

Davalos, A., Miguel, M., Bartolome, B., & Lopez-Fandino, R. (2004). Antioxidant activity of peptides derived from egg white proteins by enzymatic hydrolysis. *Journal of Food Protection®*, 67(9), 1939-1944.

Desobry, S. A., Netto, F. M., & Labuza, T. P. (1997). Comparison of Spray-drying, Drum-drying and Freeze-drying for β-Carotene Encapsulation and Preservation. *Journal of Food Science*, 62(6), 1158-1162.

Ducept, F., Sionneau, M., & Vasseur, J. (2002). Superheated steam dryer: simulations and experiments on product drying. *Chemical Engineering Journal*, 86(1), 75-83.

Favaro-Trindade, C. S., Santana, A. S., Monterrey-Quintero, E. S., Trindade, M. A., & Netto, F. M. (2010). The use of spray drying technology to reduce bitter taste of casein hydrolysate. *Food Hydrocolloids*, 24(4), 336-340.

Fellows, P. J. (2009). Food processing technology: principles and practice: Elsevier.

Ferrier, L. K., Caston, L. J., Leeson, S., Squires, J., Weaver, B. J., & Holub, B. J. (1995). alpha-Linolenic acid-and docosahexaenoic acid-enriched eggs from hens fed flaxseed: influence on blood lipids and platelet phospholipid fatty acids in humans. *The American journal of clinical nutrition*, 62(1), 81-86.

Ferrucci, L., Cherubini, A., Bandinelli, S., Bartali, B., Corsi, A., Lauretani, F., Martin, A., Andres-Lacueva, C., Senin, U., & Guralnik, J. M. (2006). Relationship of Plasma Polyunsaturated Fatty Acids to Circulating Inflammatory Markers. *Journal of Clinical Endocrinology & Metabolism*, 91(2), 439-446.

Fletcher, D., Guo, B., Harvie, D., Langrish, T., Nijdam, J., & Williams, J. (2006). What is important in the simulation of spray dryer performance and how do current CFD models perform? *Applied mathematical modelling*, 30(11), 1281-1292.

Friedman, M. (1996). Nutritional value of proteins from different food sources. A review. *Journal of Agricultural and Food Chemistry*, 44(1), 6-29.

Froiland, K., Koszewski, W., Hingst, J., & Kopecky, L. (2004). Nutritional supplement use among college athletes and their sources of information. *International journal of sport nutrition and exercise metabolism*, 14, 104-120.

Gharsallaoui, A., Roudaut, G., Chambin, O., Voilley, A., & Saurel, R. (2007). Applications of spray-drying in microencapsulation of food ingredients: An overview. *Food Research International*, 40(9), 1107-1121.

Gomes, A. M., Malcata, F. X., & Klaver, F. A. (1998). Growth Enhancement of *Bifidobacterium lactis* Bo and *Lactobacillus acidophilus* Ki by Milk Hydrolyzates. *Journal of Dairy Science*, 81(11), 2817-2825.

Grimble, G., Guilera Sarda, M., Sessay, H., Marrett, A., Kapadia, S., Bowling, T., & Silk, D. (1994). The influence of whey hydrolysate peptide chain length on nitrogen and carbohydrate absorption in the perfused human jejunum. *Clinical Nutrition*, 13, 46.

Grimble, G., Rees, R., Keohane, P., Cartwright, T., Desreumaux, M., & Silk, D. (1987). Effect of peptide chain length on absorption of egg protein hydrolysates in the normal human jejunum. *Gastroenterology*, 92(1), 136-142.

Hoffman, J. R., & Falvo, M. J. (2004). Protein - Which is best? *Journal of Sports Science and Medicine*, 3, 118-130.

Hogan, S. A., McNamee, B. F., O'Riordan, E. D., & O'Sullivan, M. (2001). Emulsification and microencapsulation properties of sodium caseinate/carbohydrate blends. *International Dairy Journal*, 11(3), 137-144.

Huang, L., Kumar, K., & Mujumdar, A. (2003). Use of computational fluid dynamics to evaluate alternative spray dryer chamber configurations. *Drying Technology*, 21(3), 385-412.

Incropera, F. P., Dewitt, D. P., Bergman, T. L., & Lavine, A. S. (2011). Fundamentals of heat and mass transfer: John Wiley & Sons.

Jakobsen, H. A., Sannæs, B. H., Grevskott, S., & Svendsen, H. F. (1997). Modeling of vertical bubble-driven flows. *Industrial & engineering chemistry research*, 36(10), 4052-4074.

Juillard, V., Guillot, A., Le Bars, D., & Gripon, J.-C. (1998). Specificity of Milk Peptide Utilization byLactococcus lactis. *Applied and environmental microbiology*, 64(4), 1230-1236.

Kagami, Y., Sugimura, S., Fujishima, N., Matsuda, K., Kometani, T., & Matsumura, Y. (2003). Oxidative stability, structure, and physical characteristics of microcapsules formed by spray drying of fish oil with protein and dextrin wall materials. *Journal of Food Science*, 68(7), 2248-2255.

Kassis, N., Drake, S. R., Beamer, S. K., Matak, K. E., & Jaczynski, J. (2010). Development of nutraceutical egg products with omega-3-rich oils. *LWT-Food Science and Technology*, 43(5), 777-783.

Kieviet, F., & Kerkhof, P. J. (1995). Measurements of particle residence time distributions in a co-current spray dryer. *Drying Technology*, 13(5-7), 1241-1248.

Kieviet, F. G. (1997). Modelling quality in spray drying: Laboratory of Separation Processes and Transport Phenomena, Department of Chemical Engineering, Eindhoven University of Technology.

Kolanowski, W. (1999). Possibilities of fish oil application for food products enrichment with omega-3 PUFA. *International journal of food sciences and nutrition*, 50(1), 39-49.

Konings, W., Poolman, B., Driessen, A., & Maloney, P. C. (1989). Bioenergetics and solute transport in lactococci. *Critical reviews in microbiology*, 16(6), 419-476.

Koopman, R., Crombach, N., Gijsen, A. P., Walrand, S., Fauquant, J., Kies, A. K., Lemosquet, S., Saris, W. H., Boirie, Y., & van Loon, L. J. (2009). Ingestion of a protein hydrolysate is accompanied by an accelerated in vivo digestion and absorption rate when compared with its intact protein. *The American journal of clinical nutrition*, 90(1), 106-115.

Kuo, K. K. (1986). Principles of combustion. *John Willey & Sons, New York*.

Kuriakose, R., & Anandharamakrishnan, C. (2010). Computational fluid dynamics (CFD) applications in spray drying of food products. *Trends in Food Science & Technology*, 21(8), 383-398.

Landy, P., Druaux, C., & Voilley, A. (1995). Retention of aroma compounds by proteins in aqueous solution. *Food Chemistry*, 54(4), 387-392.

Layman, D. K., & Rodriguez, N. R. (2009). Egg Protein as a Source of Power, Strength, and Energy. *Nutrition Today*, 44(1), 43-48.

Lenn, J., Uhl, T., Mattacola, C., Boissonneault, G., Yates, J., Ibrahim, W., & Bruckner, G. (2002). The effects of fish oil and isoflavones on delayed onset muscle soreness. *Medicine & Science in Sports & Exercise*, 34(10), 1605-1613.

Lewis, M. D., & Bailes, J. (2011). Neuroprotection for the warrior: dietary supplementation with omega-3 fatty acids. *Military medicine*, 176(10), 1120-1127.

Liu, Q., Kong, B., Xiong, Y. L., & Xia, X. (2010). Antioxidant activity and functional properties of porcine plasma protein hydrolysate as influenced by the degree of hydrolysis. *Food Chemistry*, 118(2), 403-410.

Manninen, A. H. (2009). Protein hydrolysates in sports nutrition. *Nutr Metab (Lond)*, 6, 38.

Maughan, R. J., Depiesse, F., & Geyer, H. (2007). The use of dietary supplements by athletes. *Journal of Sports Sciences*, 25(S1), S103-S113.

Meli, F., Lazzi, C., Neviani, E., & Gatti, M. (2014). Effect of Protein Hydrolysates on Growth Kinetics and Aminopeptidase Activities of Lactobacillus. *Current microbiology*, 68(1), 82-87.

Mendanha, D. V., Molina Ortiz, S. E., Favaro-Trindade, C. S., Mauri, A., Monterrey-Quintero, E. S., & Thomazini, M. (2009). Microencapsulation of casein hydrolysate by complex coacervation with SPI/pectin. *Food Research International*, 42(8), 1099-1104.

Mezhericher, M., Levy, A., & Borde, I. (2009). Modeling of droplet drying in spray chambers using 2D and 3D computational fluid dynamics. *Drying Technology*, 27(3), 359-370.

Mezhericher, M., Levy, A., & Borde, I. (2012). Three-dimensional spray-drying model based on comprehensive formulation of drying kinetics. *Drying Technology*, 30(11-12), 1256-1273.

Miguel, M., López-Fandiño, R., Ramos, M., & Aleixandre, A. (2005). Short-term effect of egg-white hydrolysate products on the arterial blood pressure of hypertensive rats. *British Journal of Nutrition*, 94(05), 731-737.

Miguel, M., Recio, I., Gómez-Ruiz, J., Ramos, M., & López-Fandiño, R. (2004). Angiotensin I-converting enzyme inhibitory activity of peptides derived from egg white proteins by enzymatic hydrolysis. *Journal of Food Protection®*, 67(9), 1914-1920.

Mine, Y. (1995). Recent advances in the understanding of egg white protein functionality. *Trends in Food Science & Technology*, 6(7), 225-232.

Moreau, D., & Rosenberg, M. (1993). Microstructure and fat extractability in microcapsules based on whey proteins or mixtures of whey proteins and lactose. *Food structure*, 12(4), 457-468.

Morsi, S., & Alexander, A. (1972). An investigation of particle trajectories in two-phase flow systems. *Journal of Fluid Mechanics*, 55(02), 193-208.

Nijdam, J. J., Guo, B., Fletcher, D. F., & Langrish, T. A. (2006). Lagrangian and Eulerian models for simulating turbulent dispersion and coalescence of droplets within a spray. *Applied mathematical modelling*, 30(11), 1196-1211.

Panyam, D., & Kilara, A. (1996). Enhancing the functionality of food proteins by enzymatic modification. *Trends in Food Science & Technology*, 7(4), 120-125.

Paris, J. R., Ross Jr, P. N., Dastur, S. P., & Morris, R. L. (1971). Modeling of the air flow pattern in a countercurrent spray-drying tower. *Industrial & Engineering Chemistry Process Design and Development*, 10(2), 157-164.

Park, P.-J., Jung, W.-K., Nam, K.-S., Shahidi, F., & Kim, S.-K. (2001). Purification and characterization of antioxidative peptides from protein hydrolysate of lecithin-free egg yolk. *Journal of the American Oil Chemists' Society*, 78(6), 651-656.

Peoples, G. E., & McLennan, P. L. (2010). Dietary fish oil reduces skeletal muscle oxygen consumption, provides fatigue resistance and improves contractile recovery in the rat in vivo hindlimb. *British Journal of Nutrition*, 104(12), 1771-1779.

Pérez-Alonso, C., Báez-González, J., Beristain, C., Vernon-Carter, E., & Vizcarra-Mendoza, M. (2003). Estimation of the activation energy of carbohydrate polymers blends as selection criteria for their use as wall material for spray-dried microcapsules. *Carbohydrate polymers*, 53(2), 197-203.

Phillips, T., Childs, A. C., Dreon, D. M., Phinney, S., & Leeuwenburgh, C. (2003). A Dietary Supplement Attenuates IL-6 and CRP after Eccentric Exercise in Untrained Males. *Medicine & Science in Sports & Exercise*, 35(12), 2032-2037.

Pokora, M., Eckert, E., Zambrowicz, A., Bobak, Ł., Szołtysik, M., Dąbrowska, A., Chrzanowska, J., Polanowski, A., & Trziszka, T. (2013). Biological and functional properties of proteolytic enzyme-modified egg protein by-products. *Food Science & Nutrition*, 1(2), 184-195.

Preston, T., Fearon, K. C. H., Robertson, I., East, B. W., & Calman, K. C. (1987). Tissue loss during severe wasting in lung cancer patients. In Ellis, K. J., Yasumura , S., & Morgan, W. P. *In Vivo* Body Composition Studies. Proceedings of an International Symposium held at Brookhaven National Laboratory, New York on September 28-October 1, 1986 pp. 60 - 69): Institute of Physical Sciences in Medicine.

Raimundo, A., Grimble, G., Rees, R., Hunjan, M., & Silk, D. (1988). The influence of fat and carbohydrate on absorption of partial enzymatic hydrolysates of casein in normal human jejenum. *GASTROENTEROLOGY*, 94, A988.

Reineccius, G. A. (1988). Spray-drying of food flavors. In Reineccius, G. A., & Risch, S. J. Flavor encapsulation. Washington, D.C: ACS Publications.

Riediger, N. D., Othman, R. A., Suh, M., & Moghadasian, M. H. (2009). A Systemic Review of the Roles of n-3 Fatty Acids in Health and Disease. *Journal of the American Dietetic Association*, 109(4), 668-679.

Risch, S. J. (1995). Review of patents for encapsulation and controlled release of food ingredients. ACS Symposium Series pp. 196-202): ACS Publications.

Salgado, P., Montagne, L., Freire, J. P. B., Ferreira, R. B., Teixeira, A., Bento, O., Abreu, M. C., Toullec, R., & Lallès, J.-P. (2002). Legume Grains Enhance Ileal Losses of Specific Endogenous Serine-Protease Proteins in Weaned Pigs. *The Journal of Nutrition*, 132(7), 1913-1920.

Schuck, P. (2002). Spray drying of dairy products: state of the art. *Le Lait*, 82(4), 375-382.

Scott, G., & Richardson, P. (1997). The application of computational fluid dynamics in the food industry. *Trends in Food Science & Technology*, 8(4), 119-124.

Simopoulos, A. P. (2007). Omega-3 fatty acids and athletics. *Current Sports Medicine Reports*, 6(4), 230-236.

Southwell, D., & Langrish, T. (2000). Observations of flow patterns in a spray dryer. *Drying Technology*, 18(3), 661-685.

Stevens, L. (1991). Egg white proteins. *Comparative Biochemistry and Physiology Part B: Comparative Biochemistry*, 100(1), 1-9.

Surai, P., & Sparks, N. (2001). Designer eggs: from improvement of egg composition to functional food. *Trends in Food Science & Technology*, 12(1), 7-16.

Tarnopolsky, M. (2000). Protein and amino acid needs for training and bulking up. *Burke, L. Deakin, V.(eds) Clinical Sports Nutrition*, 90-123.

Terjung, R. L., Clarkson, P., Eichner, E., Greenhaff, P. L., Hespel, P. J., Israel, R., Kraemer, W., Meyer, R., Spriet, L., & Tarnopolsky, M. (2000). American College of Sports Medicine roundtable. The physiological and health effects of oral creatine supplementation. *Medicine and science in sports and exercise*, 32(3), 706-717.

Tipton, K. D., & Wolfe, R. R. (2004). Protein and amino acids for athletes. *Journal of Sports Sciences*, 22(1), 65-79.

Tu, J., Yeoh, G. H., & Liu, C. (2007). Computational Fluid Dynamics: A Practical Approach: Elsevier Science.

Ummadi, M. S., & Curic-Bawden, M. (2010). Use of protein hydrolysates in industrial starter culture fermentations. Protein Hydrolysates in Biotechnology pp. 91-114): Springer.

van Loon, L. J., Saris, W. H., Verhagen, H., & Wagenmakers, A. J. (2000). Plasma insulin responses after ingestion of different amino acid or protein mixtures with carbohydrate. *The American journal of clinical nutrition*, 72(1), 96-105.

Weggemans, R. M., Zock, P. L., & Katan, M. B. (2001). Dietary cholesterol from eggs increases the ratio of total cholesterol to high-density lipoprotein cholesterol in humans: a meta-analysis. *The American journal of clinical nutrition*, 73(5), 885-891.

Whitehouse, A. S., Smith, H. J., Drake, J. L., & Tisdale, M. J. (2001). Mechanism of attenuation of skeletal muscle protein catabolism in cancer cachexia by eicosapentaenoic acid. *Cancer research*, 61(9), 3604-3609.

Wigmore, S. J., Ross, J. A., Stuart Falconer, J., Plester, C. E., Tisdale, M. J., Carter, D. C., & Ch Fearon, K. (1996). The effect of polyunsaturated fatty acids on the progress of cachexia in patients with pancreatic cancer. *Nutrition*, 12(1), S27-S30.

Xia, B., & Sun, D.-W. (2002). Applications of computational fluid dynamics (CFD) in the food industry: a review. *Computers and electronics in agriculture*, 34(1), 5-24.

Young, A. L., & Bass, I. S. (1995). Dietary Supplement Health and Education Act, The. *Food & Drug LJ*, 50, 285.

Zhang, Q., Ren, J., Zhao, H., Zhao, M., Xu, J., & Zhao, Q. (2011). Influence of casein hydrolysates on the growth and lactic acid production of Lactobacillus delbrueckii subsp. bulgaricus and Streptococcus thermophilus. *International Journal of Food Science & Technology*, 46(5), 1014-1020.

CHAPTER 2 - EFFECTS OF TEMPERAUTRE, pH, ENZYME-TO-SUBSTRATE RATIO, AND REACTION TIME ON DEGREE OF HYDROLYSIS OF EGG WHITE HYDROLYSATES

2.1 Introduction

Table eggs contain all nine essential amino acids (EAA) including histidine, isoleucine, leucine, lysine, methionine, phenylalanine, threonine, tryptophan and valine (Weggemans, Zock & Katan, 2001). Food proteins have been modified by enzymes for many years (Liu & Chiang, 2008). Enzymatic hydrolysis is a biological process that modifies the molecular conformation of native proteins to produce peptides with functional properties that can be used as additives in beverages, infant formulas, food texture enhancement and pharmaceutical ingredients (Pokora, Eckert, Zambrowicz, Bobak, Szołtysik, Dąbrowska et al., 2013). According to O'Donnell and Dornblaser (2002), amino acids and peptides (especially from soy and milk proteins) are gaining popularity in energy drinks and in other food applications due to their advantageous properties.

Certain egg white derived peptides may also play a role in controlling the development of hypertension and also have shown antioxidant properties (Davalos, Miguel, Bartolome & Lopez-Fandino, 2004; Miguel, López-Fandiño, Ramos & Aleixandre, 2005; Miguel, Recio, Gómez-Ruiz, Ramos & López-Fandiño, 2004). According to Park, Jung, Nam, Shahidi and Kim (2001), the use of protein hydrolysates with antioxidant activities may be advantageous in functional foods because they also provide other desired properties such as fat-and water-holding capacity, and emulsion capacity and stability.

Degree of protein hydrolysis (DH) is a key parameter for producing food protein hydrolysates because it defines the properties of the final product (Pokora, et al., 2013). A slight hydrolysis of proteins resulting in protein hydrolysates with DH values lower than 10% can modify the functionality of proteins (solubility, gelling, fat- and water-holding capacity, emulsion capacity and stability, and foaming capacity and stability) (Panyam & Kilara, 1996);

while, higher DH are desired for protein hydrolysates that are being used as protein supplements or in hypoallergenic foods in special medical diets (Pokora, et al., 2013).

According to Zheng, Shen, Bu and Luo (2008), response surface methodology (RSM) is an effective statistical method to optimize numerous process parameters. Several enzymatic hydrolysis processes has been successfully optimized by RSM (Fang, Zhao & Song, 2010; Ferreira, Duarte, Ribeiro, Queiroz & Domingues, 2009).

Egg white hydrolysates (EWH) have been produced using non-food grade enzymes and the process has been focused in producing hydrolysates with high antioxidant activity (Lin, Guo, You, Yin & Liu, 2012; Pokora, et al., 2013). So, the resulting hydrolysate may not be suitable for human consumption. Therefore, there is a lack of scientific literature regarding to the production of food-grade EWH which are a lactose-free source of high quality amino acids.

In the present study, egg whites were hydrolyzed using several food-grade proteases derived from *Bacillus licheniformis*, *Bacillus subtilis*, and *Aspergillus oryzae.* These food-grade proteases have a maximum activity at alkaline, neutral and acidic conditions, respectively. Therefore, the objectives of this study were to: (1) produce food-grade EWH powders using food-grade proteases, (2) determine the effect of reaction temperature, pH, enzyme-to-substrate ratio and reaction time on DH of EWH, (3) use a Central Composite Design (CCD) for RSM to obtain EWH with a maximum DH, and (4) determine the nutritional and physiochemical properties of EWH powders.

2.2 Materials and methods

2.2.1 Materials

Fresh, large, grade AA hen eggs were purchased from a local chain grocery store, in Baton Rouge, Louisiana. The eggs were stored at 4°C, and the storage time did not exceed three days.

Three commercial food-grade proteases from *Bacillus licheniformis*, *Bacillus subtilis*, and *Aspergillus oryzae* were obtained from Enzyme Development Corporation (New York, NY). All other analytical grade reagents were obtained from Sigma Aldrich (St. Louis, MO).

2.2.2 Proteolytic activity of proteases

The proteolytic activity of the food-grade proteases was determined following the method described by Merheb, Cabral, Gomes and Da-Silva (2007). A mixture of 5 mL of 0.65 (g/100g) casein solution and 5 mL (0.2 M) of sodium acetate buffer at pH 7.5 was prepared; then 50 mg of a food–grade enzyme powder were added. The reaction was carried out at 37°C for 10 min and stopped by the addition of a 5 mL of 110 mM trichloroactic acid (TCA) solution. Afterwards, 1 mL of distilled water was added and the solution was incubated at 37°C for another 10 min. After the second incubation time, the solution was filtered and 2 mL were mixed with 1 mL of Folin's reagent. The solution was heated again at 37°C for 30 min.; and the absorbance of final solution was then measured at 660 nm. Enzyme activity was determined from a standard curve prepared with a 1.1 mM tyrosine solution. The results were reported as Units/mg enzyme. One unit of enzyme activity (U) was defined as the amount in micromoles of tyrosine equivalents released from casein per minute.

2.2.3 Preparation of egg white hydrolysates (EWH)

Fresh egg whites (EW) were manually separated from egg yolks. Then, the moisture content of the EW was determined according to the official AOAC method 930.15 (AOAC, 1999). A 10±0.5 (g solids/100g) mixture containing 80g liquid egg white and 20g distilled water was prepared and homogenized using an ultra-shearing processor (OMNI, Ultrashear M, Omni International, Kennesaw, GA) for 5 min at 20,000 rpm, and then heated to 65°C in a water bath for 5 min to denature EW proteins. After heating, the mixture was cooled to room temperature.

Then, the pH of the mixture was adjusted to the require values using a 1 M citric acid and/or a 0.1 N NaOH solutions. Three EWH were prepared with food-grade proteases from *Bacillus licheniformis* (ALK), *Bacillus subtilis* (NEU), and *Aspergillus oryzae* (ACI). The enzyme-to-substrate ratio was standardized and the mixture was place in an incubator shaker at the required reaction temperature. In total four independent variables were investigated, including reaction temperature (°C) (***T***) (51.59, 55.00, 60.00, 65.00, 68.41 for ALK*;* 41.59, 45.00, 50.00, 55.00, 58.41 for NEU, and 26.59, 30.00, 35.00, 40.00, 43.41 for ACI), pH (***pH***) (7.32, 8.00, 9.00, 10.00, 10.70 for ALK, 5.32, 6.00, 7.00, 8.00, 8.68 for NEU; and 4.32, 5.00, 6.00, 7.00, 7.68 for ACI); enzyme-to-substrate ratio (U/g protein) (***[E:S]***) (79.57, 250.00, 500.00, 750.00, 920.43); and reaction time (min.) (***t***) (39.55, 60.00, 90.00, 120.00, 140.45). After the reaction time, the vessels containing the mixtures were heated to 85°C for 5 min. to inactivate the proteases. The soluble fraction of the mixture was then ultrafiltered using a 30 kDa cutoff membrane to produce HALK, HNEU, and HACI. Then, HALK, HNEU, and HACI were spray dried at 140°C inlet air temperature to produce DALK, DNEU, and DACI, respectively. Fresh egg whites were spray dried as a control (DEW). The production of EWH powders is shown in Fig. 2.1.

2.2.4 Experimental design and optimization experiments

The enzymatic hydrolysis was optimized using four independent variables including reaction temperature (*T*), pH (*pH*), enzyme-to-substrate ratio (*[E]:[S]*), and reaction time (*t*). The degree of protein hydrolysis (DH) was evaluated as the response variable (Y). Experimental design and planning was based on preliminary studies and enzymatic hydrolysis suggested by the enzyme manufacturer (Enzyme Development Corporation, New York, NY). The independent variables were optimized using a central composite design (CCD) containing five levels of each independent variable coded as –α, -1, 0, +1, +α. Where α value was calculated using Eq. 2.1:

$$\propto = F^{1/4} \quad (2.1)$$

Where, *F*= number of axial points (8). So, α=1.68

Correspondence among coded values and actual values of independent variables are summarized in Table 2.1 The five-level-four-variable CCD required 30 experiments, consisting of 16 factorial points, 8 axial points and 6 central points. The total number of experiments was determined by using Eq. 2.2.

$$N = 2^k + 2k + n_0 \quad (2.2)$$

Where, N = number of required experiments, k=number of independent variables, n_0=number of central point experiments.

The central point experiments were chosen to verify any change in the estimation procedure, as a measure of precision property. Each enzymatic experiment was run in triplicate. Experimental data was statistically analyzed using SAS software version 9.2 (SAS Institute Inc., Cary, NC, USA). The optimization data were fitted to a second-order polynomial equation (Eq. 2.3):

$$Y = \beta_{kO} + \sum_{i=1}^{4} \beta_{ki} X_i + \sum_{i=1}^{4} \beta_{kii} X_i^2 + \sum_{i=1}^{4} \sum_{j=i+1}^{4} \beta_{kij} X_i X_j \quad (2.3)$$

Where, Y = degree of protein hydrolysis (DH); β_{kO}, β_{ki}, β_{kii}, $\beta_{kij}$are the regression coefficients for the intercept, linear, quadratic, and interaction terms respectively. X_i and X_j are the independent variables.

Three-dimensional (3D) and contour plots were obtained by using the fitted model that establishes the relationship between the independent and response variables. The plots were built using the response value along with two independent variables, while the rest of the variables were fixed at their 0 level (center values of the testing ranges).

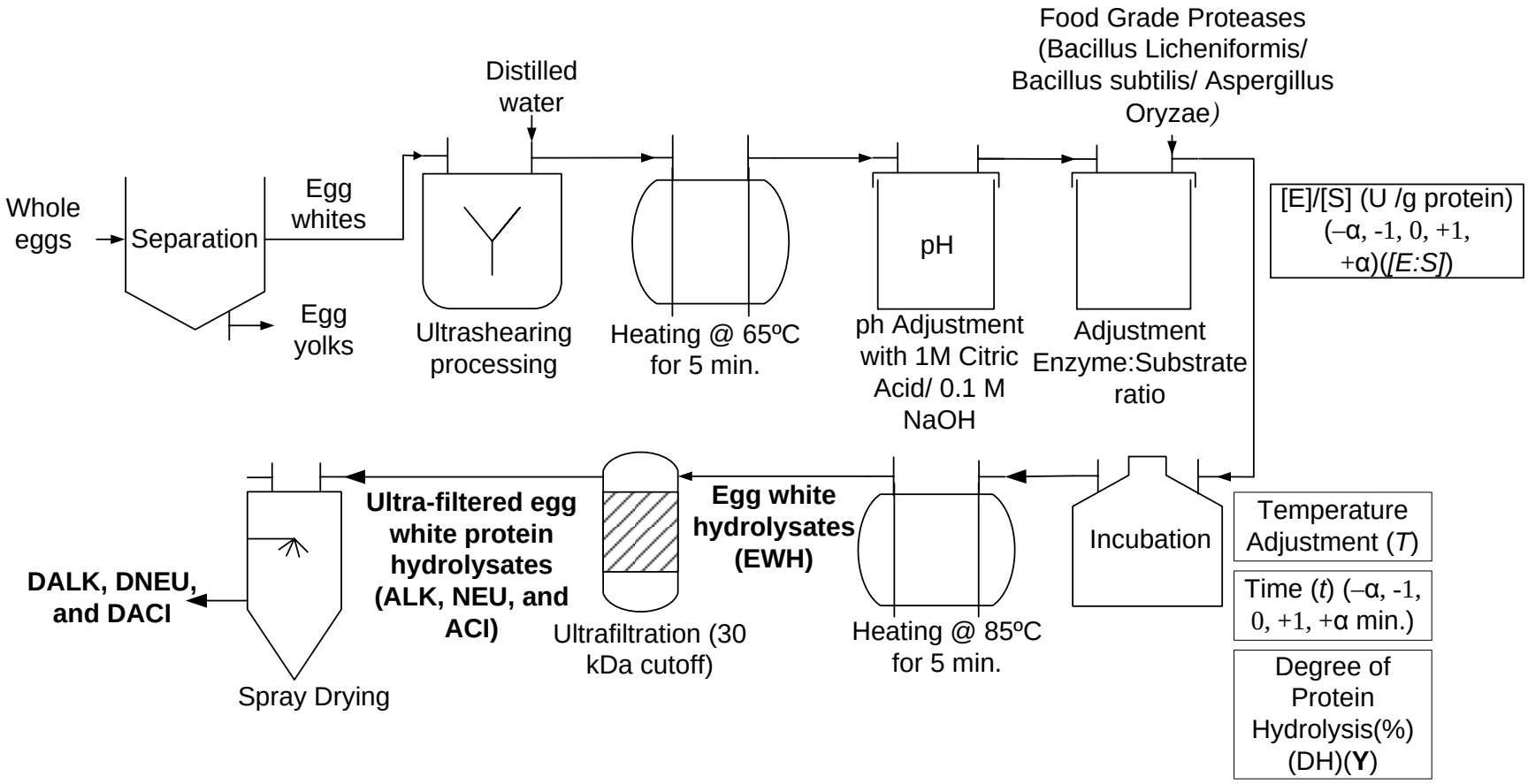

Fig. 2.1 - Production of dried egg white hydrolysates powders using food-grade proteases

Table 2.1 - Actual and coded values of independent variables at their levels in the Central Composite Design (CCD)

EWH	Protease source	Independent variable	Coded level				
			-α	**-1**	**0**	**1**	**+α**
HALK	*Bacillus licheniformis*	*T* (°C)	51.59	55	60	65	68.41
		pH	7.32	8	9	10	10.7
		[E:S] (U/g protein)	79.57	250	500	750	920.43
		t (min)	39.55	60	90	120	140.45
HNEU	*Bacillus subtilis*	*T* (°C)	41.59	45	50	55	58.41
		pH	5.32	6	7	8	8.68
		[E:S] (U/g protein)	79.57	250	500	750	920.43
		t (min)	39.55	60	90	120	140.45
HACI	*Aspergillus Oryzae*	*T* (°C)	26.59	30	35	40	43.41
		pH	4.32	5	6	7	7.68
		[E:S] (U/g protein)	79.57	250	500	750	920.43
		t (min)	39.55	60	90	120	140.45

EWH= egg white hydrolysates, HALK = EWH produced with proteases from *Bacillus licheniformis*, HNEU= EWH produce with proteseas from *Bacillus subtilis*, HACI = EWH produced with proteases from *Aspergillus oryzae*.

2.2.5 Degree of hydrolysis (DH)

The DH of the EWH was quantified using an improved method based on the reaction of primary amino groups with o-phthaldialdehyde (OPA) described in Nielsen, Petersen and Dambmann (2001). The OPA reagent was prepared by mixing 160 mg of OPA in 4 mL of ethanol, this solution was combined with another solution prepared with 7.62 g di-Na-tetraborate decahydrate, 200 mg Na-dodecyl-sulfate (SDS) and 150 mL distilled water. Then, 176 mg dithiothreitol (DTT) was added and the final mixture was made up to 200 mL with distilled water. A standard was prepared with 50 mg of serine in 500 mL distilled water. A sample solution was also prepared with 1g of liquid hydrolysates in 100 mL of distilled water. The OPA essay was carried out by adding 400 µL of the sample solution to 3 mL of OPA reagent and the mixture was vortexed for 5 s, then the absorbance of the mixture was taken after 2 min at 340 nm

using a spectrophotometer. Additionally, absorbance was recorded for solutions prepared with 400 µL standard serine solution and 3 mL of OPA. Blank measurements were carried out with distilled water. The degree of protein hydrolysis (DH) was calculated using Eq. 2.4

$$DH = \frac{h}{h_{tot}} * 100 \quad (2.4)$$

Where, h_{tot} is the total number of peptide bonds per protein equivalent (8); and *h* is the number of hydrolyzed bonds calculated using Eq. 2.5

$$h = \frac{(serine - NH_2) - \beta}{\alpha} \text{ meqv / g protein} \quad (2.5)$$

Where, α and β are constants for which the values are 1 and 0.4, respectively (Nielsen, Petersen & Dambmann, 2001). *Serine-NH_2* (meqv serine NH_2/ g protein) was determined using Eq. 2.6

$$Serine - NH_2 = \frac{OD_{sample} - OD_{blank}}{OD_{s\tan dard} - OD_{blank}} * \frac{0.9516 meqv}{L} * 0.1 * 100 * 1 * P \quad (2.6)$$

Where, *P* is the protein content (g/100g) in the sample.

2.2.6 Proximate composition of DALK, DNEU and DACI

Moisture content, total lipids, crude protein and ash were determined for DEW, DALK, DNEU and DACI. Moisture content was measured according to the AOAC official method 930.15 (AOAC, 1999). Lipids were quantified according to the official AOAC method (AOAC, 2000). A 10 g sample was dissolved in 500 mL of 2:1 chloroform:methanol solution and filtered. The filtrate was mixed with 100 mL of a 0.66% sodium chloride solution and subsequently centrifuged. The chloroform layer containing the lipids was evaporated under vacuum using a rotary evaporator at 40ºC. Crude protein content was determined according to AOAC official method 992.15 (AOAC, 2006) using a Perkin Elmer Nitrogen Analyzer (Model 2410, Perkin Elmer Instruments, Norwalk, CT). The crude protein (g/100g) was reported as 6.25 times the

nitrogen content (g/100g). Ash content was determined according to the AOAC official method 942.05 (AOAC, 1999). All of the determinations were carried out in triplicate.

2.2.7 Total amino acid and free amino acid analysis

The amino acid analysis of DEW, DALK, DNEU and DACI was conducted at the Louisiana State University - Agricultural Center (LSU AgCenter) Biotechnology Lab (Baton Rouge, LA). For total amino acid determination, hydrolysis of the samples were carried out by adding 1 mL of 6 N HCL to a 2 mg of powder; the hydrolysis was performed for 17 h at 110°C. Afterwards, 20 uL of this sample was mixed with 40 uL of 0.2 mM Nle (norleucine) solution and 940 uL of sodium azide. Total amino acids were quantified using a Dionex AAA-ICS300 Chromatography System configured for AAA-Direct equipped with an ED50 electrochemical detector with AAA-Certified disposable gold working electrode and combination pH/Ag/AgCl reference electrode in the pH mode. A microbore anion exchange column (AminoPac PA10 2x250 mm) with a ternary gradient of deionized water, 0.25 M sodium hydroxide and 1.0 M sodium acetate was used as separation device. The flow rate of the eluents was set at 0.25 mL/min. Free amino acids in the samples were quantified as described above; however, the hydrolysis step was skipped.

2.2.8 Computation of chemical score

To determine the nutritional value of DEW, DALK, DNEU and DACI powders; it is necessary to estimate their chemical score; which is the ratio of the amount of an essential amino acid present in sample to the amount of the essential amino acid present in the standard protein as described by Ovissipour, Kenari, Motamedzadegan and Nazari (2012). So, the chemical score was estimated using Eq. 2.7 as follows:

$$\text{Chemical score} = \frac{\text{EAA in sample (g/100 g)}}{\text{EAA in standard protein (g/100 g)}} \qquad (2.7)$$

Where, EAA is the essential amino acid.

2.2.9 Protein efficiency ratio (PER)

The protein efficiency ratio (PER) indicates the nutritional value of proteins. In this study, PER values were estimated by using Eq. 2.8; 2.9, and 2.10 as described in Šližytė, Daukšas, Falch, Storrø and Rustad (2005) and Lee, Elliott, Rickansrud and Hagberg (1978) as follows:

$$PER = -0.468 + 0.45[LEU] - 0.105[TYR] \quad (2.8)$$

$$PER = -1.816 + 0.435[MET] + 0.78[LEU] + 0.211[HIS] - 0.944[TYR] \quad (2.9)$$

$$PER = 0.08084[\sum AA_7] - 0.1094 \quad (2.10)$$

Where, $\sum AA_7$=threonine + valine + methionine + isoleucine + leucine + phenylalanine + lysine

And the amount of amino acids is expressed as g AA/100g protein.

2.2.10 SDS-PAGE

Samples were prepared by adding 20 µL tracking dye solution (Bio-Rad Tricine sample buffer with β-mercaptoethanol) to 20 µL liquid sample (previously prepared by dissolving 1g of sample in 10 mL distilled water) and heated to 100°C for 5 min.

The samples were then centrifuged for 1 min. at 10,000 x g. SDS-PAGE was performed by loading 20 µL of the prepared sample on 4 – 20% gradient polyacrylamide precise protein gels (Thermo scientific, Rockford IL). Gels were stained overnight in 0.1% Coomassie Brillian Blue G-250 with 50% distilled water, 40% methanol, 10% acetic acid and de-stained in distilled water.

2.2.11 Antioxidant activity

2.2.11.1 Ability to scavenge 2,2-diphenyl-1-picryhydrazyl (DPPH) free radicals

To determine the DPPH radical-scavenging activity of the EWH powders, the methods described in Klompong, Benjakul, Kantachote and Shahidi (2007) and Pokora, et al. (2013) were followed.

EWH powders were dissolved in distilled water to obtain a concentration of 40 mg protein/mL. Then, 4 mL of sample solution was mixed with 1.0 mL of 0.2 mM DPPH and incubated for 30 min at room temperature. Absorbance of the mixture was taken at 517 nm using a spectrophotometer. Also, absorbance of a control solution (non-containing EWH powders) was recorded in the same manner. DPPH radical-scavenging activity was calculated according to the Eq. 2.11.

$$\text{DPPH radical-scavenging activity (\%)} = \left(1 - \frac{A_{517}sample}{A_{517}control}\right) * 100 \qquad (2.11)$$

2.2.11.2 Reducing power

Reducing power of the EWH powders were determined by following the method described in Klompong, Benjakul, Kantachote and Shahidi (2007). A sample solution containing 40 mg protein/mL was again prepared and 0.5 mL of the this solution was mixed with 2.5 mL of 0.2 M phosphate buffer (pH 6.6) and 2.5 mL of 1 (g/100g) potassium ferricyanide. The mixture was incubated at 50°C for 20min and 2.5 mL of 10(g/100g) of trichloroacetic acid was added after the incubation time.

Then, the mixture was centrifuged at 956 x *g* for 10 min. Finally, 2.5 mL of the upper layer of solution was mixed with 2.5 mL of distilled water and 2.5 mL of 0.1 (g/100g) ferric chloride and the absorbance was recorded at 700nm. Higher absorbance values mean higher reducing power of the EWH powders.

2.2.12 Mineral analysis of DEW, DALK, DNEU and DACI

The mineral profile analysis was determined by the acid digestion method involving microwave technology (CEM microwave, MDS-2000, CEM Corp., Matthews, N.C., U.S.A.). Approximately 0.2 g of sample was placed in a vessel and 6 mL HNO3 were added. Then, the sealed vessel was heated until digestion was completed. The samples were cooled for 10 min.

The inductively couple argon plasma system (Model CIROS, SPECTRO Analytical Instruments, Kleve, Germany) was utilized to determine the mineral profile of the samples.

2.2.13 Statistical analysis

Statistical analysis of all of enzymatic optimization experiments were carried out by RSM using a CCD. The optimization experiment was conducted in triplicates. The maximum DH was determined by using a ridge analysis due to the presence of saddle points. All data was statistically analyzed by SAS software version 9.2 (SAS Institute Inc., 2008). Mean values and standard deviations from triplicate analysis were reported. Analysis of Variance (ANOVA) and Tukey's studentized range test were carried out to determine differences among treatments at the significant level of $P<0.05$.

2.3 Results and discussion

2.3.1 Optimization of hydrolysis parameters

In this study, the RSM using a CCD has been used to optimize and understand the relationship between the importance of the hydrolysis parameters (*T, pH, [E:S]*, and *t*) on the DH of EWH. In total, 30 experimental runs were carried out with different levels of the four independent variables to produce HALK, HNEU and HACI. Experimental results of the DH as a response of the independent variables are presented in Table 2.2. Although RSM is widely used to optimize several processes; this work represents the first statistical attempt to study the effect hydrolysis parameters on the DH of egg white proteins using novel food-grade proteases. Furthermore, the RSM has allowed reduction in the number experiment runs for the optimization process and to quantify the individual effect of each independent variable and their possible interaction. Table 2.2 also contains the estimated maximum DH value calculated by the resulting RSM model which regression coefficients are shown in Table 2.3.

A quadratic polynomial equation was proposed to describe the mathematical relationship between the response and the independent variables. The fit of the model was evaluated by the determination of the R^2 coefficient.

According to the ANOVA table (Table 2.4), linear, quadratic and the interaction of the regression coefficients were highly significant ($P<0.05$). Therefore, all of the RSM regression models for HALK, HNEU, and HACI were also highly significant ($P<0.05$). Highly significant RSM models are statistically valid (Fang, Zhao & Song, 2010). RSM models had an R^2 of 0.9348, 0.9209, and 0.8449 for HALK, HNEU, and HACI, respectively. Hence, more than the 84% of the variation could be explained by the RSM models. The results also indicated that a lack of fit tests, which indicates the fitness of the RSM models, were not significant; therefore, RSM models were sufficiently accurate to predict the DH for any combination of experimental independent variables within the ranges studied.

High correlation of experimental results with those predicted by RSM models for enzymatic hydrolysis have been previously reported (Bhaskar, Benila, Radha & Lalitha, 2008; Ovissipour, Kenari, Motamedzadegan & Nazari, 2012). According to the results, the *T*, *pH*, and *[E:S]* had a significantly ($p<0.05$) effect on the DH of HALK, HNEU, and HACI (Table 2.4). Meanwhile the *t* had a significantly ($P<0.05$) effect only in HALK and HACI. According Guerard, Guimas and Binet (2002), a reduction in DH is observed (in some hydrolysis cases) by increasing reaction time (after certain level) which may be the result of the formation of reaction products at high DH that may limit protease activity, reduce of the number of peptide bonds available for hydrolysis, and produce enzyme inhibition and deactivation. Higher values of the optimal levels of *T*, *pH*, and *[E:S]* results in a decrease in DH due to denaturation of enzymes and reduction of their biological activity (Ovissipour, Kenari, Motamedzadegan & Nazari, 2012).

Table 2.2 – Design and results for the CCD.

Run	*T*	*pH*	*[E:S]*	*t*	DH (%) (Y)					
					HALK		HNEU		HACI	
	Temp.(°C)	pH	(E:S)(U/g protein)	Time (min.)	Experiment	Predicted	Experiment	Predicted	Experiment	Predicted
1	-1	-1	-1	-1	45.77±0.16	43.09	41.23±0.70	41.90	38.67±1.47	36.96
2	1	-1	-1	-1	26.98±0.37	28.74	49.46±1.16	48.08	57.13±1.47	61.32
3	-1	1	-1	-1	45.61±0.89	41.70	43.88±0.80	42.84	42.04±1.69	40.20
4	1	1	-1	-1	50.89±1.67	50.49	49.73±2.27	47.59	43.16±1.04	36.66
5	-1	-1	1	-1	45.98±1.12	48.45	53.18±0.70	51.84	41.31±0.78	41.63
6	1	-1	1	-1	34.02±0.74	29.86	49.28±1.01	48.90	74.81±0.61	69.21
7	-1	1	1	-1	47.10±0.09	45.89	43.00±1.34	43.05	44.14±1.54	46.06
8	1	1	1	-1	49.66±0.88	50.46	38.21±1.36	38.69	49.76±0.66	45.73
9	-1	-1	-1	1	58.79±0.09	57.61	39.37±0.96	38.87	38.18±0.74	44.31
10	1	-1	-1	1	52.92±0.37	49.73	47.21±0.65	45.27	83.65±1.47	78.04
11	-1	1	-1	1	52.28±0.67	52.04	43.08±1.16	41.57	41.65±0.22	43.55
12	1	1	-1	1	70.16±1.04	67.31	45.22±0.81	46.54	47.61±0.73	49.39
13	-1	-1	1	1	70.32±0.81	66.32	50.97±1.07	51.22	52.44±1.34	55.25
14	1	-1	1	1	50.68±2.27	54.21	47.50±0.90	48.51	88.25±0.17	92.20
15	-1	1	1	1	61.73±0.09	59.59	42.82±1.06	44.18	57.77±0.08	55.68
16	1	1	1	1	72.35±0.16	70.63	42.61±0.43	40.05	66.70±0.08	64.73
17	+α	0	0	0	39.84±0.58	41.28	46.72±1.34	49.03	52.20±1.12	59.99
18	-α	0	0	0	38.67±0.24	44.06	47.07±1.92	47.32	36.71±1.38	31.89
19	0	+α	0	0	60.04±0.48	64.72	37.19±0.49	38.60	61.43±0.93	67.48
20	0	-α	0	0	49.93±0.91	52.10	43.75±0.83	44.91	90.91±1.68	87.84
21	0	0	+α	0	41.75±1.17	43.33	48.93±0.88	48.56	49.49±1.10	52.46
22	0	0	-α	0	30.79±1.31	36.04	42.73±0.63	45.66	35.51±1.30	35.63
23	0	0	0	+α	68.58±1.67	73.35	50.07±0.28	50.59	81.93±0.75	77.44
24	0	0	0	-α	42.11±0.86	44.18	49.95±1.02	51.99	47.81±0.96	55.28
25	0	0	0	0	48.53±0.86	47.18	52.51±0.99	52.22	71.56±1.16	69.85
26	0	0	0	0	48.17±0.69	47.18	43.61±0.49	52.22	71.01±1.52	69.85
27	0	0	0	0	47.99±1.64	47.18	52.02±0.56	52.22	69.69±1.13	69.85
28	0	0	0	0	49.14±0.48	47.18	52.68±0.79	52.22	69.63±1.04	69.85
29	0	0	0	0	47.93±1.55	47.18	53.25±0.79	52.22	70.71±0.42	69.85
30	0	0	0	0	49.26±0.69	47.18	52.43±1.10	52.22	69.33±0.65	69.85

See Table 2.1 for a brief explanation of EWH, HALK, HNEU, and HACI.

Table 2.3 - Regression coefficients of the full RSM models to estimate DH in HALK, HNEU, and HACI

	HALK		**HNEU**		**HACI**	
Parameter	**Estimate**	**Pr>|t|**	**Estimate**	**Pr>|t|**	**Estimate**	**Pr>|t|**
Intercept	741.363	0.002	-365.385	<.0001	-581.718	<.0001
T	-3.477	0.503	7.203	0.003	31.978	<.0001
pH	-133.581	<.0001	57.180	<.0001	11.971	0.548
[E:S]	0.102	0.123	0.184	<.0001	0.118	0.058
t	-0.920	0.106	-0.109	0.619	0.015	0.976
*T*T*	-0.064	0.123	-0.057	0.008	-0.338	<.0001
*pH*T*	1.158	<.0001	-0.071	0.459	-1.395	0.000
*pH*pH*	3.978	0.001	-3.710	<.0001	2.767	0.058
*[E:S]*T*	-0.001	0.301	-0.002	0.000	0.001	0.564
*[E:S]*pH*	-0.001	0.773	-0.010	<0.001	0.001	0.831
[E:S][E:S]*	0.000	0.016	0.000	<0.002	0.000	<.0001
*t*T*	0.011	0.122	0.000	0.905	0.016	0.106
*t*pH*	-0.035	0.307	0.015	0.366	-0.033	0.475
t[E:S]*	0.000	0.409	0.000	0.219	0.000	0.268
*t*t*	0.005	0.001	0.000	0.489	-0.001	0.374

See Table 2.1 for a brief explanation of HALK, HNEU, and HACI.

2.3.2 Analysis of the response surfaces

The RSM models allowed the prediction of the effect of the independent variables (*T, pH, [E:S]*, and *t*) on the response (DH). The relationship between independent and response variables is illustrated in 3D graphs of the response surfaces and 2D contour plots generated by the RSM models for DH (Fig. 2.2 for HALK, Fig. 2.3 for HNEU, and Fig. 2.4 for HACI). Moreover, the RSM analysis demonstrated a saddle point as the stationary point for all of the EWH treatments; hence, a ridge analysis was performed to reveal the critical levels of the independent variables that may produce the maximum DH (Table 2.4).

The maximum response DH was obtained at alkaline, neutral and acid conditions for the production of HALK, HNEU, and HACI. Also, the optimum reaction temperature and pH for each of the proteases was similar to those suggested by the manufacturer.

Table 2.4 – ANOVA table of DH affected by temperature, pH, [E:S] ratio and reaction time during optimization experiment

	Source	DF	Sum of square	Mean square	F value	Pr>F	Critical values
EWH	**Regression**						
HALK	Linear	4	2049.18	0.57	32.86	<.0001	
	Quadratic	4	678.98	0.19	10.89	0.0002	
	Crossproduct	6	625.77	0.17	6.69	0.0013	
	Total model	14	3353.93	0.93	15.37	<.0001	
HNEU	Linear	4	102.19	0.15	7.24	0.0019	
	Quadratic	4	325.96	0.49	23.08	<.0001	
	Crossproduct	6	188.65	0.28	8.9	0.0003	
	Total model	14	616.80	0.92	12.48	<.0001	
HACI	Linear	4	3769.69	0.48	31.78	<.0001	
	Quadratic	4	2721.03	0.35	22.94	<.0001	
	Crossproduct	6	933.18	0.12	5.24	0.0043	
	Total model	14	7423.90	0.94	17.88	<.0001	
	Residual						
HALK	Lack of fit	10	202.15	20.22	3.19	0.089	
	Pure error	5	31.68	6.34			
	Total error	15	233.83	15.59			
HNEU	Lack of fit	10	36.28	3.63	1.09	0.137	
	Pure error	5	16.69	3.34			
	Total error	15	52.96	3.53			
HACI	Lack of fit	10	400.81	40.08	4.55	0.072	
	Pure error	5	44.02	8.80			
	Total error	15	444.83	29.66			
	Factors						
HALK	Temp.(°C) (*T*)	5	652.19	130.44	8.37	0.0006	61.54
	pH (*pH*)	5	1117.86	223.57	14.34	<.0001	9.66
	[E:S](U/g prot.) (*[E:S]*)	5	246.71	49.34	3.17	0.0379	537.96
	Time (min.) (*t*)	5	1972.00	394.40	25.3	<.0001	135.28
HNEU	Temp.(°C) (*T*)	5	124.21	24.84	7.04	0.0014	45.81
	pH (*pH*)	5	400.47	80.09	22.68	<.0001	6.35
	[E:S](U/g prot.)(*[E:S]*)	5	253.25	50.65	14.34	<.0001	825.19
	Time (min.) (*t*)	5	14.45	2.89	0.82	0.555	92.41
HACI	Temp.(°C) (*T*)	5	3555.56	711.11	23.98	<.0001	38.26
	pH (*pH*)	5	1715.11	343.02	11.57	0.0001	4.59
	[E:S](U/g prot.)(*[E:S]*)	5	1942.17	388.43	13.1	<.0001	547.25
	Time (min.) (*t*)	5	1106.94	221.39	7.47	0.0011	108.51

See Table 2.1 for a full description of EWH, HALK, HNEU and HACI.

The ridge analysis also demonstrated that an increase in DH is achieved by increases in *T*, *pH*, *[E:S]*, and *t* for the production of HALK. In the case of enzymatic hydrolysis of HNEU, decreasing *T*, *pH*, and *t* (after certain level) resulted in higher DH. Meanwhile, decreasing *pH*

and increasing *T*, *[E:S]*, and *t* (after certain level) resulted in an increase in DH for the enzymatic hydrolysis of HACI. A strong dependence on reaction temperature, pH, enzyme activity, and reaction time for enzymatic hydrolysis of food proteins has been reported by Bhaskar, Benila, Radha and Lalitha (2008).

To create the 3D graphs, two independent variables were kept constant at a fixed value (coded value of 0); since only two independent variables could be plotted against the response variable (DH). For HALK, it was observed that the variables *pH*, *[E:S]*, and *t* had a clear quadratic effect on the response; meanwhile, the variable *T* showed a more linear effect on the response (Fig. 2.2). The ridge analysis revealed that the maximum predicted value of DH was around 74.63%. HALK produced using the critical values of the hydrolysis parameters (obtained by the RSM) had a DH of 69.18%. In the case of hydrolysis for HNEU, the independent variables *T*, *pH*, and *[E:S]* presented a quadratic effect; while the independent variable *t* had a more linear effect over the response (Fig. 2.3). The maximum predicted value of DH is around 52.88% obtained by the ridge analysis; meanwhile, experimental value of DH at optimum conditions for NEU was 49.78%. The effect of the independent variables for HACI is presented in Fig. 2.4. It was observed that the variables *T* and *[E:S]* had a quadratic effect; meanwhile, *pH* and *t* showed a linear effect over the response. The ridge analysis demonstrated that the maximum predicted value of DH in HACI was around 98.25%; however, experimental results showed that HACI had a DH of 92.28 % at optimum conditions obtained by RSM.

Zheng, Shen, Bu and Luo (2008) has reported a maximum DH of 32% in whey protein hydrolysates using alcalase from *Bacillus licheniformis*. However, the scope of their study was to obtain hydrolysates with the maximum antigenicity properties. In another study conducted by Pokora, et al. (2013), a DH of 20.9% is reported in protein hydrolysates using egg white by-

products left after the extraction of lysozyme and cystatin (from egg white) and a non-food grade protease from *Bacillus amyloliquefaciens* (highest activity at neutral pH conditions). Other authors have reported DH of egg white hydrolysates of 95.8, 95.3, and 79.9% using non-food grade trypsin, chymotrypsin, and elastase, respectively (Graszkiewicz, Zelazko & Trziszka, 2010). Previous studies were aimed at producing peptides with high antioxidant activity. Van der Plancken, Van Remoortere, Indrawati, Van Loey and Hendrickx (2003) reported a DH of 6.65% in egg white hydrolysates after 10 min. using a non-food grade mixture of trypsin and α-chymotrypsin. They also found that a heat-induced denaturation of egg white proteins enhances the DH. High DH (>10%) is important in protein hydrolysates which intended used are in protein supplements, hypoallergenic food and/or special medical diets (Pokora, et al., 2013).

2.3.3 Proximate composition

Proximate composition of EWH powders is shown in Table 2.5. EWH powders had similar moisture content. Also, all of the EWH powders had a high crude protein content (> 79 g/100 powder); however, DEW showed a significantly higher ($p<0.05$) protein content than the rest of the powders. This may be due to amino acid degradation during hydrolysis. In contrast, DNEU and DACI had a significantly ($p<0.05$) higher ash content compared to those of DEW and DALK. This may be the result of the addition of proteases, citric acid and/or NaOH to adjust the pH during hydrolysis. Meanwhile, fat content remained constant in all of the EWH powders. The results are similar to those reported by (AEB, 1999). The fat content in all of the EWH powders was around 2.35 – 2.66 (g/100 g powder). According to Friedman (1996), proteins are essential in the human's diet and their basic function is to supply adequate amounts of amino acids. The recommended daily allowance (RDA) for protein in the USA is 0.8 to 0.9 g/kg body weight/day; however, protein requirements for athletes can be 50 to 100% higher (Tarnopolsky, 2000).

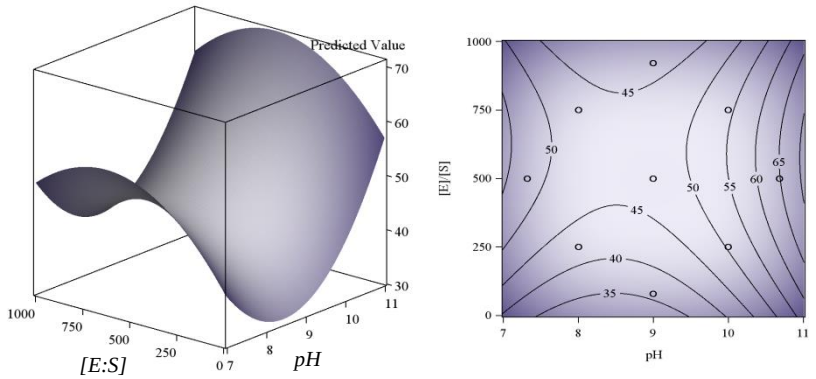

Fixed at: Time (min.)=90, Temperature(°C)=60

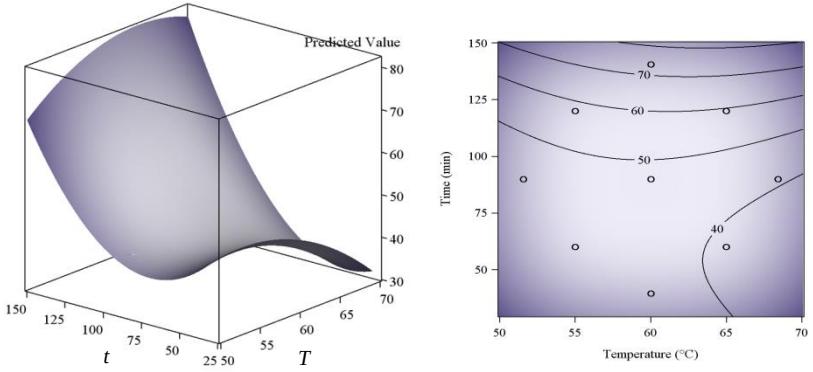

Fixed at: [E:S]=500, pH=9

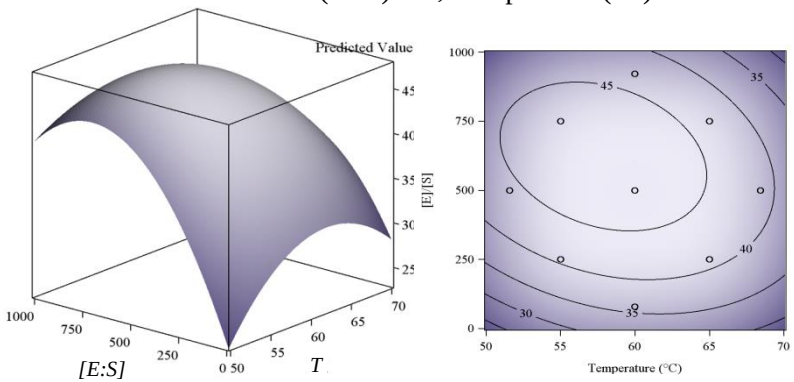

Fixed at: Time (min.)=90, pH=9

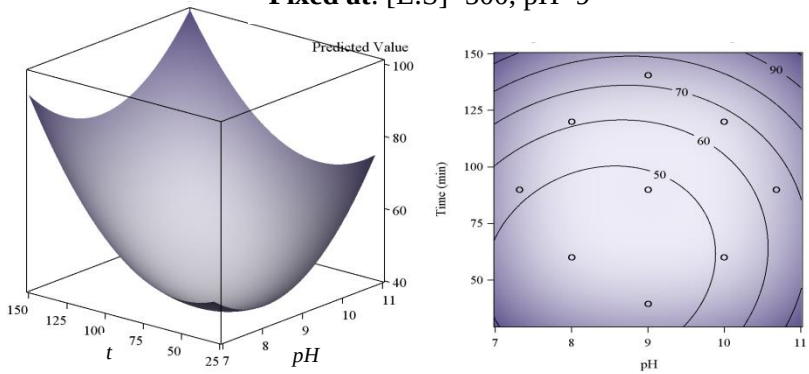

Fixed at: [E:S]=500, Temperature(°C)=60

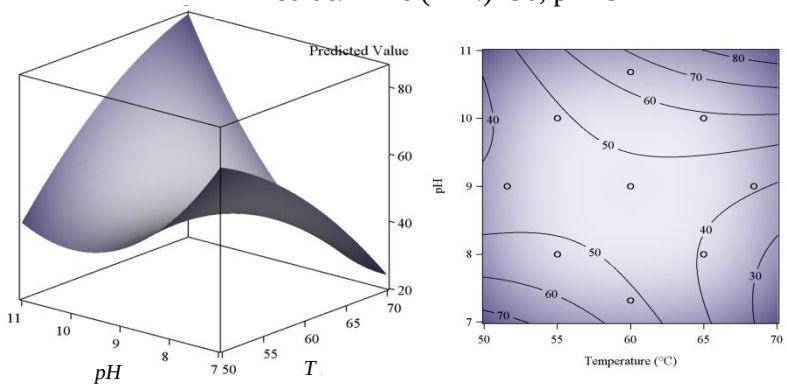

Fixed at: Time (min.)=90, [E:S]=500

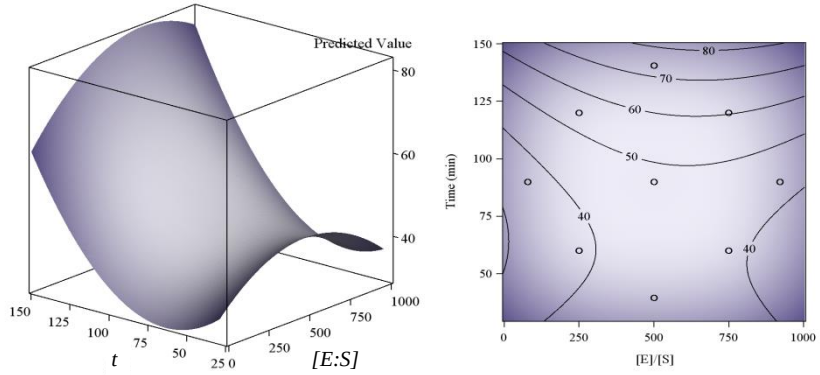

Fixed at: pH=9, Temperature(°C)=60

Fig. 2.2 - Response surface (3D) and contour plots (2D) displaying the effect of two variables on degree of degree of protein hydrolysis (DH) using proteases from *Bacillus licheniformis* to produce HALK.

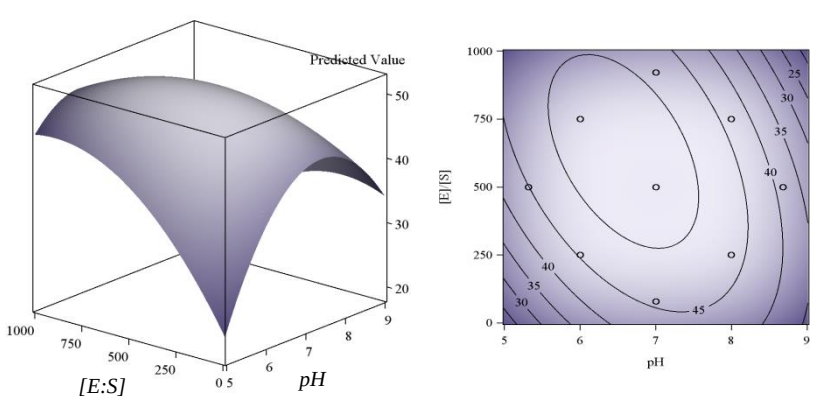

Fixed at: Time (min.)=90, Temperature(°C)=50

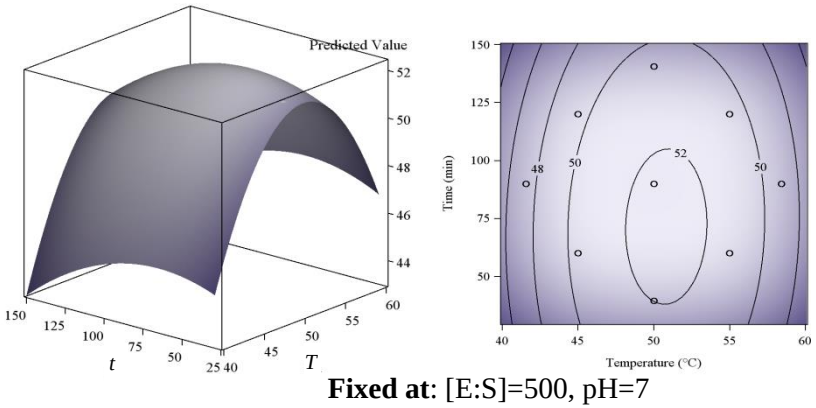

Fixed at: [E:S]=500, pH=7

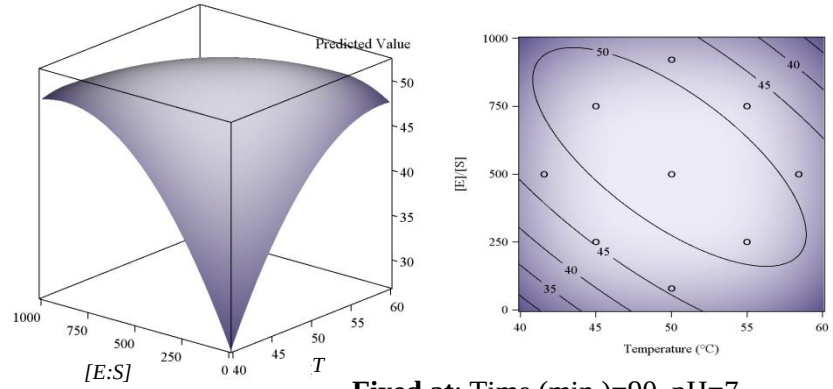

Fixed at: Time (min.)=90, pH=7

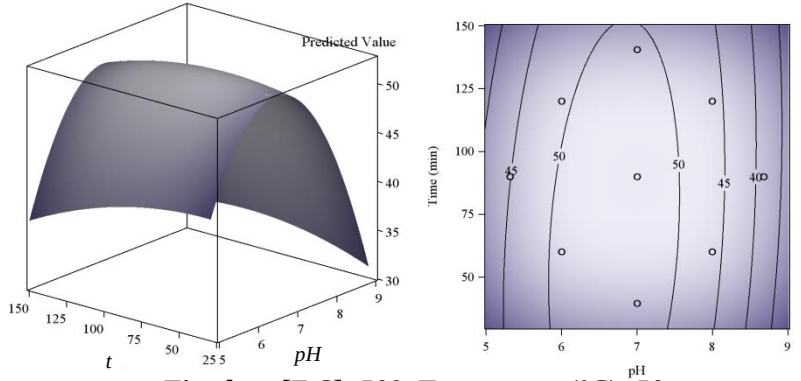

Fixed at: [E:S]=500, Temperature(°C)=50

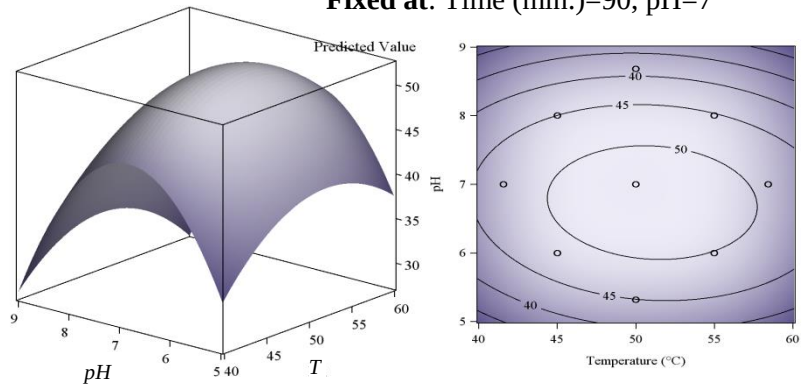

Fixed at: Time (min.)=90, [E:S]=500

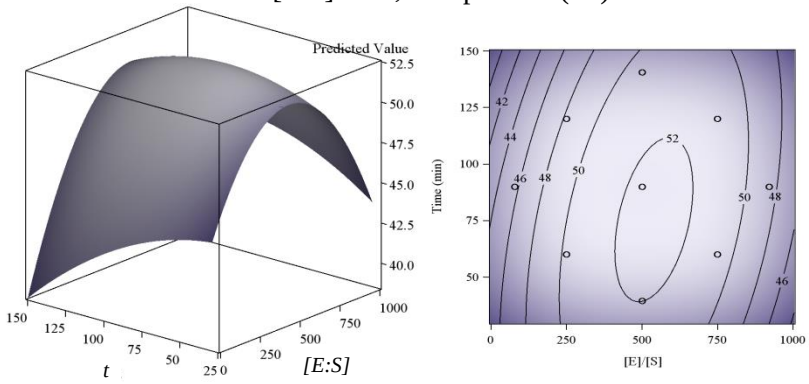

Fixed at: pH=7, Temperature(°C)=50

Fig. 2.3 - Response surface (3D) and contour plots (2D) displaying the effect of two variables on degree of degree of protein hydrolysis (DH) using proteases from *Bacillus subtilis* to produce HNEU.

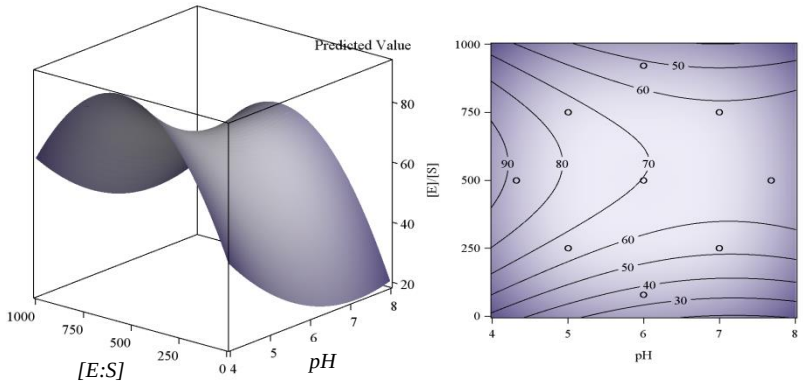

Fixed at: Time (min.)=90, Temperature(°C)=35

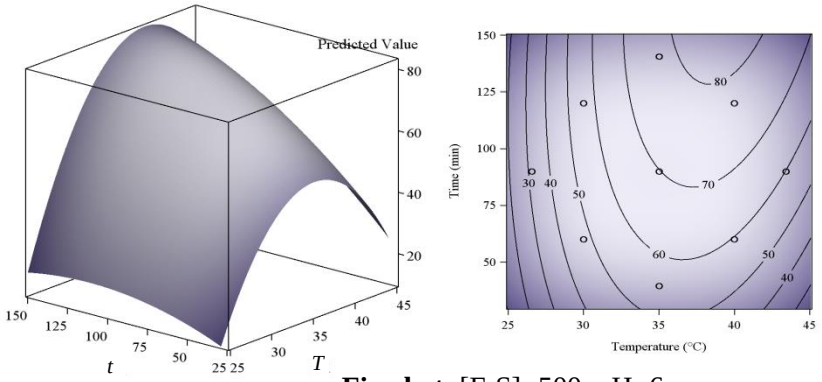

Fixed at: [E:S]=500, pH=6

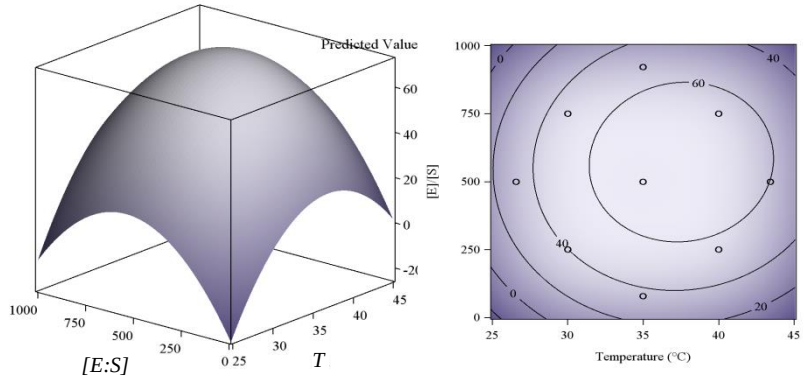

Fixed at: Time (min.)=90, pH=6

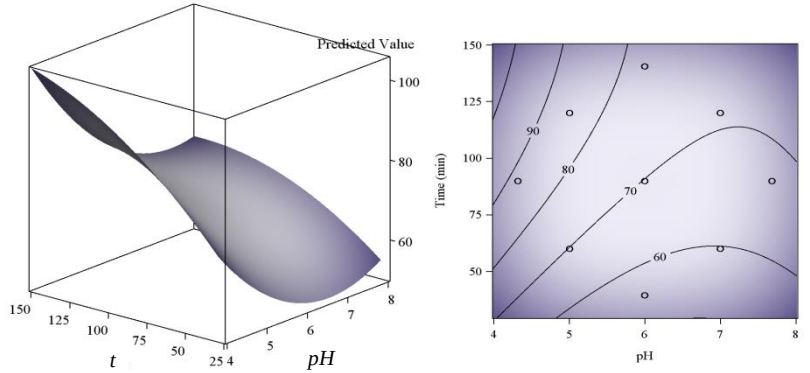

Fixed at: [E:S]=500, Temperature(°C)=35

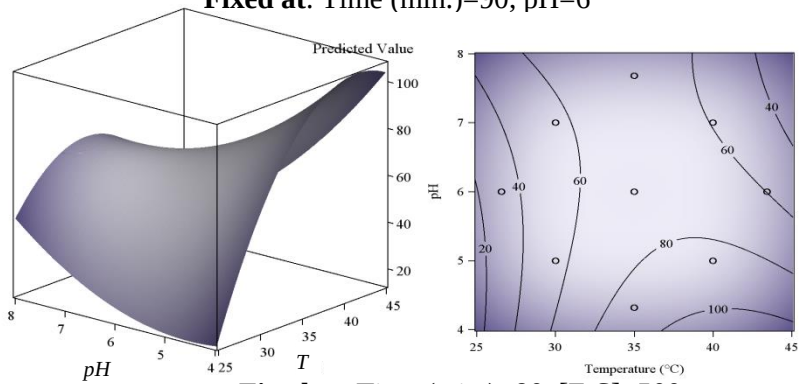

Fixed at: Time (min.)=90, [E:S]=500

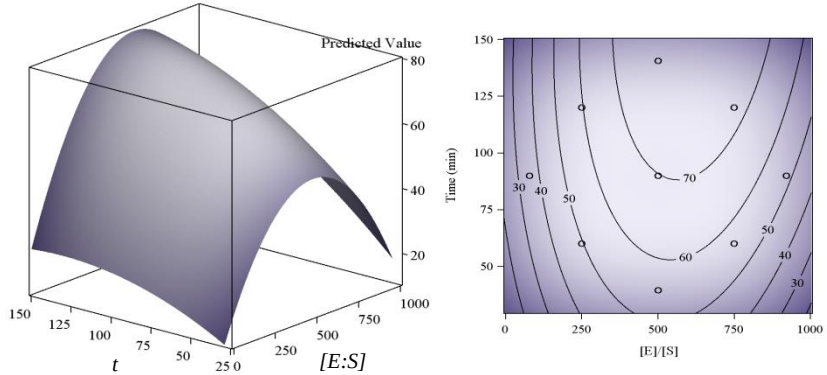

Fixed at: pH=6, Temperature(°C)=35

Fig. 2.4 - Response surface (3D) and contour plots (2D) displaying the effect of two variables on degree of degree of protein hydrolysis (DH) using proteases from *Aspergillus oryzae* to produce HACI.

Table 2.5 - Proximate composition of the egg white hydrolysates*

	DEW	DALK	DNEU	DACI
Moisture (g/100 g solids)	8.01±0.13[a]	8.20±0.16[a]	8.14±0.11[a]	8.19±0.15[a]
Protein (g/100 g solids)	82.97±0.06[a]	82.42±0.08[b]	80.42±0.10[c]	79.14±0.13[d]
Fat (g/100 g solids)	2.35±0.09[a]	2.39±0.21[a]	2.66±0.14[a]	2.62±0.14[a]
Ash (g/100g solids)	6.27±0.11[c]	6.33±0.07[c]	6.70±0.14[b]	7.26±0.08[a]

*Values are means ± SD of triplicate determination. [abcd]Means with same letter in each row are not significantly different ($p<0.05$). DEW = dried egg white, DALK= dried HALK, DNEU= dried HNEU, and DACI= dried HACI. See Table 2.1 for a description of EWH, ALK, NEU, and ACI.

2.3.4 Total amino acid and free amino acid composition

EWH powders contained all of the essential amino acids (EAA) including leucine (Table 2.6); also, DNEU and DACI showed a total essential amino content (TEAA) similar to that of DEW. Meanwhile, DALK had a significantly ($p<0.05$) lower EAA valine, isoleucine, leucine, and tyrosine than those of DEW which significantly ($p<0.05$) decreased its TEAA. Higher amino acid degradation observed in DALK may be the result of the processing. Tryptophan was not quantified in this study; however, it has been reported that EW has a tryptophan content (mg/g protein) of 12.24 (AEB, 1999). Leucine, valine, lysine and phenylalanine were the main EAA found in EWH powders. Leucine was the main EAA in all of the EWH powders. Lactic acid bacteria (LAB) requires higher amounts of alanine, arginine, leucine, isoleucine, histidine, glutamine, methionine, proline, tyrosine, tryptophan, valine and pantothenic acid for optimal growth (Safari, Motamedzadegan, Ovissipour, Regenstein, Gildberg & Rasco, 2012; Ummadi & Curic-Bawden, 2010).

Free amino acids were detected in EWH powders. However, DACI showed a significantly ($p<0.05$) higher free amino acid content compared to those of DEW, DALK, and DACI (Table 2.6). It was also observed that the EAA threonine and leucine were the main free amino acids in DACI. So, the hydrolysis procedure carried out with proteases from *Aspergillus oryzae* did release a greater amount of amino acids from the egg white proteins.

2.3.5 Chemical score

According to Ovissipour, Kenari, Motamedzadegan and Nazari (2012), the chemical score is a parameter that compares the levels of EAA between the evaluated and the standard proteins. In this study, the standard protein of FAO/WHO (1990) for adults was used as the reference protein of comparison. It was observed that all of the EWH powders provide all EAA in higher amounts compared with the suggested amino acid pattern recommended by FAO/WHO for adult humans (Table 2.7). EWH powders contained more than four times the levels of valine and threonine and more than three times the levels of leucine than in the reference protein. The EAA content in all of the EWH powders was significantly higher than in the standard protein of FAO/WHO (1990). According to Friedman (1996), proteins or hydrolysates with high biological value or quality are those containing amino acids with high chemical scores. DALK had a significantly ($p<0.05$) lower chemical score values of valine and isoleucine. Chemical score is also a good parameter to quantified amino acid degradation due to processing (Friedman, 1996). These results are comparable with the total amino acid results previously presented for EWH powders.

2.3.6 Protein efficiency ratio (PER)

The protein efficiency ratio (PER) indicates the nutritional value of proteins. PER measures the quality of proteins by feeding rats for a given period of time with a diet containing 10% of the test protein and measuring their weight gain. Due to the high cost and time required for these kind of experiments; some mathematical equations have been developed to predict the PER of proteins. PER values of EWH powders were from 2.95 to 3.33 (Table 2.8). According to Friedman (1996), food proteins with PER values below 1.5 describes a protein of low or poor quality; values between 1.5 and 2.0 are for intermediate quality proteins, and values above 2.0 are for good to high quality proteins.

Table 2.6 - Total and free amino acid content (mg AA/g Protein) of the egg white hydrolysates powders*

AA	Total Amino Acids (mg /g Protein)				Free Amino Acids (mg /g Protein)			
	DEW	DALK	DNEU	DACI	DEW	DALK	DNEU	DACI
Arginine	44.45±0.50^{a}	48.37±3.05^{a}	47.13±1.46^{a}	47.97±2.63^{a}	0.75±0.09^{c}	1.08±0.07^{b}	1.22±0.08^{b}	4.56±0.66^{a}
Lysine**	67.84±1.18^{a}	67.60±0.63^{a}	68.74±0.89^{a}	67.99±2.48^{a}	ND	ND	0.18±0.03^{b}	6.66±1.45^{a}
Alanine	57.72±0.93^{b}	60.86±0.18^{a}	56.68±0.35^{b}	57.91±0.23^{b}	ND	ND	ND	ND
Threonine**	45.44±0.95^{c}	48.72±0.41^{a}	46.73±0.15^{bc}	46.89±0.18^{b}	19.57±2.51^{b}	22.92±1.70^{ab}	16.68±4.05^{b}	27.52±5.62^{a}
Glycine	32.42±1.36^{a}	34.21±0.46^{a}	33.19±0.52^{a}	32.83±0.22^{a}	ND	ND	ND	0.31±0.54^{a}
Valine**	73.69±0.82^{a}	63.24±3.14^{b}	70.71±0.90^{a}	70.57±0.26^{a}	ND	ND	1.03±0.21^{a}	1.22±0.44^{a}
Serine	70.90±0.76^{c}	79.41±1.18^{a}	74.07±0.41^{b}	73.70±0.37^{b}	ND	ND	0.15±0.04^{b}	2.49±0.59^{a}
Proline	37.36±1.22^{a}	38.34±0.46^{a}	37.36±0.24^{a}	37.16±0.11^{a}	ND	ND	0.03±0.05^{b}	1.76±0.59^{a}
Isoleucine**	55.27±0.91^{a}	47.92±2.75^{b}	53.80±0.85^{a}	54.24±0.22^{a}	ND	ND	0.80±0.21^{b}	2.06±0.74^{a}
Leucine**	91.26±0.56^{a}	87.64±1.51^{b}	88.81±0.96^{ab}	89.15±0.36^{ab}	ND	ND	2.93±0.63^{b}	7.94±2.54^{a}
Methionine**	32.45±0.60^{a}	27.58±3.48^{ab}	24.29±4.32^{b}	29.23±1.75^{ab}	ND	ND	0.45±0.07^{b}	3.05±1.12^{a}
Histidine**	29.05±0.44^{a}	29.16±1.22^{a}	29.36±0.05^{a}	28.84±0.10^{a}	0.05±0.00^{c}	ND	1.87±0.48^{a}	1.28±0.31^{a}
Phenylalanine**	62.69±0.94^{b}	60.14±1.04^{c}	66.59±0.43^{a}	67.90±0.97^{a}	ND	ND	1.12±0.27^{b}	4.99±2.92^{a}
Glutamine	119.46±0.79^{a}	117.70±9.29^{a}	118.99±2.35^{a}	119.37±2.15^{a}	ND	0.17±0.25^{b}	ND	5.94±1.27^{a}
Asparagine	112.57±0.42^{a}	126.80±12.51^{a}	116.90±1.87^{a}	112.46±0.42^{a}	ND	ND	ND	1.75±0.39^{a}
Cysteine	25.96±0.59^{a}	23.65±1.46^{ab}	23.96±0.70^{ab}	22.49±1.10^{b}	ND	ND	0.05±0.01^{b}	0.49±0.16^{a}
Tyrosine**	42.24±0.68^{a}	38.69±1.91^{b}	40.69±1.14^{ab}	41.31±0.26^{ab}	ND	0.13±0.03^{c}	0.82±0.20^{b}	3.45±0.98^{a}
TEAA	499.94±5.23^{a}	470.68±7.13^{b}	489.72±2.82^{a}	496.11±3.63^{a}	19.62±2.51^{b}	23.02±1.79^{b}	25.43±6.06^{b}	55.12±13.65^{a}

*Values are means ± SD of triplicate determination. **Essential amino acid. ^{abcd}Means with same letter in each row are not significantly different ($p<0.05$).TEAA = total essential amino acids, ND=not detected. See Table 2.5 for a brief explanation of DEW, DALK, DNEU, and DACI.

Table 2.7 - Chemical score of the EWH powders calculated based on the requirements given by FAO/WHO (1990)

Amino Acid	TAA (g AA/100 g powder)				Reference Protein[+]	RPA***			
	DEW	DALK	DNEU	DACI		DEW	DALK	DNEU	DACI
Arg	3.62±0.04[a]	3.37±0.38[a]	3.60±0.10[a]	3.94±0.20[a]	-	-	-	-	-
Lys	5.52±0.10[a]	4.74±0.75[a]	5.25±0.09[a]	5.59±0.29[a]	1.6	3.45±0.06[a]	2.96±0.47[a]	3.28±0.06[a]	3.49±0.18[a]
Ala	4.70±0.08[a]	4.27±0.70[a]	4.48±0.02[a]	4.76±0.10[a]	-	-	-	-	-
Thr	3.70±0.08[a]	3.41±0.54[a]	3.57±0.03[a]	3.85±0.08[a]	0.9	4.11±0.09[a]	3.79±0.60[a]	3.97±0.03[a]	4.28±0.09[a]
Gly	2.64±0.11[a]	2.40±0.38[a]	2.54±0.05[a]	2.70±0.05[a]	-	-	-	-	-
Val	6.00±0.07[a]	4.43±0.73[b]	5.40±0.05[a]	5.80±0.09[a]	1.3	4.61±0.05[a]	3.41±0.56[b]	4.15±0.04[a]	4.46±0.07[a]
Ser	5.77±0.06[a]	5.57±0.91[a]	5.66±0.06[a]	6.05±0.14[a]	-	-	-	-	-
Pro	3.04±0.10[a]	2.69±0.45[a]	2.85±0.03[a]	3.05±0.07[a]	-	-	-	-	-
Ile	4.50±0.07[a]	3.36±0.60[b]	4.11±0.06[ab]	4.45±0.07[a]	1.3	3.46±0.06[a]	2.59±0.46[b]	3.16±0.04[ab]	3.43±0.06[a]
Leu	7.43±0.05[a]	6.15±1.05[a]	6.78±0.07[a]	7.32±0.16[a]	1.9	3.91±0.02[a]	3.24±0.55[a]	3.57±0.04[a]	3.85±0.09[a]
Met	2.64±0.05[a]	1.96±0.54[a]	1.86±0.33[a]	2.40±0.18[a]					
His	2.36±0.04[a]	2.03±0.25[a]	2.24±0.01[a]	2.37±0.04[a]	1.6	1.48±0.02[a]	1.27±0.16[a]	1.40±0.01[a]	1.48±0.02[a]
Phe	5.10±0.08[ab]	4.22±0.71[b]	5.09±0.04[ab]	5.58±0.13[a]	-	-	-	-	-
Glx	9.72±0.06[a]	8.32±1.95[a]	9.09±0.22[a]	9.80±0.02[a]	-	-	-	-	-
Asx	9.16±0.03[a]	8.80±0.72[a]	8.93±0.18[a]	9.24±0.20[a]	-	-	-	-	-
Cys2	2.11±0.05[a]	1.67±0.36[a]	1.83±0.05[a]	1.85±0.07[a]	-	-	-	-	-
Tyr	3.44±0.06[a]	2.72±0.54[a]	3.11±0.08[a]	3.39±0.05[a]	-	-	-	-	-
Met +Cys	4.76±0.09[a]	3.63±0.90[a]	3.69±0.37[a]	4.25±0.20[a]	1.7	2.80±0.05[a]	2.13±0.53[a]	2.17±0.22[a]	2.50±0.12[a]

[+]Profile of essential amino acid (EAA) requirements for adults suggested by (FAO/WHO, 1990).

***Chemical score calculated using the FAO/WHO reference protein.

See Table 2.5 for a brief explanation of DEW, DALK, DNEU, and DACI.

All of the EWH powders had PER values higher than 2; hence, they all were high quality proteins. It was seen that DALK had a significantly ($P<0.05$) lower PER value compared to that of DEW calculated by Eq. 2.8 and 2.10.

These results may be due to amino acid degradation and are in accordance with the results for total amino acids.

Table 2.8 - Protein efficiency ratio (PER) of DEW, DALK, DNEU and DACI*

	DEW	**DALK**	**DNEU**	**DACI**
PER[1]	3.20 ± 0.02^{a}	3.07 ± 0.08^{b}	3.10 ± 0.03^{ab}	3.11 ± 0.02^{ab}
PER[2]	3.34 ± 0.02^{a}	3.18 ± 0.24^{a}	2.95 ± 0.19^{a}	3.12 ± 0.11^{a}
PER[3]	3.36 ± 0.04^{a}	3.15 ± 0.07^{b}	3.28 ± 0.02^{a}	3.33 ± 0.03^{a}

*Values are means ± SD of triplicate determination. [abcd]Means with same letter in each row are not significantly different ($p<0.05$). See Table 2.5 for a brief explanation of DEW, DALK, DNEU, and DACI. PER^{1}= value calculated from Eq. 2.8, PER^{2}=value calculated from Eq.2.9, PER^{3}=value calculated from Eq. 2.10.

2.3.7 Antioxidant activity

Antioxidant properties of EWH powders were evaluated based on their DPPH radical scavenging activity (%) (Fig. 2.5.a) and reducing power (Fig. 2.5.b). DNEU and DACI showed a significantly ($p<0.05$) higher DPPH radical scavenging activities than those of DEW and DALK. Antioxidant activity of food protein hydrolysates is given by the proteases and the hydrolysis conditions (Klompong, Benjakul, Kantachote & Shahidi, 2007).

According to Shimada, Fujikawa, Yahara and Nakamura (1992), when DPPH (stable free radical) faces a hydrogen-donating substance, such as an antioxidant, the radical is scavenged and the absorbance is reduced.

The results indicate that the EWH powders may contain electron donor substance that may react with free radical to convert them to more stable products and terminate the radical chain reaction. It was seen that DACI had a significantly ($p<0.05$) higher reducing power compared to

the rest of the powders. Egg white hydrolysates with antioxidant properties have been previously reported (Lin, Guo, You, Yin & Liu, 2012; Pokora, et al., 2013).

According to Xia, Bamdad, Gänzle and Chen (2012), protein peptides containing the free amino acids histidine, proline, and tyrosine show a strong antioxidant activity. The results obtained in this study indicate that DACI contained greater amounts of the free amino acids histidine, proline and tyrosine than the rest of the powders (Table 2.6). Hence, the presence of these amino acids in a free form may have been a factor that enhanced the antioxidant activity of the EWH powders.

2.3.8 Electrophoresis

DEW, DALK, DNEU, and DACI had discrete protein bands with molecular weight smaller than 37,000 Da (Fig. 2.6). These patterns are consistent with soluble proteins. It was observed that the ultrafiltration procedure using a membrane with a cut-off of 30000 Da was not efficient in removing peptides of molecular weights higher than 30,000 Da.

According to Stevens (1991), the main proteins in egg white are ovalbumin (45 kDa), ovotransferrin (76.6 kDa), ovomucoid (28 kDa), lyzosyme (14.3 kDa), ovoinhibitor (49 kDa), ovoglobulin G2 (47 kDa), and ovoglobulin G3(50 kDa).

In this study, egg white proteins were hydrolyzed and the molecular weight profile of the resulting peptides was given by the protease and hydrolysis procedure.

Also, DALK, DNEU and DACI had peptides with molecular weights below 10 kDa; these results may be related with the DH of egg white hydrolysates.

Furthermore, two main peptides with molecular weights of ~35 kDa and ~24kDa were identified in the all of the EWH powders; these peptides may have been a section of a bigger protein that was not hydrolyzed by the food-grade proteases

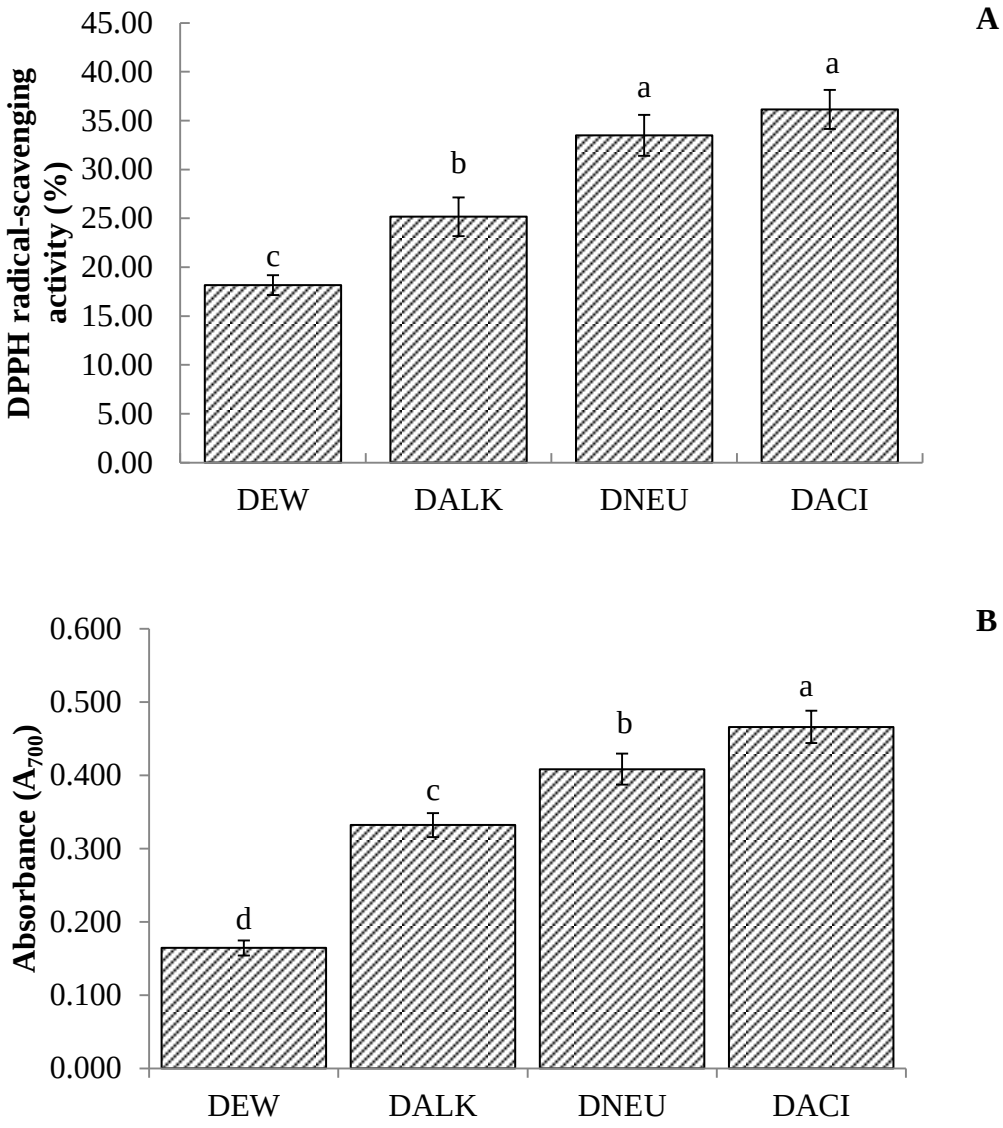

Fig. 2.5 - DPPH radical scavenging activity (%) (A) and reducing power (B) of the EWH powders. [abcd]Means with the same letter in each bar are not significantly ($p<0.05$). See Table 2.5 for a brief explanation of DEW, DALK, DNEU, and DACI.

2.3.9 Mineral profile

Potassium (P), sodium (Na), sulfur (S) and magnesium (Mg) were the main minerals found in DEW, DALK, DNEU, and DACI (Table 2.9). DEW and DALK contained greater amounts of P, and K than those of DNEU, and DACI. These results can also be associated to the addition of the commercial enzymes, which can carry minerals and other fillers, and citric acid/NaOH. EWH powders were also a good source of Cu, which is an essential element in energy metabolism, tissue synthesis and protection against free radicals (Brounds, 1993).

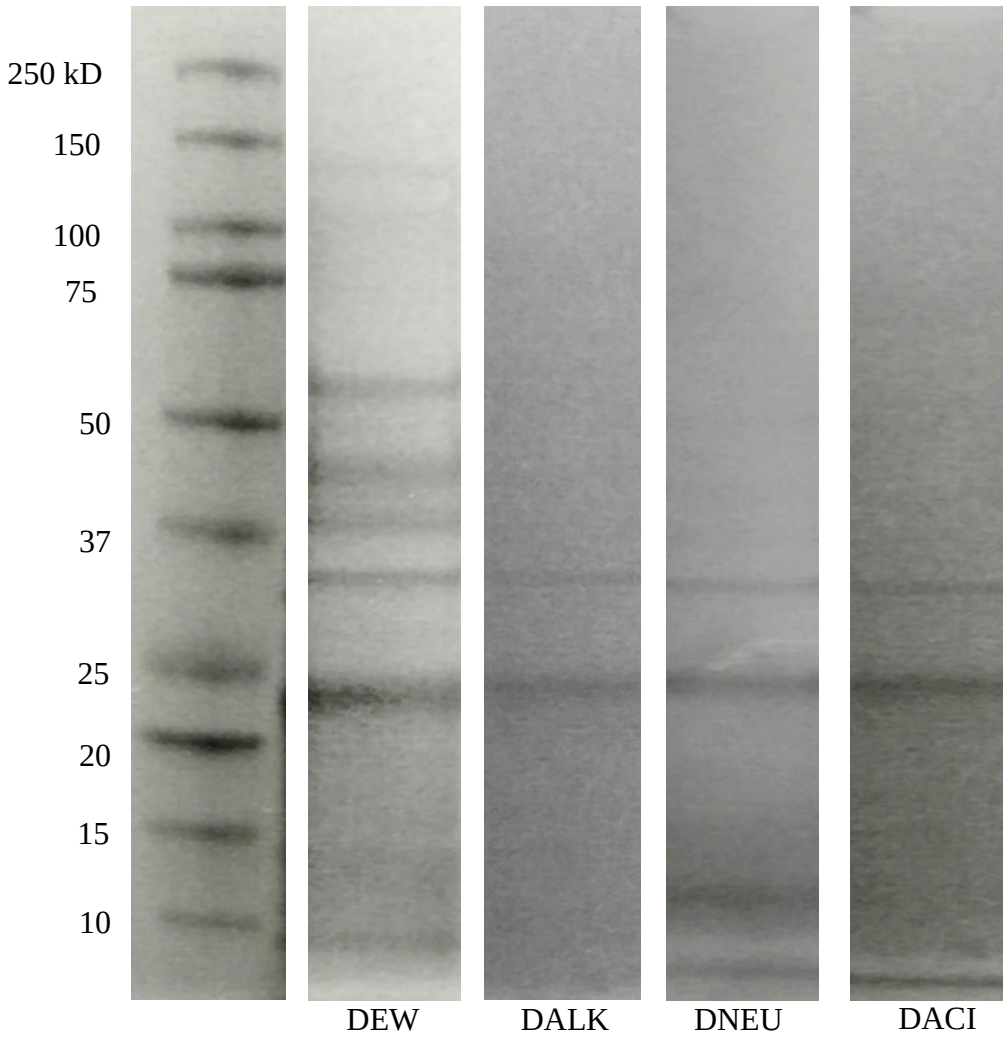

Fig. 2.6 - SDS – Page of EWH powders. See Table 2.5 for a brief explanation of DEW, DALK, DNEU, and DALK.

The recommended Na and K intakes for adults are 2,300 and 4,700 mg/day, respectively (Health & Services, 2007). Potassium is essential for the transmission of nerve impulses, muscle cell contraction, and maintenance of normal blood pressure. Na, K, Ca, Mg, Zn, and Cu are lost from the muscle cell in the urine and sweat due to cell damage during exercise (Montain, Cheuvront & Lukaski, 2007). Mg is required for biosynthetic processes, energy metabolism, gluconeogenesis, and neuromuscular transmission (Lukaski, 2011). Ca is important for muscle contraction and bone formation; while P is part of DNA, ATP, phosphocreatine, and 2,3DPG that regulates the release of oxygen to muscles during exercise (Lukaski, 2011).

Table 2.9 - Mineral profile of the egg white hydrolysates*

Element	DEW	DALK	DNEU	DACI
Aluminum (ppm)	ND	21.31±3.45[a]	ND	1.24±0.05[b]
Boron (ppm)	3.78±0.57[a]	3.51±0.50[a]	2.91±0.42[a]	3.05±1.19[a]
Calcium (g/100g)	0.05±0.00[a]	0.05±0.00[a]	0.05±0.00[a]	0.05±0.00[a]
Copper (ppm)	1.58±0.04[c]	2.30±0.33[a]	1.77±0.02[bc]	2.14±0.02[ab]
Iron (ppm)	4.83±1.92[b]	13.37±3.29[ab]	11.21±0.24[ab]	31.18±17.77[a]
Magnesium (g/100g)	0.10±0.00[a]	0.09±0.00[b]	0.10±0.00[a]	0.10±0.00[a]
Manganese (ppm)	ND	ND	ND	ND
Molybdenum (ppm)	ND	ND	ND	ND
Phosphorus (g/100g)	0.10±0.00[a]	0.10±0.00[a]	0.09±0.00[b]	0.09±0.00[b]
Potassium (g/100g)	1.22±0.02[a]	1.21±0.01[a]	1.12±0.01[b]	1.09±0.01[b]
Sodium (ppm)	12904.82±151.18[b]	17818.98±124.18[a]	12621.46±172.71[b]	11750.47±283.04[c]
Sulfur (g/100g)	1.40±0.01[a]	1.37±0.01[b]	1.37±0.01[b]	1.33±0.01[c]
Zinc (ppm)	ND	3.61±0.22[b]	1.28±0.20[c]	4.95±0.24[a]

*Values are means ± SD of triplicate determination. [abcd]Means with same letter in each row are not significantly different ($p<0.05$). See Table 2.5 for a brief explanation of DEW, DALK, DNEU, and DACI.

2.4 Conclusions

The study demonstrated that egg white hydrolysate powders with antioxidant properties can be effectively produced by using food-grade proteases obtained from *Bacillus licheniformis*, *Bacillus subtilis*, and *Aspergillus oryzae*. Maximum degree of protein hydrolysis in the egg white hydrolysates was achieved by optimizing the reaction temperature, pH, enzyme:substrate ratio, and reaction time of the hydrolysis procedure using the response surface methodology.

Egg white hydrolysates produced with proteases from *Aspergillus oryzae* contained greater amounts of free amino acids and showed higher antioxidant activity and protein efficiency ratio values than the rest of the hydrolysates. All of the egg white hydrolysates powders with a high biological value contained all of the essential amino acids including leucine, valine and lysine. Also, they were a good source of potassium, and sodium; hence, they may be used either as a protein supplement for athletes performing high intensity exercise or as effective nitrogen source for microbial growth media.

2.5 References

AEB. (1999). Eggcyclopedia - The incredible edible egg. Park Ridge, IL: American Egg Board.

AOAC. (1999). Official method of analysis.Ass.of Official Analytical Chemists, Arlington, VA

AOAC. (2000). Official method of analysis.Ass.of Official Analytical Chemists, Arlington, VA

AOAC. (2006). Official method of analysis.Ass.of Official Analytical Chemists, Arlington, VA

Bhaskar, N., Benila, T., Radha, C., & Lalitha, R. G. (2008). Optimization of enzymatic hydrolysis of visceral waste proteins of Catla (*Catla catla*) for preparing protein hydrolysate using a commercial protease. *Bioresource technology*, 99(2), 335-343.

Davalos, A., Miguel, M., Bartolome, B., & Lopez-Fandino, R. (2004). Antioxidant activity of peptides derived from egg white proteins by enzymatic hydrolysis. *Journal of Food Protection®*, 67(9), 1939-1944.

Fang, H., Zhao, C., & Song, X.-Y. (2010). Optimization of enzymatic hydrolysis of steam-exploded corn stover by two approaches: Response surface methodology or using cellulase from mixed cultures of *Trichoderma reesei* RUT-C30 and *Aspergillus niger* NL02. *Bioresource technology*, 101(11), 4111-4119.

FAO/WHO. (1990). Energy and Protein Requirements. Report of joint FAO/WHO/ONU Expert Consultation Technical Report. FAO/WHO and United Nations University, Geneva, Series No. 724. 166 -129.

Ferreira, S., Duarte, A. P., Ribeiro, M. H., Queiroz, J. A., & Domingues, F. C. (2009). Response surface optimization of enzymatic hydrolysis of *Cistus ladanifer* and *Cytisus striatus* for bioethanol production. *Biochemical Engineering Journal*, 45(3), 192-200.

Friedman, M. (1996). Nutritional value of proteins from different food sources. A review. *Journal of Agricultural and Food Chemistry*, 44(1), 6-29.

Graszkiewicz, A., Zelazko, M., & Trziszka, T. (2010). Application of pancreatic enzymes in hydrolysis of egg-white proteins. *Polish Journal of Food and Nutrition Sciences*, 60(1).

Guerard, F., Guimas, L., & Binet, A. (2002). Production of tuna waste hydrolysates by a commercial neutral protease preparation. *Journal of Molecular Catalysis B: Enzymatic*, 19, 489-498.

Health, U. D. o., & Services, H. (2007). US Department of Agriculture (2005) Dietary Guidelines for Americans, 2005. *Washington, DC: US Government Printing Office*.

Klompong, V, Benjakul, S, Kantachote, D, & Shahidi, F. (2007). Antioxidative activity and functional properties of protein hydrolysate of yellow stripe trevally (*Selaroides leptolepis*) as influenced by the degree of hydrolysis and enzyme type. *Food Chemistry*, 102(4),1317-27.

Lee, Y. B., Elliott, J. G., Rickansrud, D. A., & Hagberg, E. Y. C. (1978). Predicting protein efficiency ratio by the chemical determination of connective tissue content in meat. *Journal of Food Science*, 43(5), 1359-1362.

Lin, S., Guo, Y., You, Q., Yin, Y., & Liu, J. (2012). Preparation of antioxidant peptide from egg white protein and improvement of its activities assisted by high-intensity pulsed electric field. *Journal of the Science of Food and Agriculture*, 92(7), 1554-1561.

Liu, B.-L., & Chiang, P.-S. (2008). Production of hydrolysate with antioxidative activity and functional properties by enzymatic hydrolysis of defatted sesame (Sesamum indicum L.). *International Journal of Applied Science and Engineering*, 6(2), 73-83.

Lukaski, H. C. (2011). Vitamins and Minerals. In Campell, B. I., & Spano, M. NSCA's Guide to Sport and Exercise Nutrition: Human Kinetics.

Merheb, C. W., Cabral, H., Gomes, E., & Da-Silva, R. (2007). Partial characterization of protease from a thermophilic fungus, Thermoascus aurantiacus, and its hydrolytic activity on bovine casein. *Food Chemistry*, 104(1), 127-131.

Miguel, M., López-Fandiño, R., Ramos, M., & Aleixandre, A. (2005). Short-term effect of egg-white hydrolysate products on the arterial blood pressure of hypertensive rats. *British Journal of Nutrition*, 94(05), 731-737.

Miguel, M., Recio, I., Gómez-Ruiz, J., Ramos, M., & López-Fandiño, R. (2004). Angiotensin I-converting enzyme inhibitory activity of peptides derived from egg white proteins by enzymatic hydrolysis. *Journal of Food Protection®*, 67(9), 1914-1920.

Montain, S. J., Cheuvront, S. N., & Lukaski, H. C. (2007). Sweat mineral-element responses during 7 h of exercise-heat stress. *International Journal of Sport Nutrition and Exercise Metabolism*, 17(6), 574-582.

Nielsen, P. M., Petersen, D., & Dambmann, C. (2001). Improved Method for Determining Food Protein Degree of Hydrolysis. *Journal of Food Science*, 66(5), 642-646.

O'Donnell, C., & Dornblaser, L. (2002). Amino acids/peptides. *Prepared Foods*, 117, 72-73.

Ovissipour, M., Kenari, A. A., Motamedzadegan, A., & Nazari, R. M. (2012). Optimization of enzymatic hydrolysis of visceral waste proteins of yellowfin tuna (Thunnus albacares). *Food and Bioprocess Technology*, 5(2), 696-705.

Panyam, D., & Kilara, A. (1996). Enhancing the functionality of food proteins by enzymatic modification. *Trends in Food Science & Technology*, 7(4), 120-125.

Park, P.-J., Jung, W.-K., Nam, K.-S., Shahidi, F., & Kim, S.-K. (2001). Purification and characterization of antioxidative peptides from protein hydrolysate of lecithin-free egg yolk. *Journal of the American Oil Chemists' Society*, 78(6), 651-656.

Pokora, M., Eckert, E., Zambrowicz, A., Bobak, Ł., Szołtysik, M., Dąbrowska, A., Chrzanowska, J., Polanowski, A., & Trziszka, T. (2013). Biological and functional properties of proteolytic enzyme-modified egg protein by-products. *Food Science & Nutrition*, 1(2), 184-195.

Safari, R., Motamedzadegan, A., Ovissipour, M., Regenstein, J. M., Gildberg, A., & Rasco, B. (2012). Use of hydrolysates from yellowfin tuna (Thunnus albacares) heads as a complex nitrogen source for lactic acid bacteria. *Food and Bioprocess Technology*, 5(1), 73-79.

Shimada, K., Fujikawa, K., Yahara, K., & Nakamura, T. (1992). Antioxidative properties of xanthan on the autoxidation of soybean oil in cyclodextrin emulsion. *Journal of Agricultural and Food Chemistry*, 40(6), 945-948.

Šližytė, R., Daukšas, E., Falch, E., Storrø, I., & Rustad, T. (2005). Characteristics of protein fractions generated from hydrolysed cod (Gadus morhua) by-products. *Process Biochemistry*, 40(6), 2021-2033.

Stevens, L. (1991). Egg white proteins. *Comparative Biochemistry and Physiology Part B: Comparative Biochemistry*, 100(1), 1-9.

Tarnopolsky, M. (2000). Protein and amino acid needs for training and bulking up. *Burke, L. Deakin, V.(eds) Clinical Sports Nutrition*, 90-123.

Ummadi, M. S., & Curic-Bawden, M. (2010). Use of protein hydrolysates in industrial starter culture fermentations. Protein Hydrolysates in Biotechnology pp. 91-114): Springer.

Van der Plancken, I., Van Remoortere, M., Indrawati, Van Loey, A., & Hendrickx, M. E. (2003). Heat-induced changes in the susceptibility of egg white proteins to enzymatic hydrolysis: a kinetic study. *Journal of Agricultural and Food Chemistry*, 51(13), 3819-3823.

Weggemans, R. M., Zock, P. L., & Katan, M. B. (2001). Dietary cholesterol from eggs increases the ratio of total cholesterol to high-density lipoprotein cholesterol in humans: a meta-analysis. *The American journal of clinical nutrition*, 73(5), 885-891.

Xia, Y., Bamdad, F., Gänzle, M., & Chen, L. (2012). Fractionation and characterization of antioxidant peptides derived from barley glutelin by enzymatic hydrolysis. *Food Chemistry*, 134(3), 1509-1518.

Zheng, H., Shen, X., Bu, G., & Luo, Y. (2008). Effects of pH, temperature and enzyme-to-substrate ratio on the antigenicity of whey protein hydrolysates prepared by Alcalase. *International Dairy Journal*, 18(10), 1028-1033.

CHAPTER 3 - GROWTH KINETICS AND LACTIC ACID PRODUCTION OF *Lactobacillus plantarum* NRRL B-4496, *L. acidophilus* NRRL B-4495, *and L. reuteri* B-14171 IN MEDIA CONTAINING EGG WHITE HYDROLYSATES

3.1 Introduction

Lactic acid bacteria (LAB) are used as starter cultures for producing many fermented foods including yogurt, cheese, fermented sausages, fish, fermented beverages, sauerkraut, etc. According to Fioramonti, Theodorou and Bueno (2003), probiotic LAB show beneficial interactions with the human gastrointestinal tract and its microflora and provide health benefits to the host when they are consumed in adequate amounts (Safari, Motamedzadegan, Ovissipour, Regenstein, Gildberg & Rasco, 2012). Some of the health benefits attributed to the consumption of probiotic LAB include improving the health of the intestinal tract and immune system, increasing the bioavailability of nutrients, and decreasing the risk of certain cancer (Kopp-Hoolihan, 2001). Among the LAB are the genus *Lactobacillus*, which are one of the most economically important bacteria groups for the food industry (Ummadi & Curic-Bawden, 2010).

Lactobacillus spp. require a growth media that must contains a carbon source, amino acids, peptides, fatty acids, vitamins, and nucleic acids. This media is available as a standard laboratory medium known as Man Rogosa Sharpe (MRS) (Meli, Lazzi, Neviani & Gatti, 2014). MRS is used to promote the growth of *Lactobacillus spp*. for laboratory studies; and contains beef, yeast extracts and peptone as its main nitrogen sources. According to Ummadi and Curic-Bawden (2010), every species of *Lactobacillus spp.* has its distinctive growth requirements for essential energy, carbon and nitrogen sources. The selection of the right raw ingredients and the formulation of the optimum fermentation media is the most important step in the production of concentrated LAB starter cultures. Different nutritional requirements are observed for several species of LAB including those of the genus *Lactobacillus spp.*; moreover, the type of carbon

and nitrogen source in the fermentation media has a tremendous effect on the growth of the *Lactobacillus spp.* (Ummadi & Curic-Bawden, 2010). Some LAB have a limited capacity to synthesize amino acids; therefore, they depend on exogenous sources of amino acids and peptides (Foucaud, Hemme & Desmazeaud, 2001).

Due to the high prices of ingredients that are used as nitrogen sources in MRS, the commercial application of MRS is limited (Martone, Borla & Sánchez, 2005); even more, the presence of ingredients from bovine or porcine origin restricts its application in *halal* and *kosher* products (Safari, Motamedzadegan, Ovissipour, Regenstein, Gildberg & Rasco, 2012). It is suggested that the use of MRS may be avoided due to risks related to the occurrence of bovine spongiform encephalopathy (Aspmo, Horn & Eijsink, 2005). According to Castro and Sato (2014), the production of protein hydrolysates containing bioactive peptides from animal and plant sources using enzymatic hydrolysis has attracted attention in recent years due to their positive effects on the growth stimulation of probiotic bacteria. The growth stimulation of LAB provided by protein hydrolysates may be due to their ability to provide free amino acids, low molecular weight peptides, and growth factors (Ummadi & Curic-Bawden, 2010). Hence, the use of protein hydrolysates may be an alternative for the growth of probiotic LAB compared to the use of whole proteins; this may result in a higher growth rate and biomass yield of LAB (Juillard, Guillot, Le Bars & Gripon, 1998).

Ummadi and Curic-Bawden (2010) have reported that the amino acid composition, the form of the amino acids (only L-stereoisomers or L-amino acids can be incorporated into the cell biomass), and the form of the peptide (oligopeptide, di- and tri-peptides, or as free amino acids) determine the biological value of a particular protein hydrolysate as a nitrogen source in a fermentation media for LAB growth. The effect of using protein hydrolysates on the growth of

certain strains of *Lactobacillus spp.* has been previously reported (Juillard, Guillot, Le Bars & Gripon, 1998; Ravula & Shah, 1998; Ummadi & Curic-Bawden, 2010). Nevertheless, most of these studies on growth kinetics of LAB have conducted using protein hydrolysates from dairy proteins. According to Kassis, Drake, Beamer, Matak and Jaczynski (2010), eggs are one of the best and low cost sources of high quality protein because they contain high amounts of proline, arginine, and glutamine which are essential amino acids for the growth of *Lactobacillus spp.*(Ummadi & Curic-Bawden, 2010). The effect of fermentation media containing food-grade egg white hydrolysates on the growth and lactic acid production of *L. plantarum* B-4496, *L. acidophilus* B-4495, and *L. reuteri* B-14171 has not been reported in the scientific literature. Hence, the aim of this study was to evaluate the performance of fermentation media containing food-grade egg white hydrolysates and/or dried egg white with MRS on the growth of LAB.

3.2 Materials and Methods

3.2.1 Materials

Fresh, large, grade AA hen eggs were purchased from a local chain grocery store, in Baton Rouge, Louisiana. The eggs were stored at 4°C, and the storage time did not exceed three days. A food-grade protease from *Aspergillus oryzae* was obtained from Enzyme Development Corporation (New York, NY). The MRS media was obtained from Neogen Corporation (Lansing, MI). All other chemicals were analytical grade and were obtained from Sigma Aldrich (St. Louis, MO).

3.2.2 Preparation of food-grade egg white hydrolysates (EWH)

Fresh egg whites (EW) were manually separated from egg yolks. Then, the moisture content of the EW was determined according to the official AOAC method 930.15 (AOAC, 1999). A mixture containing 80 g EW and 20 g distilled water was prepared and homogenized using an

ultra-shearing processor (OMNI, Ultrashear M, Omni International, Kennesaw, GA) for 5 min at 20,000 rpm, and then heated to 65°C in a water bath for 5 min to denature some of the proteins. After heating, the mixture was cooled down to room temperature. Then, the pH of the mixture was adjusted to 4.60 using a 1 M citric acid solution. The enzymatic hydrolysis was carried using a food-grade protease obtained from *Aspergillus oryzae*. The enzyme-to-substrate ratio [E:S] was standardized to 550 (U enzyme/g protein) and the fermentation vessel was place in an incubator shaker at 38 °C for 110 min. After the reaction time, the fermentation vessel containing the mixtures was heated to 85°C for 5 min to inactivate the enzymes. The degree of protein hydrolysis (DH) was determined by following the method descried in Chapter 2. Then, the resulting mixture containing the hydrolysates were homogenized using an ultra-shearing processor and spray dried using a Pilot-Scale spray dryer (FT80 Tall Form Spray Dryer Armfield Inc., Ringwood, UK) under co-current drying conditions at 140°C inlet air temperature.

3.2.3 Microorganisms

Lyophilized culture of *L. plantarum* NRRL B-4496, *L. acidophilus* B-4495 and *L. reuteri* B-14171 were provided by ARS Culture Collection (Washington, DC, US). The strains were maintained as cultures stocks in 20% glycerol (w/v) at -30°C. One mL of the culture stock was activated in 9 mL of MRS fermentation media and incubated at 37°C for 24 h. Afterwards, 15 mL of MRS fermentation media was added to the fermentation vessel and was kept at 37°C for another 8 h. and the resulting twenty five mL of every strain was subsequently inoculated into 500 mL of a fermentation media.

3.2.4 Media composition

The composition of each of the fermentation media is summarized in Table 3.1. In total, four fermentation media were evaluated including the standard MRS media, the MRS with no

nitrogen source (MRSN), MRSN with egg white hydrolysates (MRSN-EWH), and MRSN with dried egg white (MRSN-DEW). Before inoculation, all of the fermentation media were sterilized at 121 °C for 15 min. at a pressure of 1.1 atm using an autoclave (SM-32, Yamato Scientific America Inc. Orangeburg, NY).

Table 3.1 - Composition of the fermentation media in the microbial essays

Ingredient	Fermentation Media			
	MRS (g/L)	**MRSN–EWH (g/L)**	**MRSN-DEW (g/L)**	**MRSN (g/L)**
Enzymatic digest of animal tissue	10	-	-	-
Beef extract	10	-	-	-
Yeast extract	5	-	-	-
Egg white hydrolysates (EWH)	-	25	-	-
Egg white powder (DEW)	-	-	25	-
Dextrose	20	20	20	20
Sodium acetate	5	5	5	5
Polysorbate 80	1	1	1	1
Potassium phosphate	2	2	2	2
Ammonium citrate	2	2	2	2
Magnesium sulfate	0.1	0.1	0.1	0.1
Manganese sulfate	0.05	0.05	0.05	0.05

MRS = Man Rogosa and Sharpe media
MRSN = MRS media with not nitrogen source
MRSN-EWH = MRSN media with egg white hydrolysates as a nitrogen source
MRSN-DEW= MRSN media with dried egg white as a nitrogen source

3.2.5 Analytical methods

3.2.5.1 Growth curves

Twenty five mL of *L. plantarum* NRRL B-4496, *L. acidophilus* B-4495 and/or *L. reuteri* B-14171 were inoculated in 500 mL of fermentation media and incubated at 37°C for 24 h. Growth curves were constructed by measuring the optical density at 600 nm (OD_{600}) of the cell cultures using a spectrophotometer (Genesis 20, Thermo scientific instruments, LLC, Madison, WI). The maximum cell density (OD_{max}) was obtained when the growth curves reached stationary phase; meanwhile, the maximum specific growth rate (μ_{max}) was obtained by computing the slope of the

exponential growth phase (μ_{max} = $\Delta \ln(OD_{600})/ \Delta t$) as described by Horn, Aspmo and Eijsink (2005). The doubling time (T_d) was calculated by using Eq. 3.1

$$T_d = \frac{\text{Ln } 2}{\mu_{max}} \qquad \text{Eq. (3.1)}$$

3.2.5.2 pH and titratable acidity

The pH of the samples was measured using a Thermo Scientific Orion 4 Star Benchtop pH meter (Thermo Fisher Scientific Inc.). Titratable acidity (TA) was determined by following the method described in Xie, Ye, Liu and Ying (2011) with some modifications. A 10 mL aliquot of fermented broth was mixed with 10 mL of distilled water in a 50 mL beaker. Then, the mixture was neutralized using a 0.1 N sodium hydroxide (NaOH) solution. The end point was set at pH 8.2. The TA was calculated using Eq. 3.2.

$$\text{TA (g/100 mL)} = \frac{(\text{mL NaOH})\ (\text{Normality of NaOH sol.})\ (\text{Equivalent Wt. of lactic acid})}{(10)(\text{mL of sample})} \quad \text{(Eq. 3.2)}$$

Where, the equivalent wt. of lactic acid is 90.08.

The results are expressed in terms of (g/mL) of lactic acid.

3.2.6 Statistical methods

All of the resulting data was statistically analyzed by SAS statistical software version 9.2 (SAS Institute Inc., 2008). Means and standard deviations from triplicate analysis were reported. Analysis of Variance (ANOVA) and Tukey's studentized range test were carried out to determine differences among treatments at the significant level of $P<0.05$.

3.3 Results and discussion

3.3.1 Growth curves

Three strains of the *Lactobacillus spp.* were grown on four different media: MRS, MRSN-EWH, MRSN-DEW, and MRSN. Their growth was monitored during 24 h. It was observed that

the three LAB did grow in each of the four mediums. The growth curves for *L. plantarum* NRRL B-4496 are shown in Fig. 3.1.A. The results demonstrated that its growth was affected by the fermentation media (Table 3.2). Its maximum cell density (OD_{max}) and specific growth rate (μ_{max}) were significantly ($p<0.05$) higher on MRS and on MRSN-EWH media (Table 3.2). Even more, the doubling time (T_d) of *L. plantarum* was significantly ($p<0.05$) lower on MRS and on MRSN-EWH media. Hence, both MRS and MRSN-EWH showed the same performance for the growth of *L. plantarum* after 24 h. The results also revealed that media containing dried egg white hydrolysates (MRSN-EWH) performed better than the media containing dried egg white (MRSN-DEW). These results may be due to the higher amount of low molecular weight peptides and free amino acids in egg white hydrolysates. Horn, Aspmo and Eijsink (2005) have reported an increase of 10% in biomass yield of *L. plantarum* using a media containing a mixture of cod viscera hydrolysates and yeast extract after 24 h of fermentation. According to Safari, Motamedzadegan, Ovissipour, Regenstein, Gildberg and Rasco (2012), *L. plantarum* requires significant amounts of arginine, isoleucine, tyrosine, valine and pantothenic acid for optimal growth. The results demonstrated that EWH had a degree of protein hydrolysis (%) of 92.28 and contained a greater amount of total essential free amino acids (mg/g protein) (55.12) than that of dried egg white (19.62).

Growth curves and growth parameters (μ_{max} and OD_{max}) of *L. acidophilus* NRRL B-4495 are shown in Fig. 3.1.B and Table 3.2, respectively. The results indicated that significantly ($p<0.05$) higher μ_{max} and OD_{max} values were obtained on *L. acidophilus* grew on MRSN-EWH media. These results indicate that a higher cell biomass yield was obtained with MRSN-EWH. Meanwhile, a significantly ($p<0.05$) lower doubling time (T_d) was obtained for *L. acidophilus* grown on MRS and MRSN-EWH compared when it grown on MRSN-DEW and MRSN. These

results suggested that the media containing EWH as nitrogen source performed better than MRS on the growth of *L. acidophilus*. Similar results were obtained by Castro and Sato (2014). They reported a higher cell growth of *L.acidophilus* by supplying the fermentation media with a mixture of protein hydrolysates from whey and egg whites at a dose of 25 mg/mL. Liu, Kong, Xiong and Xia (2010) indicates that protein hydrolysates may show desirable functional properties due to their higher concentration of free amino and carboxyl groups compared to native proteins. According to Ummadi and Curic-Bawden (2010), *L. acidophilus* is a probiotic LAB widely used in the production of fermented milk. Moreover, it requires proline, arginine, and glutamine in high amounts for optimal growth. The results obtained in Chapter 2 showed that EWH had a proline, arginine and glutamine content (mg/ g protein) of 37.16, 47.97, and 119.37, respectively. Also, EWH had a significantly ($p<0.05$) higher free proline, arginine and glutamine content than DEW. According to Hebert, Raya and De Giori (2000), *L. acidophilus* also requires significant amounts of aromatic amino acids (phynylalanine, tryptophan, tyrosine, and histidine) because it does not have a fully functional pentose phosphate pathway.

The growth curves of *L. reuteri* B-14171 on different fermentation media are shown in Fig. 3.1.C. Meanwhile, the results for μ_{max} and OD_{max} of *L. reuteri* are presented in Table 3.2.
It was observed that *L. reuteri* grown on MRSN-EWH had a significantly ($p<0.05$) higher OD_{max} than the rest of the treatments. Furthermore, *L. reuteri* grown on MRS showed a significantly ($p<0.05$) higher μ_{max} than the rest of the treatments. Meanwhile, T_d values of *L. reuteri* grew on MRS were significantly ($p<0.05$) lower than those of the rest of the treatments.

These results suggest that a higher cell biomass yield was produced using MRSN-EWH media. Similar findings were previously described for the growth of *L. acidophilus* using MRSN-EWH. Ummadi and Curic-Bawden (2010) indicates that *L. reuteri* are one of most

fastidious organisms with probiotic properties. They are used in a free or encapsulated freeze-dried form to produce several nutraceutical products. Also, they require sufficient quantities of methionine, glutamine, tyrosine, tryptophan, histidine, leucine, valine and alanine in the fermentation media for optimal growth. In this study, the superior performance of MRSN-EWH media may due to the peptides, free amino acids and growth factors provided by EWH. EWH had a DH (%) of 92.28, therefore, it had a significantly ($p<0.05$) higher free amino acid content compared to that of DEW (Chapter 2). EWH was also an excellent source of minerals. According to Safari, Motamedzadegan, Ovissipour, Regenstein, Gildberg and Rasco (2012), hydrolysates with a high degree of hydrolysis are rapidly absorbed by LAB. Ummadi and Curic-Bawden (2010) indicates that protein hydrolysates with a high biological value also provide growth factors and minerals that can stimulate bacteria growth. The results obtained in this study also showed that *L. plantarum* NRRL B-4496 had a significantly ($p<0.05$) higher OD_{max} than those of *L. acidophilus* NRRL B-4495, and *L.reuteri* B-14171 in all of the fermentation media. This suggests that *L. plantarum* had a higher cell biomass yield compared to the rest of the LAB.

3.3.2 pH

Changes in the pH of the fermentation media during the growth of *L. plantarum* NRRL B-4496 are shown in Fig. 3.2.A. MRS and MRSN-EWH had a significantly ($p<0.05$) lower pH than those of MRSN-DEW and MRSN. MRS and MRSN-EWH had pH values lower than 3.75 after 24 h of fermentation. Furthermore, MRS, MRSN-EWH, MRSN-DEW, and MRSN had a decrease in pH of 2.86, 2.54, 2.27, and 2.14 (after 24 h of fermentation), respectively. The pHs of the fermentation mediums did not significantly changed after 12 h. This may be due to the fact that *L. plantarum* reached a steady-state growth after 12 hours. Also, the pH changes may be the result of bacterial lactic acid production.

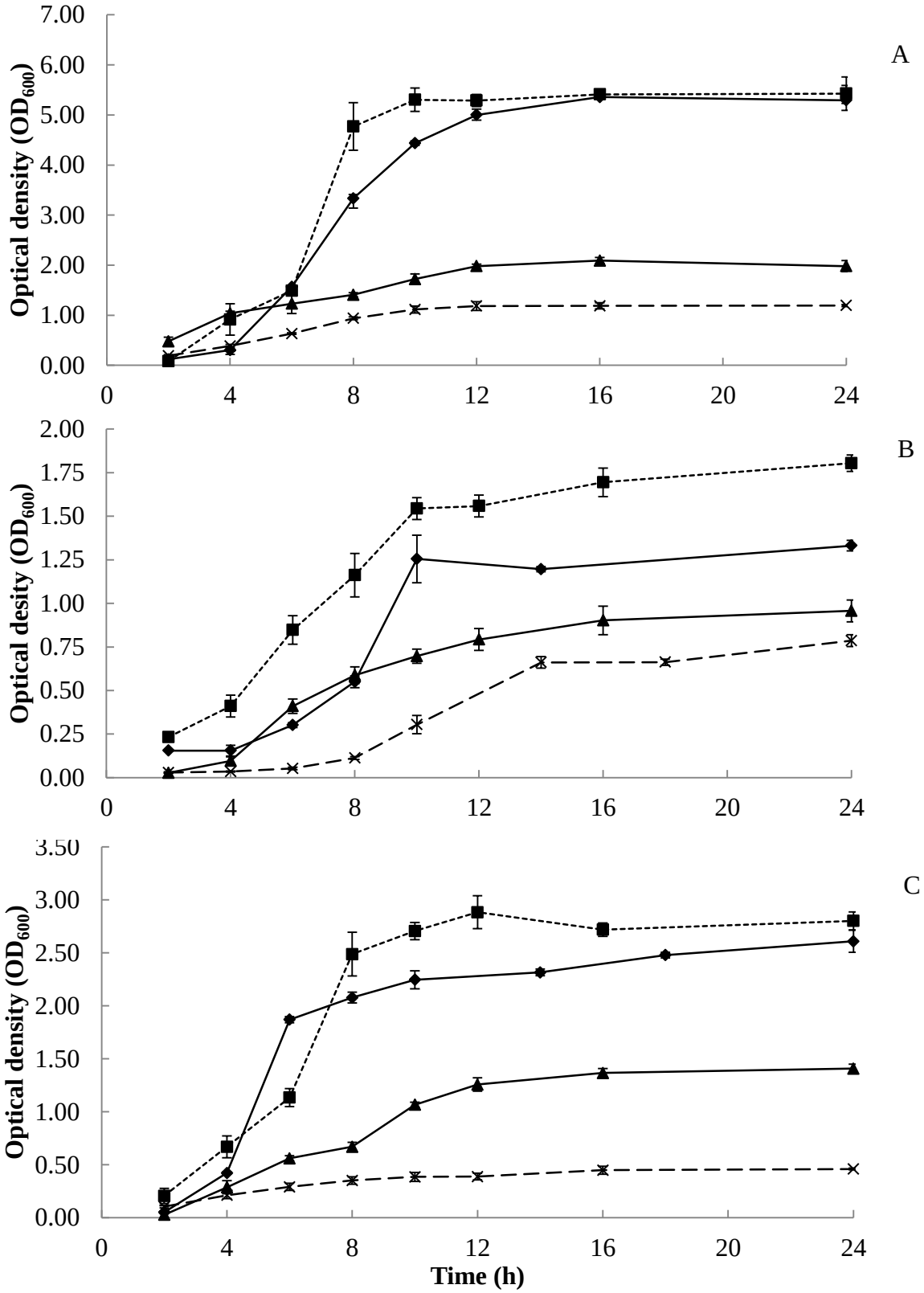

Fig. 3.1 - Growth of *L. plantarum* NRRL B-4496 (A), *L. acidophilus* NRRL B-4495 (B), and *L. reuteri* B-14171 (C) measured as optical density (OD_{600}) using different fermentation media. —◆— =MRS ; - -■- -·= MRSN +EWH; —▲— = MRSN+DEW; —✕— = MRSN.

Table 3.2 - Maximum specific growth (μ_{max}) and maximum cell density (OD_{max}) of *L. plantarum* NRRL B-4496, *L. acidophilus* NRRL B-4495 (B), and *L. reuteri* B-14171 cultured in different media*

	Fermentation Media	*L. plantarum* NRRL B-4496	*L. acidophilus* NRRL B-4495	*L. reuteri* B-14171
μ_{max} (h^{-1})	MRS	0.48 ± 0.01^{aA}	0.26 ± 0.02^{bB}	0.46 ± 0.02^{aA}
	MRSN-EWH	0.50 ± 0.08^{aA}	0.24 ± 0.02^{bB}	0.33 ± 0.03^{bB}
	MRSN-DEW	0.14 ± 0.02^{bC}	0.43 ± 0.06^{aA}	0.31 ± 0.02^{bB}
	MRSN	0.22 ± 0.01^{bB}	0.29 ± 0.03^{bA}	0.16 ± 0.01^{cC}
OD_{max}	MRS	5.36 ± 0.30^{aA}	1.33 ± 0.03^{bC}	2.61 ± 0.10^{bB}
	MRSN-EWH	5.58 ± 0.08^{aA}	1.80 ± 0.08^{aC}	2.80 ± 0.09^{aB}
	MRSN-DEW	2.10 ± 0.04^{bA}	1.01 ± 0.09^{cC}	1.41 ± 0.04^{cB}
	MRSN	1.21 ± 0.03^{cA}	0.79 ± 0.03^{dB}	0.47 ± 0.02^{dC}
T_d(h)	MRS	1.44 ± 0.04^{cB}	2.65 ± 0.18^{aA}	1.50 ± 0.07^{cB}
	MRSN-EWH	1.41 ± 0.23^{cC}	2.85 ± 0.29^{aA}	2.13 ± 0.23^{bB}
	MRSN-DEW	4.86 ± 0.64^{aA}	1.62 ± 0.21^{bB}	2.21 ± 0.13^{bB}
	MRSN	3.13 ± 0.20^{bB}	2.38 ± 0.25^{aC}	4.44 ± 0.35^{aA}

*Values are means ± SD of triplicate determination. ^{abcd}Means with same letter in each column are not significantly different ($p<0.05$). ^{ABC}Means with same letter in each row are not significantly different. See table 3.1 for description of MRSN-EWH, MRSN-DEW, and MRSN.

Fig. 3.2.B shows the pHs of the fermentation media during the growth of *L. acidophilus* NRRL B-4495 after 24 h. It was seen that MRS and MRSN-EWH reached final pH values below 4.5. The MRS, MRSN-EWH, MRSN-DEW, and MRSN had a decrease in pH of 2.33, 1.99, 2.25 and 0.64, respectively. As previously seen for the growth of *L.plantarum*, the pH of the fermentation media did not have any significantly changes after 12 of fermentation. Meanwhile, the pH results for the growth of *L. reuteri* B-14171 in different media are shown in Fig. 3.2.C. After 24 h of fermentation, lower pH values were obtained for MRS and MRSN-EWH which were 4.31 and 4.13, respectively. These results are similar to those obtained during the growth of *L. plantarum* and *L. acidophilus*. Also, MRS, MRSN-EWH, MRSN-DEW, and MRSN had a pH decrease of 2.28, 2.08, 1.98, and 1.55 respectively. According to Zotta, Asterinou, Rossano, Ricciardi, Varcamonti and Parente (2009), the decrease in pH during a LAB fermentation is due to the production of lactic acid and is not correlated to the number of viable cells.

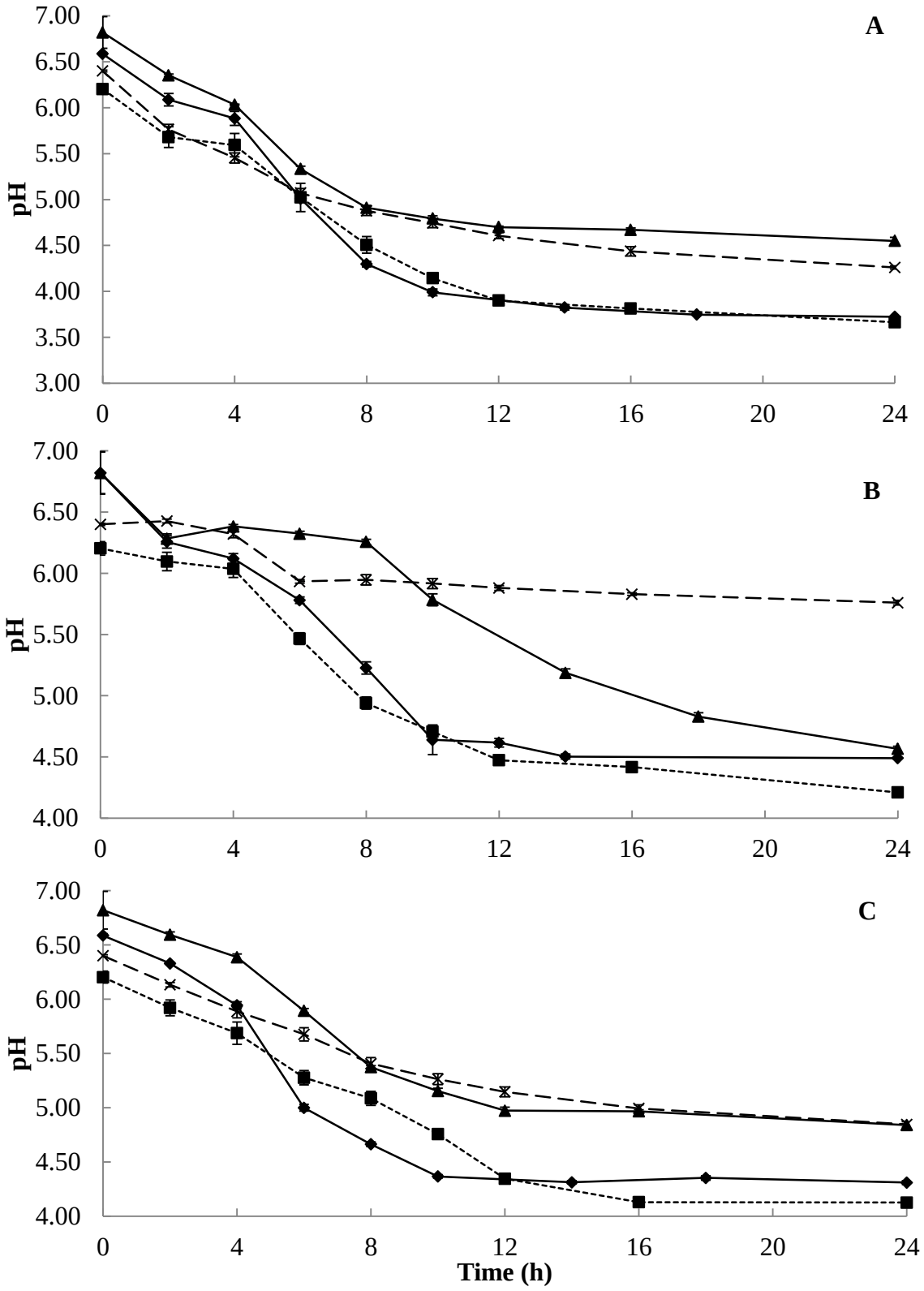

Fig. 3.2 - PH of fermentation media during the growth of *L. plantarum* NRRL B-4496 (**A**), *L. acidophilus* NRRL B-4495 (**B**), and *L. reuteri* B-14171 (**C**).
—◆— =MRS ; - -■- -·= MRSN +EWH; —▲— = MRSN+DEW; —✕— = MRSN.

The results indicated that a greater decrease in pH was observed in LAB grown on MRSN-EWH than on MRSN-DEW.

3.3.3 Titratable acidity (TA)

Titratable acidity was quantified in terms of equivalent weight of lactic acid. According to Ummadi and Curic-Bawden (2010) LAB can transform the available source of carbohydrates in the media into acid (mainly lactic acid); this process results in a decrease in the pH and organoleptic changes in the fermentation media. The amount of lactic acid produced is a LAB strain-specific characteristic which can be enhanced (up to a certain limit) by improving the cultivation conditions (Petrov, Urshev & Petrova, 2008). The influence of the fermentation media on the titratable acidity for *L. plantarum* NRRL B-4496 is shown in Fig. 3.3.A. A significantly ($p<0.05$) higher titratable acidity (g/100 mL) was obtained with MRS (1.73) followed by MRSN-EWH (1.61) after 24 h. Therefore, *L. plantarum* produced 7% more titratable acidity when growing in MRN than in MRSN-EWH. Also, the production of TA reached its maximum value after 20 h of fermentation; meanwhile, the pH of the fermentation media reached its minimum value after 12 h. According to Boulton (1980), pH is the logarithmic of the concentration of the free protons or free hydrogen ions in the media; meanwhile, TA is the number of protons recuperated during a titration with a base and both parameters are not proportionally correlated. Also, it was seen that *L. acidophilus* NRRL B-4495 grown on MRSN-EWH had a significantly ($p<0.05$) higher TA (g/100 mL) (0.71) compared to those of MRS (0.66), MRSN-DEW (0.59), and MRSN (0.55), respectively (Fig. 3.3.B). This implies that *L. acidophilus* secreted 7% more TA when it was grown on MRSN-EWH than in MRS. The results for TA during the growth of *L. reuteri* B-14171 are presented in Fig. 3.3.C. It was observed that after 24 h of fermentation, the titratable acidity (g/100 mL) of *L. reuteri* grown on MRS, MRSN-

EWH, MRSN-DEW, and MRSN was 1.05, 1.12, 0.57, and 0.39, respectively. In this case, *L. reuteri* grown on MRSN-EWH produced a significantly ($p<0.05$) higher titratable acidity than on the rest of the treatments. The growth of *L. reuteri* generates 6.25% more titratable acidity on MRSN-EWH than on MRS after 24 h of fermentation. An enhancement in lactic acid production by LAB using casein hydrolysates in the fermentation media have been previously reported by Zhang, Ren, Zhao, Zhao, Xu and Zhao (2011). The authors attributed the results to the supplementation of the hydrolysates containing small peptides (<3000 Da). Also, Gomes, Malcata and Klaver (1998) have reported an increase in lactic acid production from *Bifidobacterium lactis* by adding milk hydrolysates during the fermentation of skim milk. However, the authors did not observe the same effect using *L. acidophilus*; which can be attributed to its slow growth. The use of egg white protein hydrolysates as a nitrogen source in a LAB fermentation media improved the production of lactic acid during a fermentation using *L. acidophilus* and *L. reuteri*. Also, egg white hydrolysates (containing small peptides and large amount of amino acids) were better nitrogen sources than dried egg white for the growth of *L. plantarum* NRRL B-4496, *L. acidophilus* NRRL B-4495, and *L. reuteri* B-14171.

3.4 Conclusion

It was demonstrated that dried egg white hydrolysates can be effectively used as a nitrogen source for media that supports the growth of *L. plantarum* NRRL B-4496, *L. acidophilus* NRRL B-4495, and *L. reuteri* B-14171. Also, higher yields of cell biomass and production of titratable acidity was observed in *L. acidophilus* NRRL B-4495 and *L. reuteri* B-14171when they grew in a media containing dried egg white hydrolysates which suggested that dried egg white hydrolysates with higher free amino acid contents are a better nitrogen source than dried egg white; this may enable the LAB cultures to survive further processing; therefore, prolonging their shelf life at room temperature.

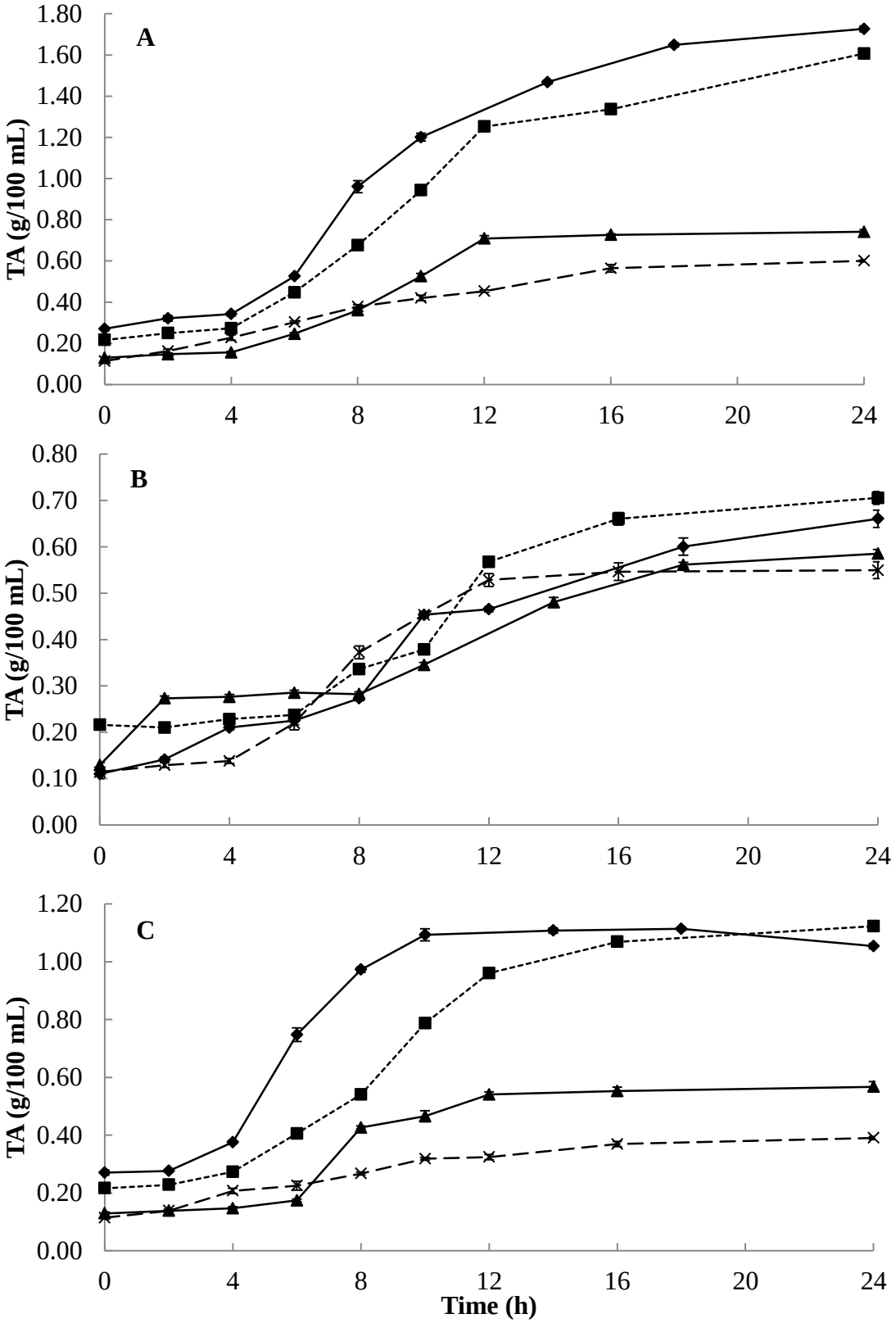

Fig. 3.3 - Titratable acidity of the fermentation media during the growth of *L. plantarum* NRRL B-4496 (**A**), *L. acidophilus* NRRL B-4495 (**B**), and *L. reuteri* B-14171 (**C**).
—◆— =MRS ; - -■- ·= MRSN +EWH; —▲— = MRSN+DEW; —✕— = MRSN.

3.5 References

AOAC. (1999). Official methods of analysis. Arlington, VA: Association of Official Analytical Chemists.

Aspmo, S. I., Horn, S. J., & Eijsink, V. G. (2005). Hydrolysates from Atlantic cod (*Gadus morhua L.*) viscera as components of microbial growth media. *Process Biochemistry*, 40(12), 3714-3722.

Boulton, R. (1980). The Relationships between Total Acidity, Titratable Acidity and pH in Wine. *American Journal of Enology and Viticulture*, 31(1), 76-80.

Castro, R. J. S. d., & Sato, H. H. (2014). Functional properties and growth promotion of bifidobacteria and lactic acid bacteria strains by protein hydrolysates using a statistical mixture design. *Food Bioscience*.

Fioramonti, J., Theodorou, V., & Bueno, L. (2003). Probiotics: what are they? What are their effects on gut physiology? *Best Practice & Research Clinical Gastroenterology*, 17(5), 711-724.

Foucaud, C., Hemme, D., & Desmazeaud, M. (2001). Peptide utilization by Lactococcus lactis and Leuconostoc mesenteroides. *Letters in Applied Microbiology*, 32(1), 20-25.

Gomes, A. M., Malcata, F. X., & Klaver, F. A. (1998). Growth Enhancement of *Bifidobacterium lactis Bo* and *Lactobacillus acidophilus Ki* by Milk Hydrolyzates. *Journal of Dairy Science*, 81(11), 2817-2825.

Hebert, E. M., Raya, R. R., & De Giori, G. S. (2000). Nutritional requirements and nitrogen-dependent regulation of proteinase activity of Lactobacillus helveticus CRL 1062. *Applied and environmental microbiology*, 66(12), 5316-5321.

Horn, S., Aspmo, S., & Eijsink, V. (2005). Growth of Lactobacillus plantarum in media containing hydrolysates of fish viscera. *Journal of Applied Microbiology*, 99(5), 1082-1089.

Juillard, V., Guillot, A., Le Bars, D., & Gripon, J.-C. (1998). Specificity of Milk Peptide Utilization byLactococcus lactis. *Applied and environmental microbiology*, 64(4), 1230-1236.

Kassis, N., Drake, S. R., Beamer, S. K., Matak, K. E., & Jaczynski, J. (2010). Development of nutraceutical egg products with omega-3-rich oils. *LWT-Food Science and Technology*, 43(5), 777-783.

Kopp-Hoolihan, L. (2001). Prophylactic and Therapeutic Uses of Probiotics: A review. *Journal of the American Dietetic Association*, 101(2), 229-241.

Liu, Q., Kong, B., Xiong, Y. L., & Xia, X. (2010). Antioxidant activity and functional properties of porcine plasma protein hydrolysate as influenced by the degree of hydrolysis. *Food Chemistry*, 118(2), 403-410.

Martone, C. B., Borla, O. P., & Sánchez, J. J. (2005). Fishery by-product as a nutrient source for bacteria and archaea growth media. *Bioresource technology*, 96(3), 383-387.

Meli, F., Lazzi, C., Neviani, E., & Gatti, M. (2014). Effect of Protein Hydrolysates on Growth Kinetics and Aminopeptidase Activities of Lactobacillus. *Current microbiology*, 68(1), 82-87.

Petrov, K., Urshev, Z., & Petrova, P. (2008). l (+)-Lactic acid production from starch by a novel amylolytic *Lactococcus lactis* subsp.lactis B84. *Food microbiology*, 25(4), 550-557.

Ravula, R., & Shah, N. (1998). Effect of acid casein hydrolysate and cysteine on the viability of yogurt and probiotic bacteria in fermented frozen dairy desserts. *Australian Journal of Dairy Technology*, 53(3), 175-179.

Safari, R., Motamedzadegan, A., Ovissipour, M., Regenstein, J. M., Gildberg, A., & Rasco, B. (2012). Use of hydrolysates from yellowfin tuna (Thunnus albacares) heads as a complex nitrogen source for lactic acid bacteria. *Food and Bioprocess Technology*, 5(1), 73-79.

Ummadi, M. S., & Curic-Bawden, M. (2010). Use of protein hydrolysates in industrial starter culture fermentations. Protein Hydrolysates in Biotechnology pp. 91-114): Springer.

Xie, L., Ye, X., Liu, D., & Ying, Y. (2011). Prediction of titratable acidity, malic acid, and citric acid in bayberry fruit by near-infrared spectroscopy. *Food Research International*, 44(7), 2198-2204.

Zhang, Q., Ren, J., Zhao, H., Zhao, M., Xu, J., & Zhao, Q. (2011). Influence of casein hydrolysates on the growth and lactic acid production of Lactobacillus delbrueckii subsp. bulgaricus and Streptococcus thermophilus. *International Journal of Food Science & Technology*, 46(5), 1014-1020.

Zotta, T., Asterinou, K., Rossano, R., Ricciardi, A., Varcamonti, M., & Parente, E. (2009). Effect of inactivation of stress response regulators on the growth and survival of *Streptococcus thermophilus* Sfi39. *International journal of food microbiology*, 129(3), 211-220.

CHAPTER 4 - CO-CURRENT AND COUNTER-CURRENT SPRAY DRYING COMPUTATIONAL FLUID DYNAMICS (CFD) SIMULATION STUDIES TO PREDICT THE QUALITY OF MICROENCAPSULATED FISH OIL WITH EGG WHITE HYDROLYSATES POWDERS

4.1 Introduction

Spray drying is a processing technique of transforming a liquid feed into a low-moisture content powder and is widely used in several industries including food manufacturing (Fletcher, Guo, Harvie, Langrish, Nijdam & Williams, 2006). Several attempts have been proposed to model the physical phenomena that govern the spray drying process; however, these models are inadequately correlated with final quality of the spray-dried powders (Kuriakose & Anandharamakrishnan, 2010). Also, basic mass transport assumptions that occur in the drying chamber are applied and the physical phenomena that takes place at other important parts of the spray dryer like the cyclone separator is normally neglected (Kuriakose & Anandharamakrishnan, 2010; Mezhericher, Levy & Borde, 2009). Therefore, more accurate spray drying models need to be built to understand and predict thermal degradation of bioactives during spray drying. To experimentally study the spray drying process is challenging and difficult due to the complexity in measuring and describing the drying air flow, heat, and mass transfer mechanisms within the spray dryer (Birchal, Huang, Mujumdar & Passos, 2006).

According to Kieviet (1997), prediction of the final quality of spray-dried products is extremely difficult because parameters like moisture content, thermal degradation of bioactives, aroma retention, stickiness, particle structure and size are normally associated with product quality. In addition, quality of spray-dried powders is highly linked with the spray drying processing conditions (temperature, humidity, etc.) (Kieviet & Kerkhof, 1995; Paris, Ross Jr, Dastur & Morris, 1971). Due to the complexity of experimentally predicting the final quality of spray-dried powders, several models of the spray drying process have been reported in the

literature using a computational fluid dynamics approach (CFD) (Birchal, Huang, Mujumdar & Passos, 2006); however, most of these attempts are based on experimental calculations of drying kinetics of discrete droplets immersed into a current of hot air (Mezhericher, Levy & Borde, 2012).

CFD is as a powerful simulation tool that has been utilized in basic and applied research and has attracted the interest of the food processing sector in recent years (Kuriakose & Anandharamakrishnan, 2010). CFD uses powerful computers and applied mathematics to model fluid flow processes. This simulation tool requires solving equations for the conservation of mass, momentum and energy using numerical methods to predict velocity, temperature and pressure inside of a spray dryer (Scott & Richardson, 1997).In the case of spray drying, CFD can be used to predict the drying air flow pattern and food particle histories such as temperature, velocity, and residence times. These parameters are extremely difficult and expensive to be measured in large and/or pilot-scale spray dryers. Also, CFD can be successfully employed to study the effect of chamber design on drying behavior of food materials. Therefore, CFD is a useful tool to scale-up spray drying chambers from pilot to full industrial scale (Mezhericher, Levy & Borde, 2009).

Microencapsulation of fish oil by spray drying has been used to reduce lipid oxidation during storage. However, lipid oxidation of the microencapsulated oil can happen during the spray drying process due to the high drying air temperatures. Tonon, Grosso and Hubinger (2011) have reported that increasing drying air temperatures produces greater lipid oxidation in microencapsulated flaxseed oil. Furthermore, longer particle residence time (RT) at high drying air temperatures during spray drying increases thermal degradation and oxidation of lipids (Bimbenet, Bonazzi & Dumoulin, 2002).

Measuring the particle residence time (RT) during spray drying is extremely challenging because it involves several parameters such as spray drying configuration, drying air velocity and temperature, emulsion flow rate, and feed atomization conditions; therefore, CFD simulations have been effectively used to predict the RT of spray dried particles (Ducept, Sionneau & Vasseur, 2002). According to Huang, Kumar and Mujumdar (2003a) most of the CFD spray drying simulations are carry out using co-current spray drying configurations. So, there is a lack of scientific information about CFD spray drying simulations in counter-current conditions. CFD simulations have allowed the improvement on device design and somehow predict the final quality of powders; nevertheless, predicting the quality of powders using only the computational tool is complicated due to the number of parameters that intervene during the process such as droplet evaporation, collision, breakups, agglomeration, heat and mass exchange between the droplets and drying medium and so on (Gharsallaoui, Roudaut, Chambin, Voilley & Saurel, 2007). Therefore, combining CFD simulations with experimental tools is a more feasible and practical approach for predicting the final quality of spray-dried food powders.

There is a lack of scientific literature regarding the use CFD simulations with experimental methods to study the final quality of microencapsulated fish oil with egg white hydrolysates by spray drying. Also, comparison studies between the performance of co-current and counter-current spray drying configurations on the quality of the powder are needed. So, the objectives of this study were: (1) to produce microencapsulated fish oil with egg white hydrolysates powders by spray drying; (2) to develop 3D-CFD models to study the drying air flow pattern and particle histories during spray drying of microencapsulated fish oil powders; and (3) to study the effects of inlet air temperature, emulsion flow rate, and spray drying configuration on the quality of the microencapsulated fish oil powders using CFD simulations and experimental tools.

4.2 Materials and Methods

4.2.1 Experimental procedure

Microencapsulated fish oil powders were physically produced by spray drying in order to generate experimental data that can be compared with the predicted results obtained with the 3D-CFD simulations.

4.2.1.1 Materials

Fresh, large, grade AA hen eggs were purchased from a local chain grocery store, in Baton Rouge, Louisiana. The eggs were stored at 4°C, and the storage time did not exceed three days. A commercial food-grade protease from *Bacillus subtilis* was obtained from Enzyme Development Corporation (New York, NY). Menhaden fish oil (MO) was obtained from a commercial vendor (VooDoo Offshore, Pleasant, S.C.). All other analytical grade reagents were obtained from Sigma Aldrich (St. Louis, MO).

4.2.1.2 Preparation of liquid egg white hydrolysates (LEWH)

Fresh egg whites (EW) were manually separated from egg yolks. Then, the moisture content of the EW was determined according to the official AOAC method 930.15 (AOAC, 1999). A 10±0.5 (g solids/100g) mixture containing 80g liquid egg white and 20 g distilled water was prepared and homogenized using an ultra-shearing processor (OMNI, Ultrashear M, Omni International, Kennesaw, GA) for 5 min. at 20,000 rpm, and then heated to 65°C in a water bath for 5 min. Afterwards, the mixture was cooled down to room temperature and its PH was adjusted to 4.60 using a 1 M citric acid solution. The enzymatic hydrolysis was carried out at 38 °C for 110 min using food-grade protease obtained from *Aspergillus oryzae* with the enzyme-to-substrate ratio [E:S] standardized at 550 (U enzyme/g protein). To stop the enzymatic activity,

the fermentation vessel (containing LEWH) was heated to 85°C for 5 min. and homogenized at room temperature.

4.2.1.3 Emulsion preparation

Oil-in-water emulsions containing MO and LEWH were prepared to produce microencapsulated menhaden oil with egg white hydrolysates. Based on our preliminary studies from our lab reported by Yin, Pu, Wan, Xiang, Bechtel and Sathivel (2010), stable emulsions (E-MO-LEWH) were obtained with 3 (g/100g) MO, and 97 (g/100g) LEWH. LEWH had a solid content of approximately 12g/100 mL; therefore, E-MO-LEWH contained 15 (g/100g) solids. The emulsion preparation conditions were selected following the procedure reported by Yin, Pu, Wan, Xiang, Bechtel and Sathivel (2010). The emulsions were homogenized for 5 min using an ultrasonic processor (500 Watt Model CPX 500, Cole-Parmer Instrument Co. Vernon Hill, IL) fitted with a 22 mm tip diameter at 82% amplitude with 2x1 pulses (with 1 s delay between pulses) and then using an ultra-shearing processor for 5 min. at 20,000 rpm. Samples were held in an ice bath at 4°C during the procedure.

4.2.1.4 Spray drying of E-MO-LEWH

E-MO-LEWH was dried using a pilot-scale spray dryer (FT80 Tall Form Spray Dryer Armfield Inc., Ringwood, UK) under co-current (CO) and counter-current (CNT) conditions at a flow rate (Kg/h) of 0.5, 0.75 and/or 1. Inlet air temperature was set to 130, 150 and/or 170°C. Details of the CO and CNT conditions are described in section 4.2.2.1.1. Inlet air velocities and temperatures were measured inside the drying chamber in order to validate the results of the 3D-CFD simulations. Air temperature and velocity inside the drying chamber of the spray dryer was measured using an anemometer (Kanomax 6162 Anemomaster, Japan) as shown in Fig. 4.1. The data was collected once the drying air reached steady state conditions. The resulting spray-dried

powders and dust were separated at the cyclone and filter bag, respectively. In total, eighteen (18) spray-dried powders were obtained (Table 4.1). The procedure was carried out in triplicate. Powders were stored in amber bottles and kept in a desiccator until needed for analysis.

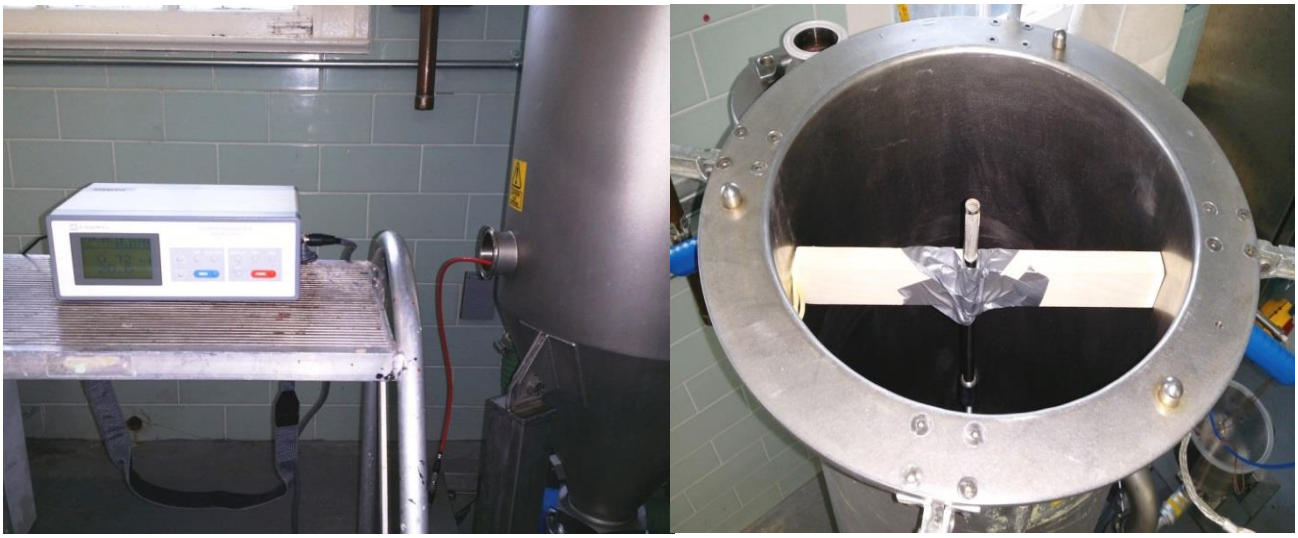

Fig. 4.1 - Determination of drying air velocity and temperature using an anemometer to validate CFD simulations

Table 4.1 - Description of the spray-dried powders obtained at different processing conditions

Spray Drying Configuration	**Flow rate (kg/h)**	**Inlet Air Temperature (°C)**		
		130	**150**	**170**
Co-current (CO)	0.50	50-E-130	50-E-150	50-E-170
	0.75	75-E-130	75-E-150	75-E-170
	1	100-E-130	100-E-150	100-E-170
Counter-current (CNT)	0.50	50-E-130CNT	50-E-150CNT	50-E-170CNT
	0.75	75-E-130CNT	75-E-150CNT	75-E-170CNT
	1	100-E-130CNT	100-E-150CNT	100-E-170CNT

4.2.1.5 Characterization of spray dried powders

4.2.1.5.1 Moisture and water activity (a_w)

Moisture content was measured according to the AOAC official method 930.15 (AOAC, 1999). Water activity (a_w) was determined using an AquaLab water activity meter (Model Series 3 TE, Decagon Devices, Inc., Pullman, WA, USA). Determinations were carried out in triplicate.

4.2.1.5.2 Microencapsulation efficiency (ME)

The total lipid content (OT) of the microencapsulated includes encapsulated oil (EO) and surface oil (OS). The EO was determined as EO=OT–OS. The OT and OS were determined to calculate ME using Eq. 4.1 as described in Wanasundara and Shahidi (1995).

$$ME = [Total\ oil - Surface\ oil)/Total\ oil] \times 100 \quad (4.1)$$

4.2.1.5.3 Lipid oxidation

a. Peroxide value (PV)

The PV of the spray-dried powders was determined by following the IDF method described in Shantha and Decker (1993) with some modifications. An iron (II) chloride solution was prepared by dissolving 0.4 barium chloride dehydrate in 50 mL of distilled water; then, to this solution was added an iron (II) sulfate solution (0.5 g $FeSO_4.7H_2O$ dissolved in 50 mL distilled water). Afterwards, two mL of 10N hydrochloric acid were added and the barium sulfate precipitate was filtered off and stored in a brown bottle and kept in the dark.

To determine the PV of the powders, 0.3 g of sample was mixed with 9.8 mL chloroform-methanol (7+3, v/v) and vortexed for 4 s. Then, 50 µL of ammonium thiocyanate solution and 50 uL iron (II) solution were added and the mixture was vortexed for 4 s. After 5 min incubation at room temperature, the absorbance of the samples was recorded at 500 nm against a blank that contained all the reagents except the sample. A standard curve of Fe^{3+} concentration vs. absorbance was constructed to quantify PV. The PV, expressed as milliequivalents of peroxide per kilogram of sample, was calculated by using the following Eq. 4.2

$$Peroxide\ Value = \frac{(A_s - A_b) * m}{55.84 * m_0 * 2} \quad (4.2)$$

Where, A_s= absorbance of the sample; A_b= absorbance of the blank; m=slope (from the standard curve); m_0 = mass of the sample (g); 55.84 =atomic weight of iron.

b. Thiobarbituric acid reactive substances (TBARS)

TBARS of the powders were determined according to method described in Mei, McClements, Wu and Decker (1998). A solution of thiobarbituric acid (TBA) was prepared by mixing 15g of tricholoroactic acid, 0.375 g of TBA, 1.76 mL of 12 N HCL, and 82.9 mL of H_2O. The TBA solution (100 mL) was mixed with 3 mL of 2 (g/100 mL) butylated hydroxytoluene in ethanol. Then, 2 mL of the resulting solution were mixed with 1 mL of a sample prepared with 0.5 g of powder and 5 mL of distilled water. The mixture was vortexed for 10 s and heated in a boiling water bath for 15 min. Then, it was allowed to cool to room temperature at 25°C and centrifuged at 3400 x g (5600 rpm) for 25 min. The absorbance of the supernatant was measured at 530 nm. Concentrations of TBARS were determined from standard curves prepared with 0-0.02 mmol/L of 1,1,,3,- tetraethoxypropane. The results were expressed in mmol of equivalents of malonaldehyde per kg oil.

4.2.1.5.4 Microstructure and particle size analysis

Scanning Electron Microscopy (SEM) micrographs were obtained at the Louisiana State University - Institute for Advance Materials. The microstructure of the powders was evaluated by SEM (JSM-6610LV, JEOL Ltd. Japan). The samples were mounted on aluminum SEM stubs, and then coated with gold:palladium (60:40) in an Edwards S150 sputter coater (Edwards High Vacuum International, Wilmington, MA). The powders were systematically observed at 1000X of magnification. Particle size analysis was carried out at the Composites and Engineered Wood Products Laboratory of the LSU-School of Renewable Natural Resources. Particle size was measured by a Microtrac S3500 system (MicroTrac, Largo FL). The system is equipped with three solid state lasers fixed at 780 nm. Powder samples were placed into the test chamber with circulating ethanol. A 10s period of ultrasound mixing at 20 watts was used before each test.

Then the sample was pumped through the sample cell at 40% of the maximum flow rate. Light was scattered from the tri-lasers from low to high angles (0-163 degrees). The volume distribution of the particle size was calculated using modified MIE-scattering technique.

4.2.1.5.5 Statistical analysis

Experimental data was statistically analyzed by SAS software version 9.2 (SAS Institute Inc., 2008). Mean values and standard deviations from triplicate analysis were reported. A factorial experimental design was used to carry out the Analysis of Variance (ANOVA). A Tukey's studentized range test was carried out to determine differences among treatments at the significant level of $P<0.05$.

4.2.2 Computational fluid dynamics (CFD) simulation methodology

In this study, two sub-processes were separately studied to successfully model the spray drying procedure using CFD; this approach allowed reaching convergence faster during the CFD simulations. The drying phenomena occurring in the drying chamber was studied in the first case; meanwhile, the second case was defined as the separation of the dried particles at the cyclone separator. The CFD code ANSYS FLUENT 15.0 was used to develop the spray drying simulations in a 3D-geometry using a pseudo-transient-method; which is a form of implicit under-relaxation for steady-state conditions for air flow and particle injections under CO and CNT spray drying configurations using a pressure nozzle with a solid-cone spray. Also, a hybrid solution initiation was used to improve the convergence of the simulations. A 3D model of the spray dryer was created in Autodesk Inventor (Fig.4.2) with the same dimensions of the pilot scale spray dryer. The convergence of the numerical solution has been checked by means of residuals of the governing equations and also by net imbalances between the entering and leaving mass flow and heat transfer rates.

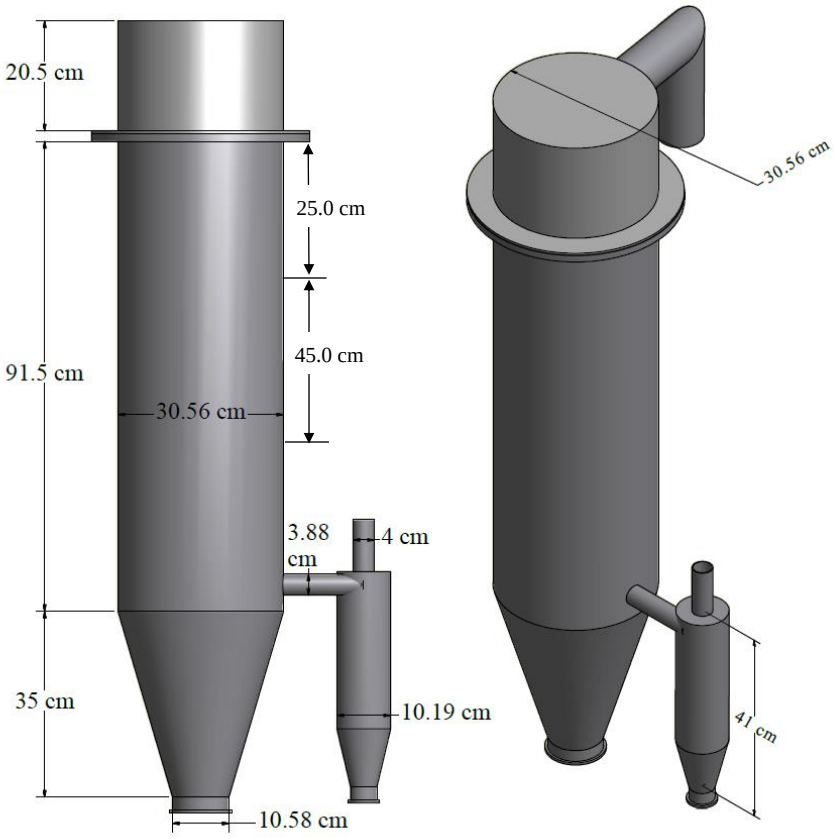

Fig. 4.2 - Three-dimensional pilot scale spray dryer model

4.2.2.1 Case 1 - Drying chamber

4.2.2.1.1 Simulation conditions

In the first CFD simulation case, drying hot air at different temperatures and sprayed feed droplets at different feed rates were introduced into the spray chamber at quasi-steady state conditions. Feed had a moisture content of 85 (g/100g) and was sprayed by a nozzle either from the top (CO) (Fig. 4.3A) or from the bottom (CNT) (Fig. 4.3B) of the drying chamber. In this case, the flow pattern, temperature, and velocity of the drying air were modeled. Also, the particles histories: residence time (RT), temperature, velocity, moisture content and particle size distribution at the outlet of the spray dryer chamber were predicted. To successfully develop the CFD simulations; the 3D model of the spray dryer chamber was simplified (Fig 4.3). The 3D model of the spray dryer chamber had 57,847 grill cells (Fig. 4.3C).

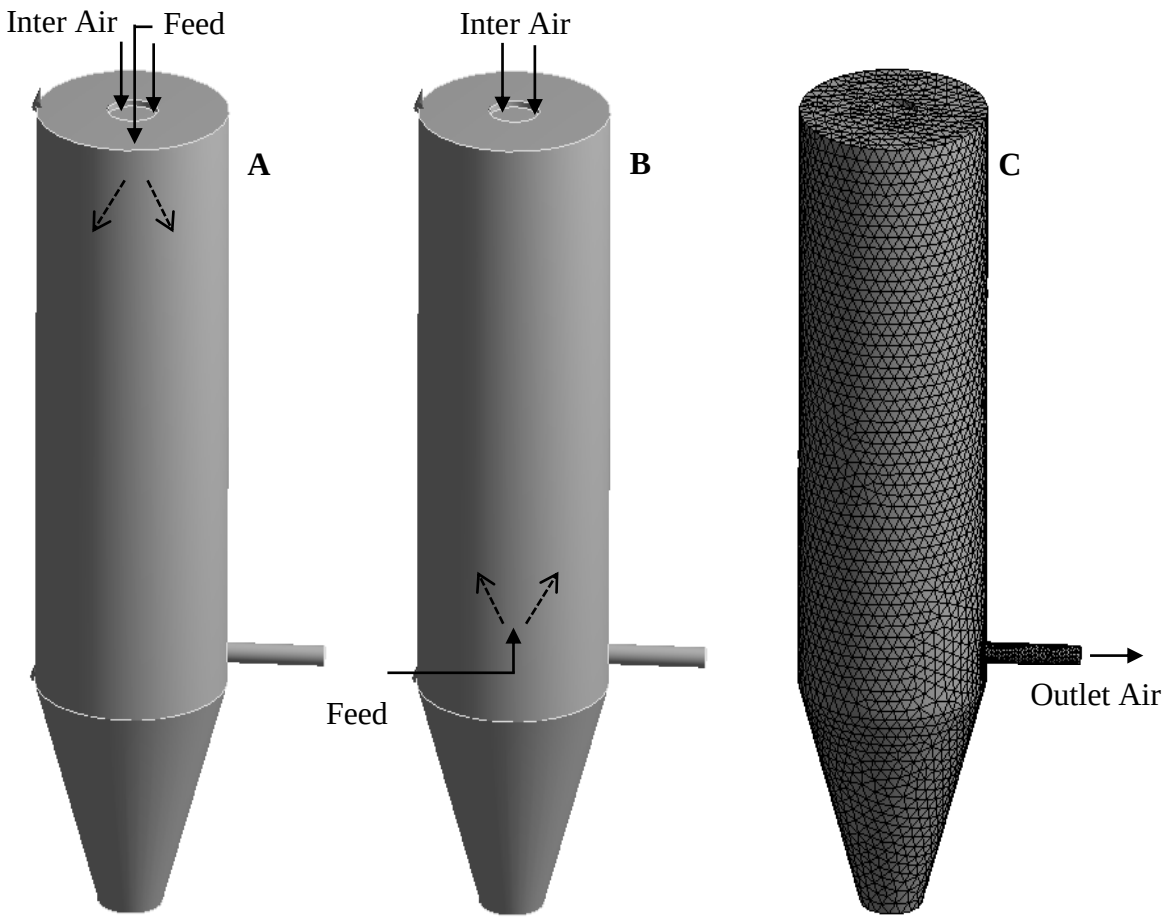

Fig. 4.3 - Spray Dryer Chamber: (A) Co-current (CO) configuration, (B) Counter-current (CNT) configuration, and (C) Computational domain and meshing.

The boundary conditions for this case are described in Table 4.2. Initial droplet size distribution was given by a fit of the Rosin-Rammler distribution which was discretized into 10 particle size classes ranging from 35 to 75 μm. Also, the finite volume approach was utilized to resolve the set of partial differential equations of a two-way coupled Euler-Lagrange method for the continuous and discrete phases. Using this approach, there is a feedback mechanism in which the continuous and dispersed phase flows interact. The governing equation for the continuous and dispersed phases are detailed in Huang, Kumar and Mujumdar (2004). The discrete phase was defined as multicomponent evaporating droplets available in Ansys Fluent. Feed with two components (solids and water) were included in the model, being water the evaporative element.

4.2.2.1.2 Turbulence model

The realizable *k-ε* turbulent model was used in this CFD simulation. According to Huang, Kumar and Mujumdar (2003b), low swirl is expected in a spray drying chamber; so, the *k-ε* turbulent model is appropriate to simulate the air flow inside the chamber. Moreover, in the realizable *k-ε*, the term "realizable" means that the model satisfies certain mathematical constraints on the normal stresses, consistent with the physics of turbulent flows (Kuriakose & Anandharamakrishnan, 2010). Eqs. 4.3–4.5 were used to estimate the *k* and *ε* values as described in (Langrish & Zbicinski, 1994)

$$k = \frac{3}{2}(v_{inlet} I)^2 \quad (4.3)$$

Where, *I* is the intensity of turbulence at the inlet, *I* was calculated by using Eq. 4.4

$$I = 0.2\, Re^{-1/8} \quad (4.4)$$

Where, *Re* is the Reynolds number at the inlet. The energy dissipation (*ε*) was calculated by using Eq. 4.5.

$$\varepsilon = \frac{{C_\mu}^{3/4} k^{3/2}}{l} \quad (4.5)$$

Where, *l* is the length scale of the turbulence (in this case is the diameter of the inlet opening to the dryer chamber), v_{inlet} is the inlet gas velocity, C_μ is a constant. Particles histories were obtained from the simulation results using ANSYS CFD post-processing.

4.2.2.2 Case 2 – Cyclone separator

To carry out the 3D-CFD simulations for the second case, three different inlet air temperatures were used 130, 150 and/or 170, respectively. The CFD simulations were carried out by following the set up conditions described in Chu, Wang, Xu, Chen and Yu (2011). Using this approach, all of the particles were treated as spherical; this required less computational effort. The simplified 3D-model of the cyclone had 57, 584 grill cells Figs. 4.4-A, and B.

Table 4.2 - Conditions for the CFD simulation –Case 1

Inlet Air		**Feed spray from nozzle**	
Temperature (°C)	130, 150, 170	Feed rate (Kg/h)	0.50, 0.75, 1.0
Mass Flow rate (Kg/s)	17.5929	Feed temperature (°C)	25
Velocity (m/s)	3.5	Moisture content (g/100g)	85
Outlet condition (Pa)	-100	Spray angle (full angle)	60
Turbulent Model		Minimum droplet diameter (μm)	35
Turbulent *k*-value (m^2/s^2) (Eq.4.3)	0.09	Maximum droplet diameter (μm)	75
Turbulent ε-value (m^2/s^3) (Eq. 4.5)	0.055	Average droplet diameter (μm)	50
Chamber wall conditions		Droplet velocity at nozzle exit (m/s)	8
Chamber wall thickness (mm)	5	Rosin-Rammler spread parameter	3.5
Wall material	Steel		
Wall heat transfer coefficient (W/m^2K)	0		
Interaction between wall and droplet	Reflect		

Fig. 4.5 shows the CFD simulation steps. First, the simulation of the drying air flow was solved until reaching steady state flow conditions; then, dried particles were introduced at the inlet of the cyclone. After the drying air reaches its steady state flow, the pressure drop was estimated by the average difference in static pressure at the inlet and at the outlet of the cyclone. The boundary conditions for the second CFD case are described in Table 4.3. The initial particle size distribution was taken from the data previously generated from CFD case 1. As in case 1, the particle size distribution followed a fit of the Rosin-Rammler (RR) distribution which was discretized into 10 particle size classes. The finite volume approach was used to resolve the set of partial differential equations as previously described for CFD case 1.

4.2.2.2.1 Turbulent model

Several works have tested different turbulent models to predict the flow behavior of air inside cyclones and the Reynolds Stress Model (RSM) turbulent model has produced satisfactory results (Chu, Wang, Xu, Chen & Yu, 2011). So, in this study the RSM turbulent model was used.

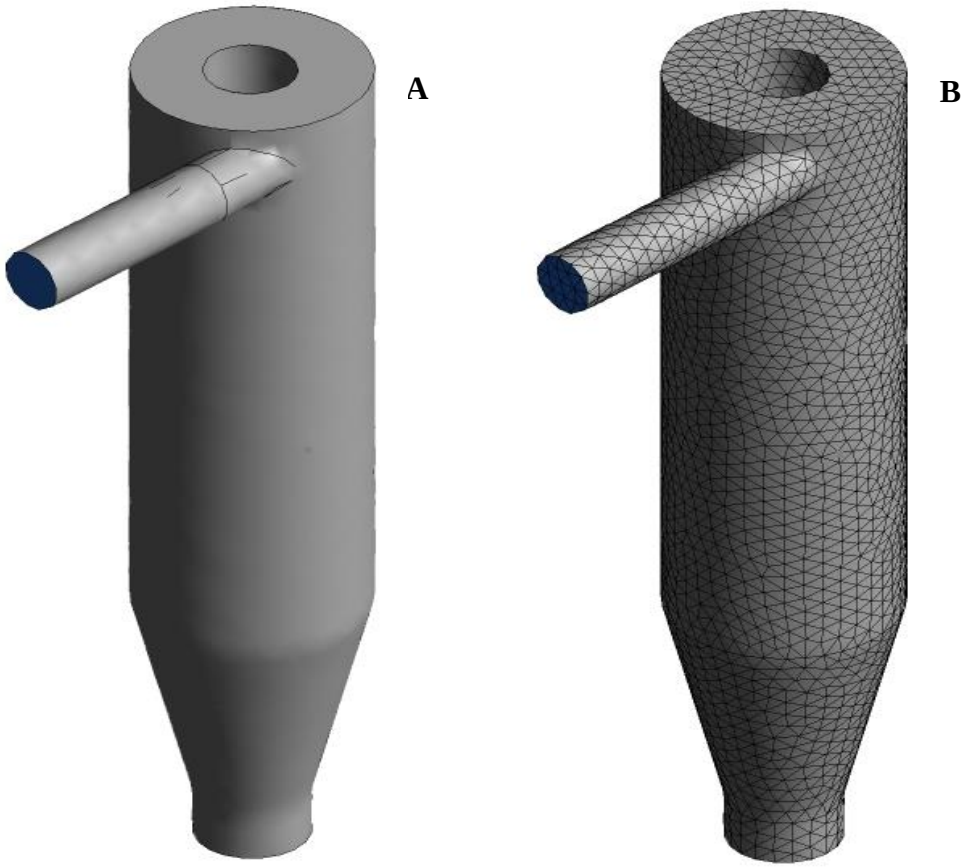

Fig. 4.4 - Cyclone separator: (A) 3D model for CFD, (B) Computational domain and meshing.

Table 4.3 - Conditions for the CFD simulation – Case 2.

Inlet air		**Dried particles**	
Temperature (°C)	130, 150, 170	Feed rate (Kg/s)	0.00002254
Mass Flow rate (Kg/s)	17.5929	Particles' temperature (°C)	130, 150, 170
Velocity (m/s)	25	Moisture content (g/100g)	0
Outlet condition (Pa)	-200	Minimum droplet diameter (µm)	14
Turbulent model		Maximum droplet diameter (µm)	37
Reynolds Stress Model (RSM)		Mean droplet diameter (µm)	24
Chamber wall conditions		Rosin-Rammler spread parameter	3.5
Chamber wall thickness (mm)	5		
Wall material	Steel		
Wall heat transfer coefficient (W/m^2K)	0		
Interaction between wall and droplet	Reflect		

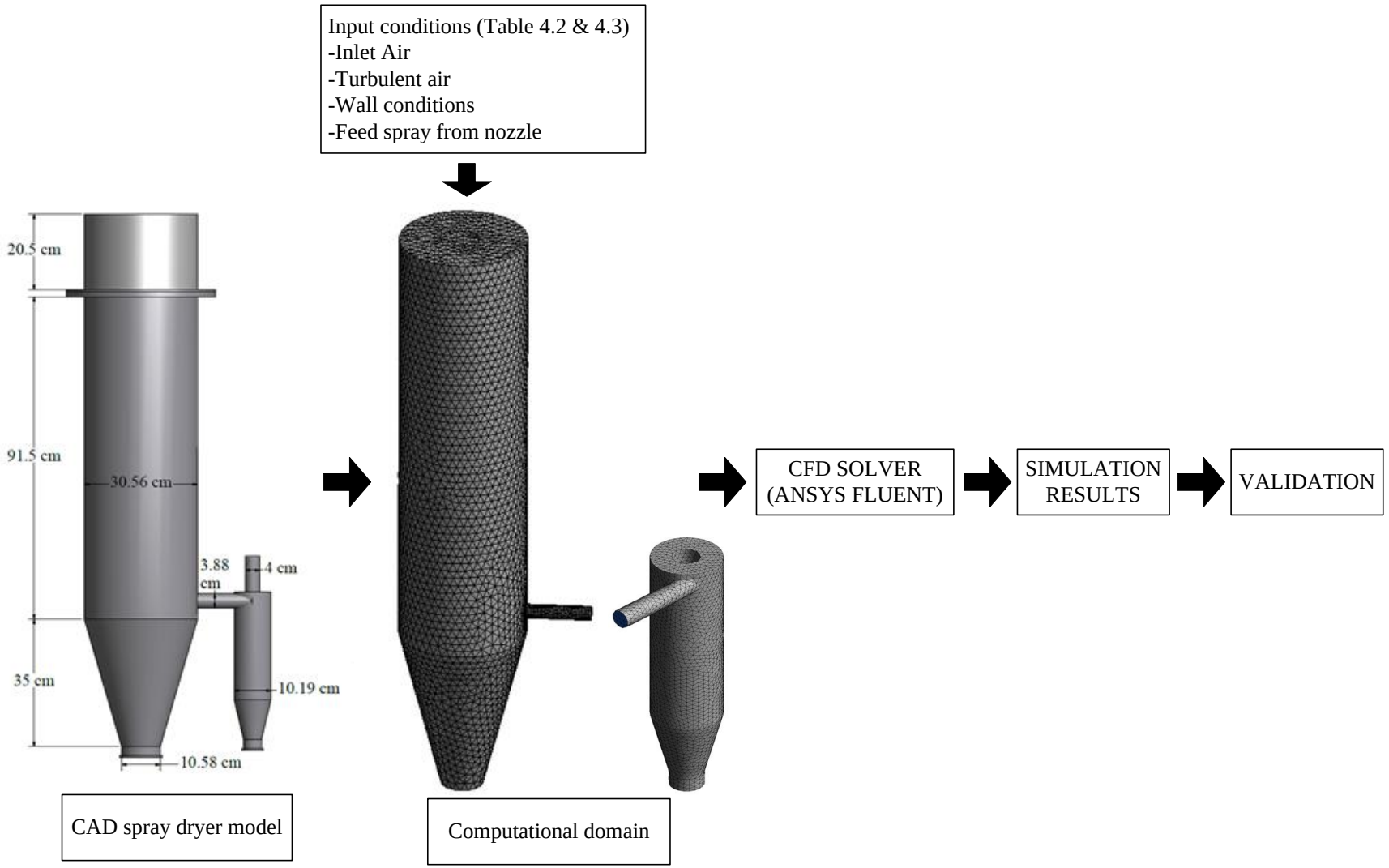

Fig. 4.5 - CFD simulation steps.

4.3 Results and discussion

The development of 3D-CFD simulations is essential to accurately predict drying air flow patterns and particle histories and trajectories inside the spray dryer (Mezhericher, Levy & Borde, 2009). According to Kuriakose and Anandharamakrishnan (2010), 3D-CFD simulations are better than 2D-CFD simulations because the asymmetry of the drying air flow patterns and particle trajectories can be predicted and therefore more accurate results are obtained. However, 3D-CFD simulations require higher computational power; so, they are recommended for detailed spray drying studies.

As previously discussed, the two main sections of the pilot-scale spray dryer used in this study are the dryer chamber and the cyclone separator. Due to the complexity of the drying phenomena taking place inside the spray dryer, each section of the spray dryer has been studied separately. This simplification allowed the convergence of the 3D-CFD simulations.

The first part of this study (case 1) focused on the drying phenomena occurring at the drying chamber of the spray dryer. Meanwhile, the second case focused on the separation of the spray-dried particles from the drying air flow inside the cyclone separator.

4.3.1 Case 1

4.3.1.1 Experimental validation

4.3.1.1.1 Drying air velocity

The measured and predicted drying air velocities inside the drying chamber are shown in Fig. 4.5. According to Mezhericher, Levy and Borde (2009), air velocity inside the spray dryer is one of the most important parameters of the spray drying process because it influences the particle residence time inside the drying chamber. Experimental air velocities were measured during CO and CNT spray drying conditions.

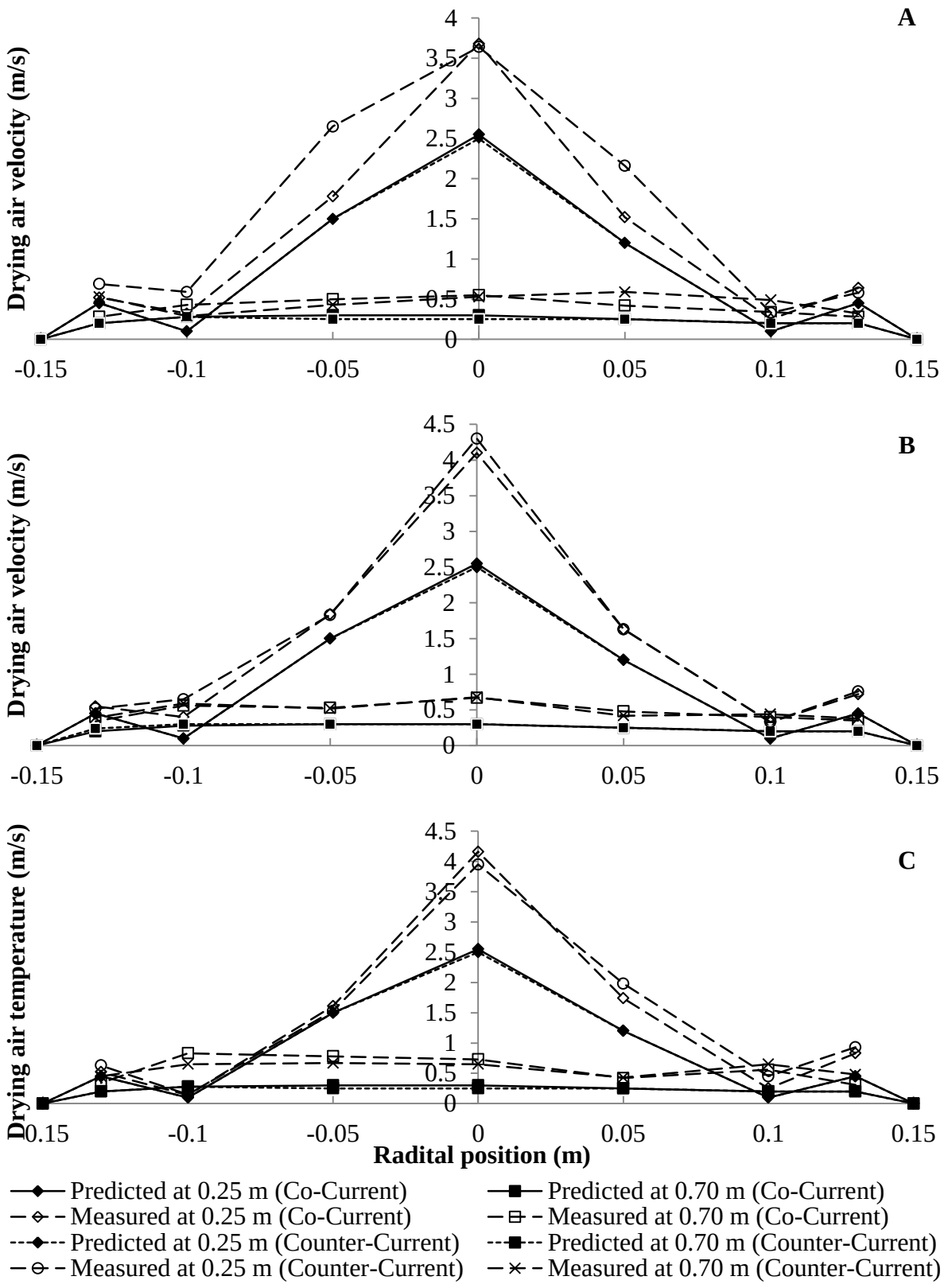

Fig. 4.6 - Predicted and measured drying air velocities at 0.25 and 0.70 m from the ceiling of the drying chamber of the spray dryer using inlet air temperatures of (A) 130, (B) 150 and (C) 170°C.

Furthermore, experimental air velocity values were taken at a distance of 0.25m and 0.70m from the ceiling of the drying chamber (Fig. 4.2); and the results were compared with those predicted by the 3D-CFD model at the same points.

Experimental and predicted drying air velocities showed higher drying air velocities at the core (radial center) of the drying chamber which may be due to the fact that the drying air enters the drying chamber at the inlet opening located at the top and radial center of the drying chamber as seen in Fig.4.3.

Moreover, experimental measurement values were slightly higher than predicted values; and higher drying air velocities were obtained at 0.25 m compared to those obtained at 0.70 m which can be attributed to the proximity of the inlet opening to the recording location inside the drying chamber. Experimental and predicted data demonstrated no significant variations in drying air velocities were between CO and CNT spray drying configurations at 130, 150 and/or 170°C inlet air temperatures (Fig. 4.5 A, B, and C). Similar results for air velocities in spray dryers have been obtained by Mezhericher, Levy and Borde (2009) and Anandharamakrishnan, Gimbun, Stapley and Rielly (2009) with satisfactory agreement.

4.3.1.1.2 Drying air temperature

Air temperature values inside the drying chamber were recorded to validate the results of the CFD simulations. The results for air temperatures inside the drying chamber for spray drying of E-MO-LEWH at 130, 150, and 170°C using CO and CNT spray drying configurations are shown in Figs. 4.6 A, B, and C. According to Huang, Kumar and Mujumdar (2003a), numerical simulations of the spray drying process can generate reliable results similar to experimental data in terms of velocity, temperature and humidity of the drying air. In this study, experimental and predicted results showed lower drying air temperatures at the core (radial center) of the drying

chamber for measurements taken at 0.70m than those recorded at 0.25m. Furthermore, greater drops in air temperature values were recorded at 0.25 m for CO compared to those of CNT spray drying. In contrast, greater drops in air temperature values were recorded at 0.70 m for CNT than for CO spray drying. This effect can be explained by the location of the nozzle inside the drying chamber during CO and CNT spray drying configurations. During spray drying, the feed is directly sprayed into the drying chamber either from the top (CO) or from the bottom (CNT); this produces high heat and mass transfer rates in the nozzle zone due to relatively high velocities between the hot drying air and the feed droplets with large temperature driving forces (Huang, Kumar & Mujumdar, 2003a). Our results are in good agreement with those reported by Huang, Kumar and Mujumdar (2003b) and Birchal, Huang, Mujumdar and Passos (2006) for CO spray drying configurations.

According to Mezhericher, Levy and Borde (2009) experimental data is the result of time-averaged values of measurements done with some accuracy; however, variations up to 70% between the predicted and experimental data can be obtained.

4.3.1.2 Simulation results

Results for predicted flow patterns, temperature, velocities of the drying air are presented in this section. Also, predicted results for particle histories are discussed and compared against experimental results. For the 3D-CFD simulations, two parameters were tracked during the numerical iteration: residuals and outlet velocity.

The criteria for convergence were established based on the results for the residuals. Feed droplets were introduced into the drying chamber after the outlet reached quasi-steady-state conditions (at 200 iterations). This approach allowed reaching convergence in the simulations which was achieved after 800 iterations.

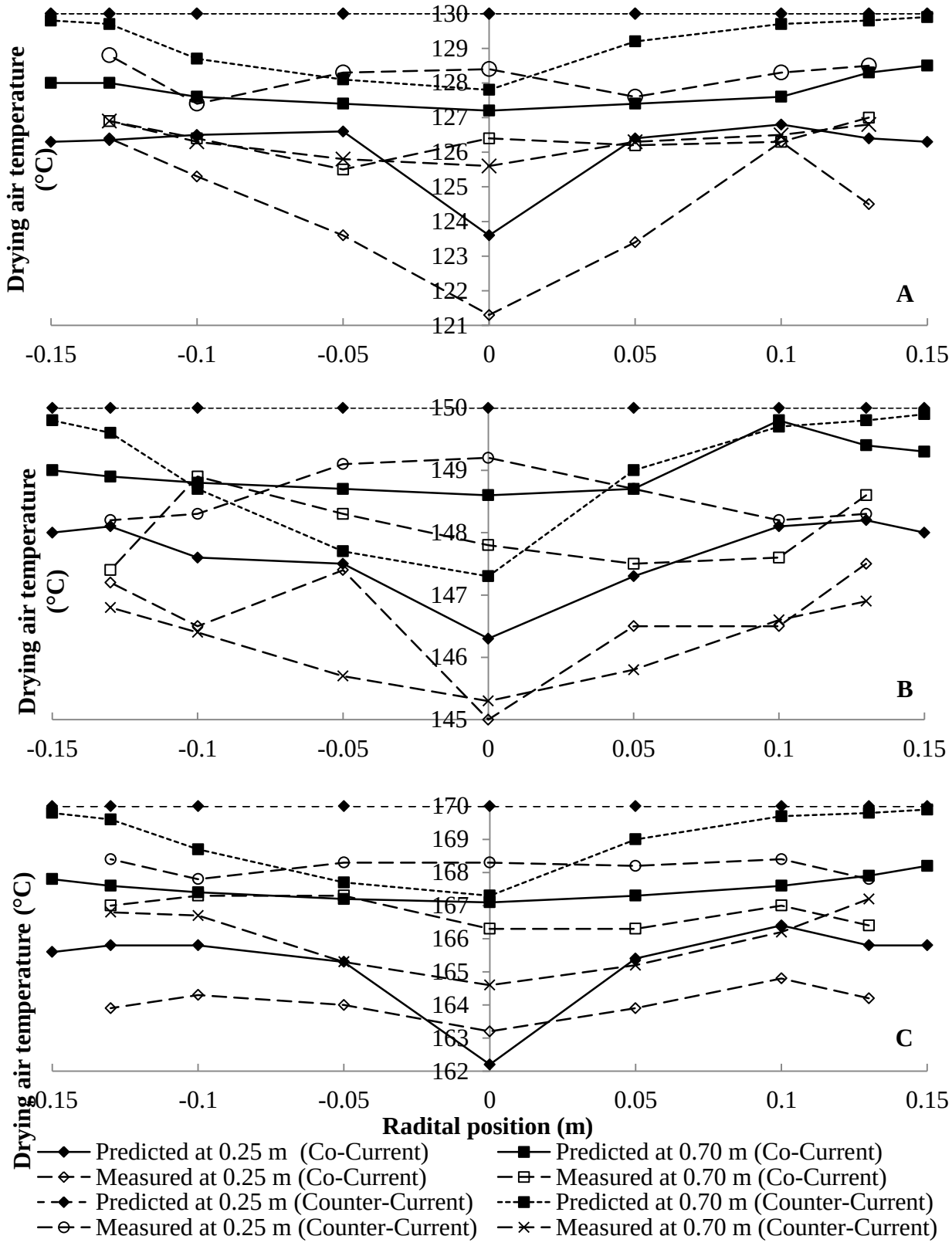

Fig. 4.7 - Predicted and measured drying air temperatures at 0.25 and 0.70 m from the ceiling of the drying chamber of the spray dryer using inlet air temperatures of (A) 130, (B) 150 and (C) 170°C

4.3.1.2.1 Drying air flow pattern

The drying air flow patterns inside the drying chamber during spray drying are shown in Figs. 4.7, 4.8, and 4.9 for CO and CNT spray drying. It can be observed that the drying air flow patterns are similar for both CO and CNT spray drying configurations.

According to the results obtained by the 3D-CFD model, no air recirculation occurs inside the drying chamber at all of the tested conditions, this effect is desirable because air recirculation inside the drying chamber increases RT and thermal degradation of bioactives. Additionally, no reverse air flows are identified across the drying chamber during CO and CNT spray drying configurations. The results suggested that neither the inlet air temperatures nor the feed rate (data not shown) affected the drying air flow patterns inside the drying chamber.

Using the 3D-CFD simulations, it was possible to predict the asymmetric drying air flow patterns inside the drying chamber. Drying air flow patterns are affected by the drying chamber design and 3D-CFD simulations can effectively predict flow patterns of the drying air using an adequate turbulence model (Kuriakose & Anandharamakrishnan, 2010). Several studies have previously reported a precise prediction of the flow pattern of the drying air using CFD (Langrish, Williams & Fletcher, 2004; Mezhericher, Levy & Borde, 2009; Oakley & Bahu, 1993).

In accordance with Huang, Kumar and Mujumdar (2003a), the k - ε turbulent model is a suitable model to simulate the air flow inside the drying chamber because there is not high swirling flow inside of it. Furthermore, the realizable k - ε turbulent model satisfies certain mathematical constraints on the normal stresses which are consistent with the physics of turbulent flows. This model provides better results for predicting air flow patterns under strong pressure gradients, separation and recirculation (Kuriakose & Anandharamakrishnan, 2010).

4.3.1.2.2 Drying air temperature profile

Time-temperature profile of the drying air flow pattern is shown in Figs. 4.7-A, 4.8-A, and 4.9-A for the spray drying of microencapsulated powders at inlet air temperatures of 130, 150, and 170°C, respectively. The simulation results demonstrated that drying air enters into the drying chamber at the adjusted inlet air temperatures in CO and CNT spray drying.

Moreover, in the case of CO spray drying, the drying air immediately gets in contact with the feed droplets at the top of the drying chamber; this effect produces a drop in the drying air temperatures up to 7.3, 4.1, and 4.5 Celsius degrees for spray drying at inlet air temperatures of 130, 150, and 170°C, respectively. According to Birchal, Huang, Mujumdar and Passos (2006), a drop in the drying air temperature inside the drying chamber is due to the heat transfer between the drying air and the feed droplets. Gharsallaoui, Roudaut, Chambin, Voilley and Saurel (2007) reported that higher evaporation rates are observed at this region of the drying chamber during CO spray drying, therefore, higher moisture evaporation rates are expected in this zone.

In the case of CNT spray drying, the feed droplets reach the drying air approximately below the center region of the drying chamber as seen in Figs. 4.7-A, 4.8-A, and 4.9-A. This produces greater drops in drying air temperature in this zone. It is also observed that at this section of the drying chamber, the drying air flow is fully developed.

Furthermore, predicted results demonstrated that changes in feed rate did not have any effect in the temperature of the drying air flow pattern neither in CO nor CNT spray drying configurations (data not shown). Drying air temperatures, feed temperatures, and feed droplet size have a significant impact on drying rate and overall quality of spray-dried powders (Kuriakose & Anandharamakrishnan, 2010). As previously discussed, there is a lack of scientific information about the temperature profiles of the drying air in CNT spray drying configuration.

So, 3D-CFD simulations can help to understand the drying phenomena inside the spray dryer. This is the first attempt to use computational tools to compare temperatures of the drying air flow pattern inside the drying chamber using different spray drying configurations.

4.3.1.2.3 Drying air velocity prolife

The time - drying air velocity profiles for CO and CNT spray drying are shown in Figs. 4.7-B, 4.8-B, and 4.9-B for inlet air temperatures of 130, 150, and 170°C, respectively. The 3D-CFD simulations suggested that drying air velocities were not affected either by the inlet air temperature or spray drying configuration. Furthermore, inlet drying air enters the drying chamber at 3.5 m/s; however, this velocity quickly decreased due to the expansion of the inlet air inside the drying chamber. Predicted results also revealed that greater drying air velocities at the outlet of the drying chamber (up to 31.5 m/s) are due to the high volumetric flow rates of the drying air at the small-diameter drying chamber's outlet. Similar observations were reported by Huang, Kumar and Mujumdar (2004).

To effectively develop the 3D-CFD simulations, the coupled Euler-Lagrange approach was used; this method allowed treating the drying air as the continuous phase and the feed droplets as the discrete phase. This approach also allowed the drying air to affect the momentum and trajectories of the drying particles and vice versa. The predicted results showed that the drying particles did not produce significant changes in the drying air velocities during CO and CNT spray drying. According to Xia and Sun (2002), drying rate is highly influenced by the air flow and air velocity; therefore, it is very important to identify the drying area inside the drying chamber to assure a proper drying process. Furthermore, 3D-CFD simulations are useful to predict air velocities inside the drying chamber because they are usually extremely difficult to obtain experimentally.

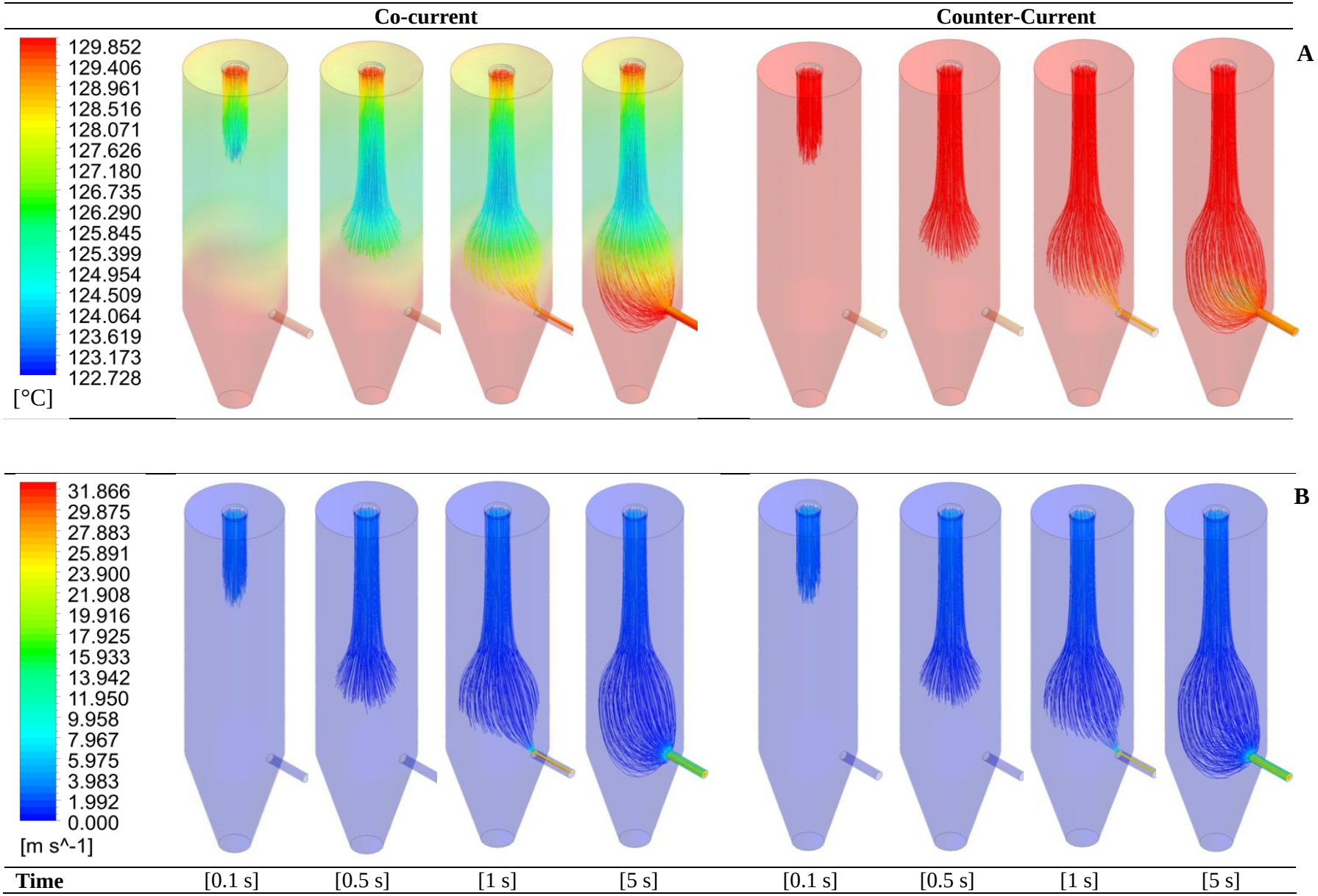

Fig. 4.8 - Time-temperature (A) and time-velocity (B) profiles of drying air inside of the drying chamber during the spray drying of a emulsion at 0.50 Kg/h feeding rate and 130°C inlet temperature under co-current and counter-current conditions

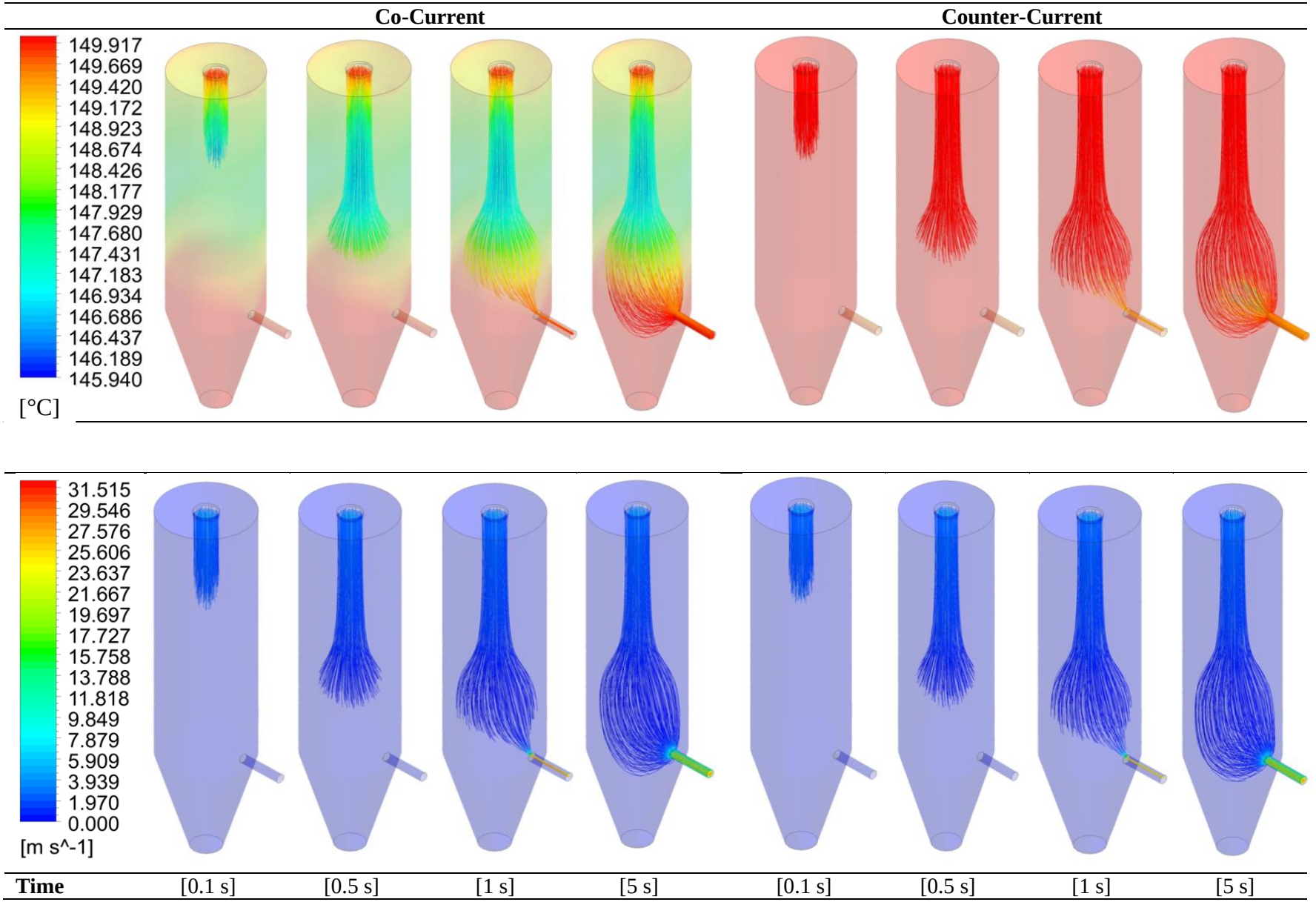

Fig. 4.9 - Time-temperature (A) and time-velocity (B) profiles of drying air inside of the drying chamber during the spray drying of a emulsion at 0.50 Kg/h feeding rate and 150°C inlet temperature under co-current and counter-current conditions

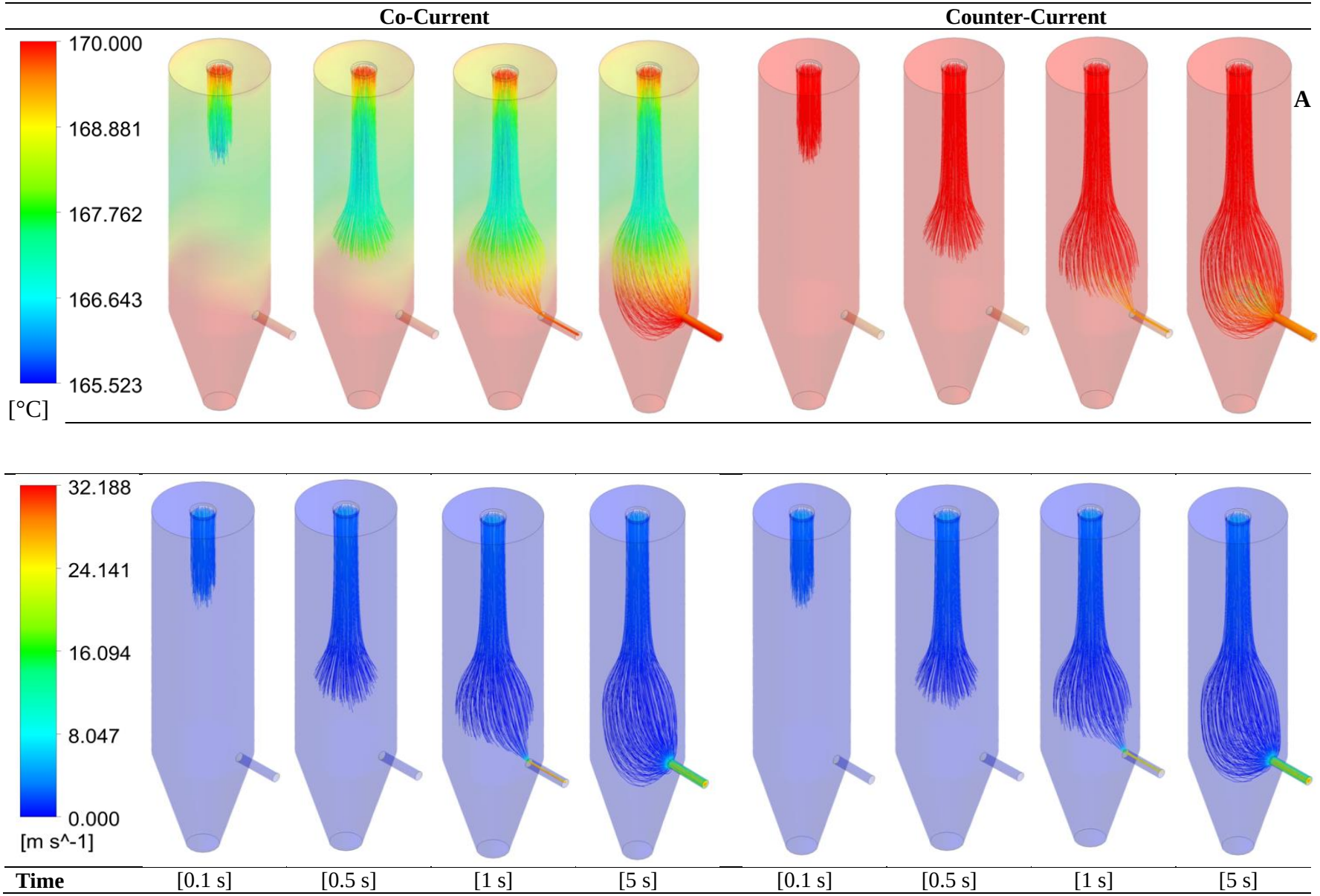

Fig. 4.10 - Time-temperature (A) and time-velocity (B) profiles of drying air inside of the drying chamber during the spray drying of a emulsion at 0.50 Kg/h feeding rate and 170°C inlet temperature under co-current and counter-current conditions

4.3.1.2.4 Particle residence time (RT)

Using CFD, the RT was calculated by tracking a high number of particles through the flow domain and recording the time that each particle spent from the atomizer to the outlet of the dryer chamber. Using the coupled Euler-Lagrange approach, the RT was given by the trajectory of the particles; which is affected by the drying air flow pattern. In this study, the maximum, mean and minimum RT are shown in Figs. 4.12 A, B, and C, respectively.

According to the CFD results, greater RT values were observed in CO spray drying compared to those of CNT spray drying. Moreover, the results revealed that the mean and maximum RT values for CO spray drying were from 2.5 to 3s and from 12 to 14 s, respectively. Meanwhile, the mean and maximum RT values for CNT spray drying were from 0.5 to 0.75s and from 6 to 9s. Neither the drying air temperature nor the feed rate clearly affected the RT. These results may be due to the longer distances that the particles needed to travel and particle recirculation in CO spray drying configurations (Fig. 4.10). Fig. 4.11 shows the trajectories of particles based on their size inside the drying chamber. It was observed that in CO spray drying, smaller particles have more recirculation (outside the core region of the drying chamber) than larger particles. These results are in agreement with those reported by Anandharamakrishnan, Gimbun, Stapley and Rielly (2009) for CO spray drying design.

Using 3D-CFD simulations produced asymmetry particle flows in the spray drying chamber which is more accurate to the real conditions. Therefore, this type of approach is more powerful than 2D-CFD simulations (Mezhericher, Levy & Borde, 2009). According to Kuriakose and Anandharamakrishnan (2010), RT is a very important parameter to develop spray drying processes and have a huge impact on product quality.

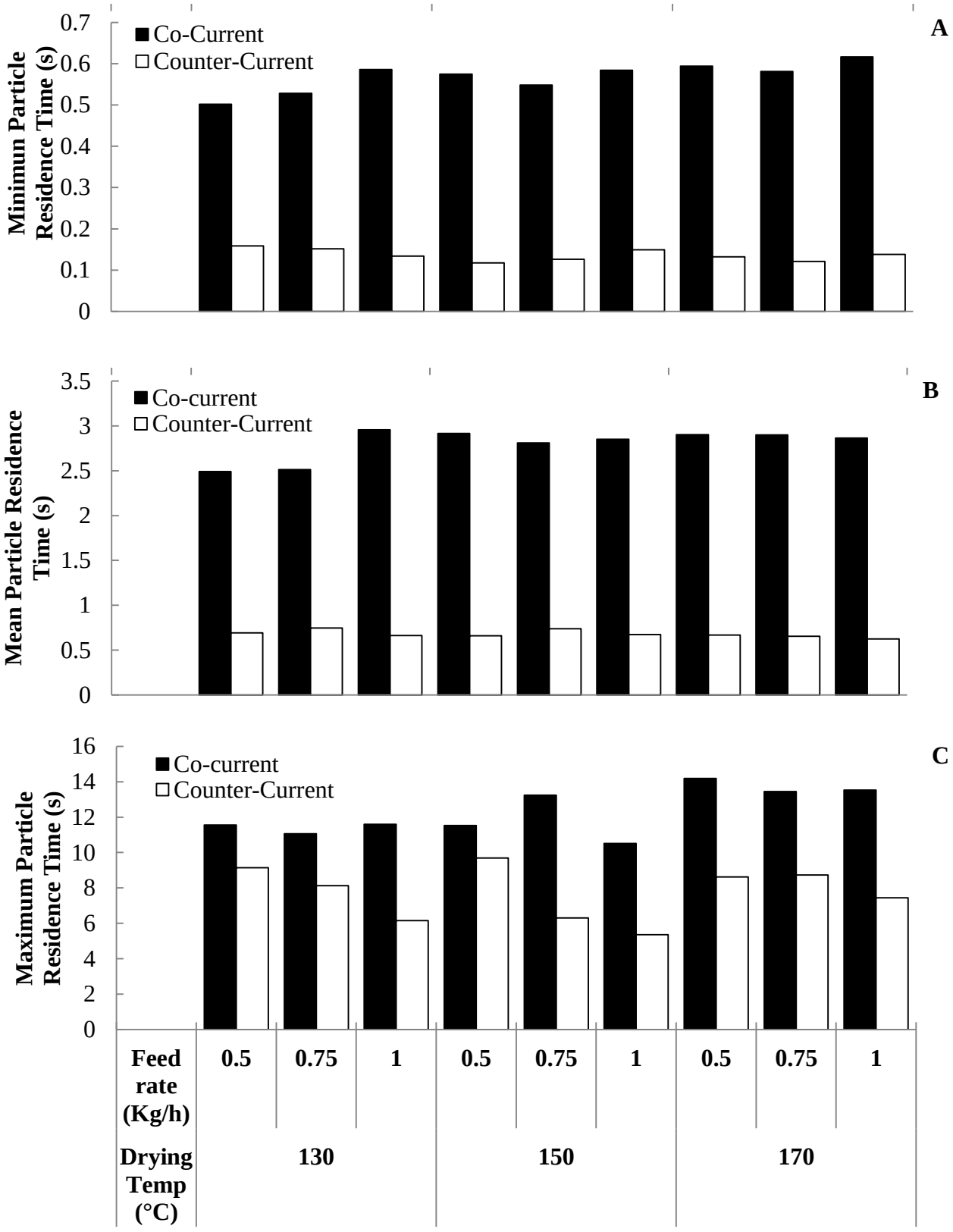

Fig. 4.11 - Predicted particle residence times inside the drying chamber during co-current and counter-current spray drying (A) Minimum values, (B) Average values, and (C) Maximum values

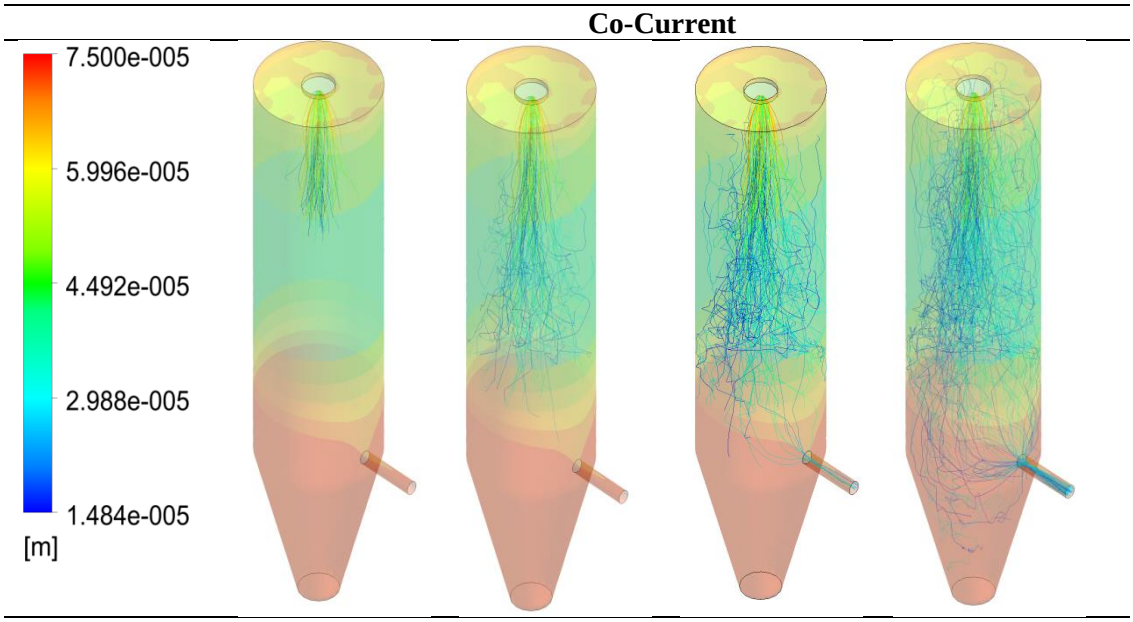

Fig. 4.12 - Simulated particle trajectories based on their diameter (m) inside the drying chamber in co-current and counter-current spray drying configurations at 130°C inlet air temperature.

4.3.1.2.5 Particle temperature

Particle -temperature profiles based on particle trajectories during spray drying is shown in Fig. 4.12. It is observed that powder particles quickly reached drying air temperature in both CO and CNT spray drying configurations. Combining these results and those previously discussed

for particle trajectories based on particle sizes, it can be seen that smaller particles quickly reached temperatures of the drying air and remain inside the drying chamber for longer times (higher RT). This effect is more evident in CO spray drying. This information may be valuable to explain thermal degradation of bioactives during spray drying using CO and CNT spray drying configurations. Hence, it is assumed that smaller spray-dried particles (below 15µm) experienced more thermal degradation and moisture evaporation than larger particles. However, the quantification of these differences is of out the scope of this study. According to Huang, Kumar and Mujumdar (2003b), particles of the same initial diameter can exit the drying chamber with different temperatures and moisture contents; and these parameter are highly influenced by the flow and temperature of the drying air.

4.3.1.3 Microencapsulated powders

4.3.1.3.1 Moisture content

In this study, CFD simulations predicted almost the total moisture evaporation from the feed droplets during the spray drying process (Fig. 4.13). However, experimental results demonstrated that the spray dried powders had moisture contents from 5.12 to 7.29 (g/100 g). It is believed that most of the remaining moisture (experimentally quantified) is molecular and bound water that remained in the powders after the drying process.

The initial moisture content of the feed was 85 (g/100 g). Free water was the only type of water included into the CFD model; meanwhile, molecular and bound water were neglected to simplify the simulations. Therefore, the CFD simulation slightly overestimated the moisture removal from the feed during spray drying. Lower predicted values compared to those experimentally obtained for moisture were also obtained by Pinto, Kemp, Bermingham, Hartwig and Bisten (2014) during CO spray drying simulations.

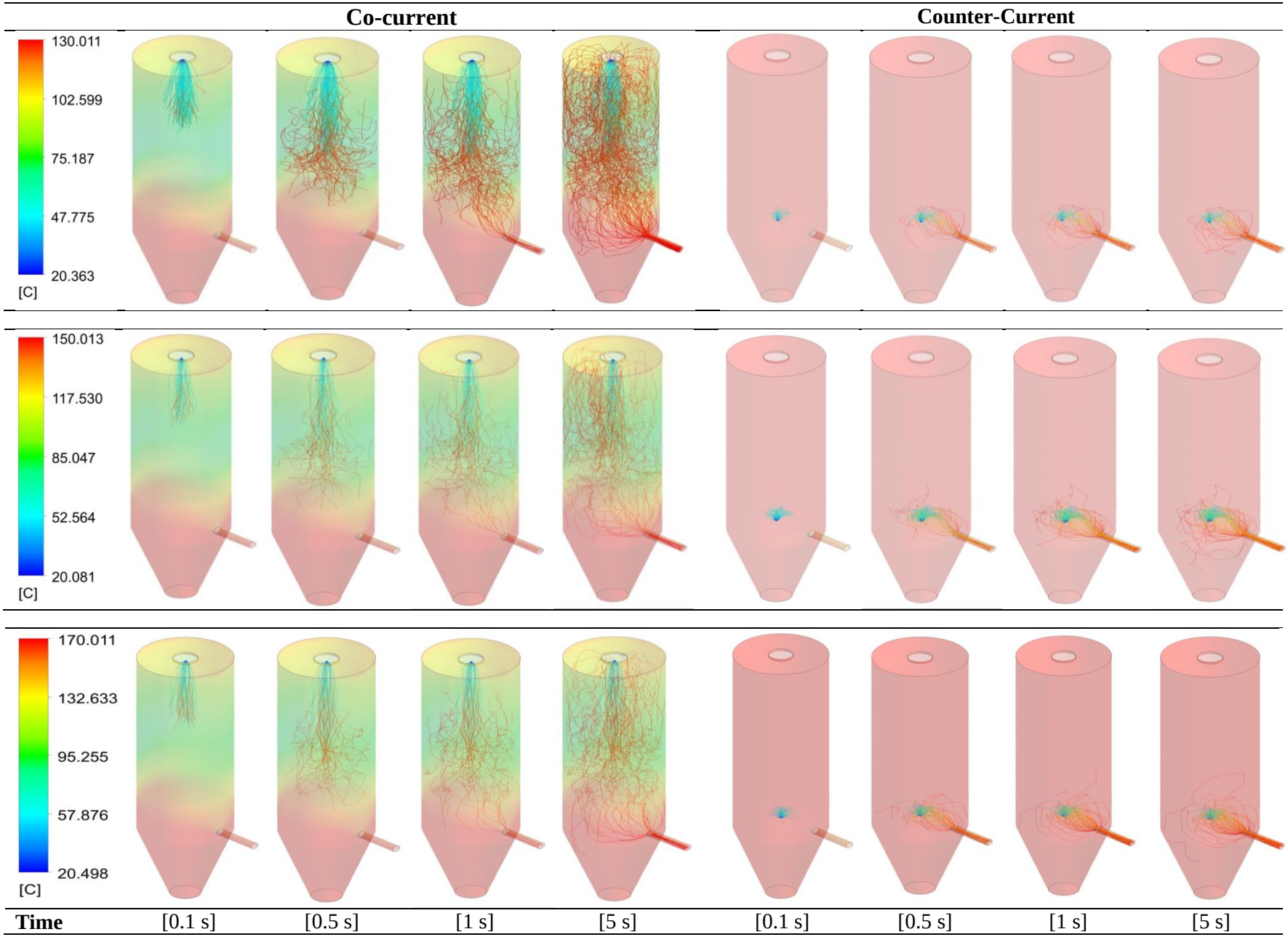

Fig. 4.13 - Time-temperature profiles of drying particles during the spray drying of an emulsion at 0.50 Kg/h feeding rate and 130 (A), 150 (B) and 170°C (C) inlet air temperature under co-current and counter-current conditions

Moreover, the experimental data demonstrated that moisture content was significantly ($p<0.05$) affected by the inlet air temperature, spray drying configuration and interaction of both effects.

Therefore, powders produced in CO spray drying had significantly ($p<0.05$) lower moisture content than the powders produced in CNT spray drying (at 170°C inlet air temperatures).The feed rate did not have a significant ($P<0.05$) effect on the final moisture content of the powders (Fig. 4.13).

CFD simulations demonstrated that most of the moisture evaporation occurs immediately after the feed droplets are sprayed inside the drying chamber (Fig. 4.14). Also, it was seen that higher inlet air temperatures increases evaporation rates in CO spray drying (Figs. 4.14, A, B, and C); meanwhile this effect is less evident in counter-current spray drying.

These results are in agreement with those reported by Woo, Daud, Mujumdar, Wu, Meor Talib and Tasirin (2008). Furthermore, particle recirculation can be observed in co-current spray drying which increased RT and affected the moisture content of the resulting dried particles.

Besides the atomization conditions, temperature and humidity of the drying air, and moisture content and temperature of the feed can also affect the final moisture content of spray dried powders (Pinto, Kemp, Bermingham, Hartwig & Bisten, 2014).

Prediction of moisture evaporation from atomized droplets is extremely difficult due to the presence of solutes and changes in the morphology of the particles such as crust formation and shrinkage.

However, 3D-CFD simulations are powerful tools that can produce reliable results for moisture evaporation in spray drying operations (Woo, Daud, Mujumdar, Wu, Meor Talib & Tasirin, 2008).

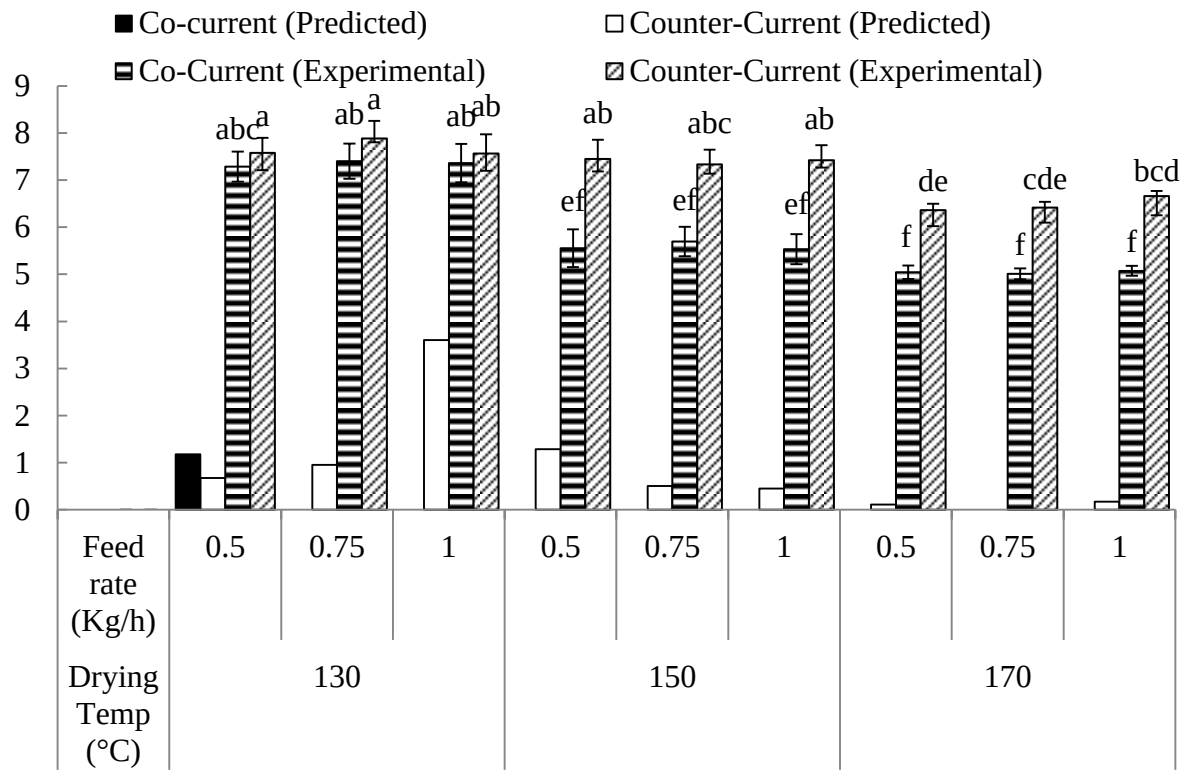

Fig. 4.14 - Predicted and experimental moisture content of powders dried at different inlet air temperatures in co-current and counter-current spray drying configurations. [a-f]Means with same letters are not significantly (P<0.05) different between experimental values.

4.3.1.3.2 Water activity (a_w)

Water activity (a_w) is an important index to determine food stability, safety, and microbial growth (Damodaran, Parkin & Fennema, 2008). Experimental results showed that a_w were significantly (P<0.05) affected by inlet air temperature, spray drying configuration and interaction between these two effects. Hence, inlet air temperatures of 170°C produced powders with lower a_w (Fig. 4.15). Also, powders produced in CO conditions had lower a_w compared to those produced in CNT conditions. These results are in agreement with those obtained for moisture content. All of the powders had a_w values below 0.4. Microbiologically stable foods have a_w less than 0.6 (Quek, Chok & Swedlund, 2007). Jimenez, García and Beristain (2004) have reported a very good oxidation stability of microencapsulated conjugated linoleic acid at a_w=0.743 for at least 60 days.

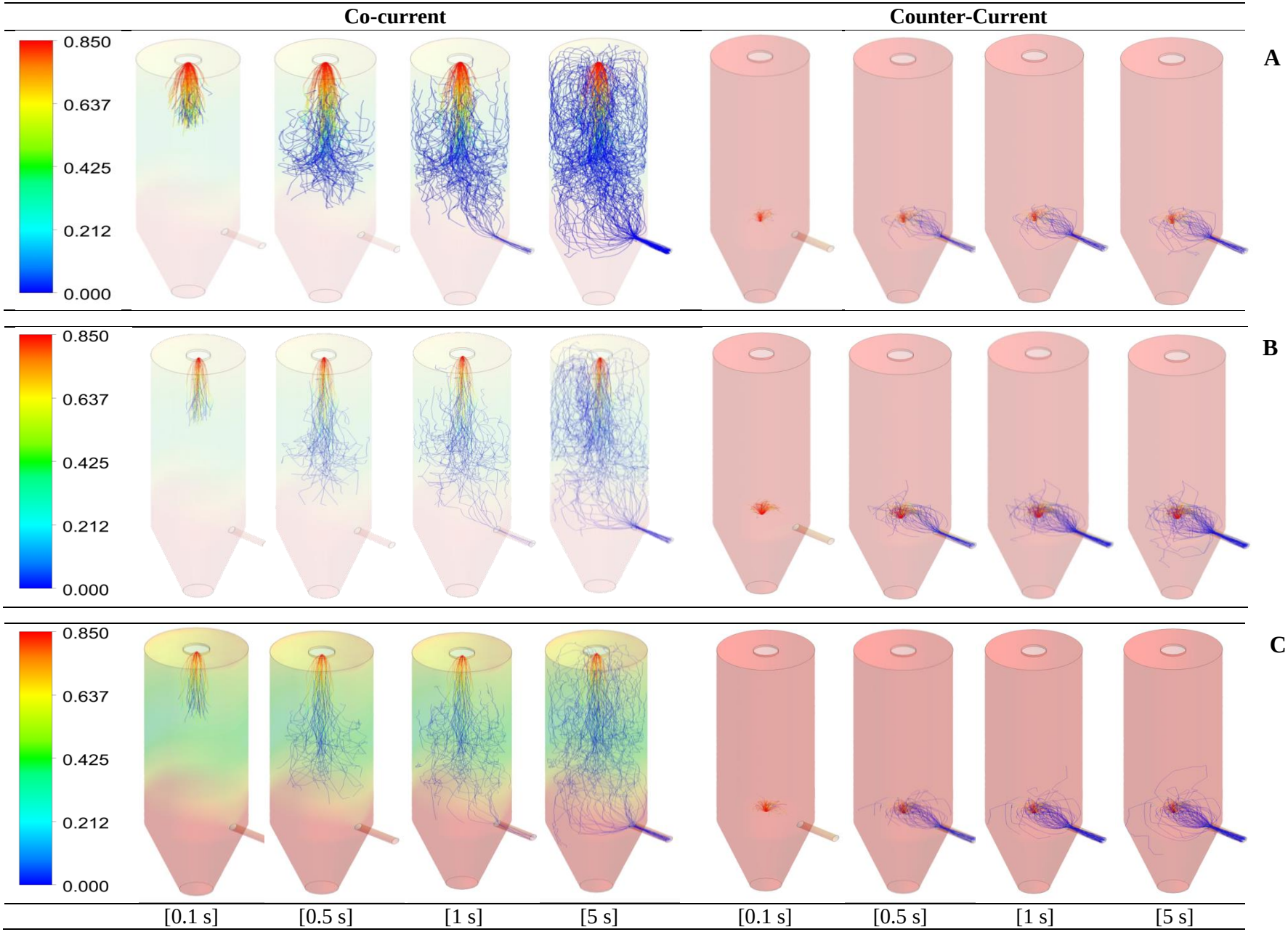

Fig. 4.15 - Time-moisture fraction profiles of drying particles during the spray drying of an emulsion at 0.50 Kg/h feeding rate and 130 (A), 150 (B) and 170°C (C) inlet air temperature under co-current and counter-current conditions

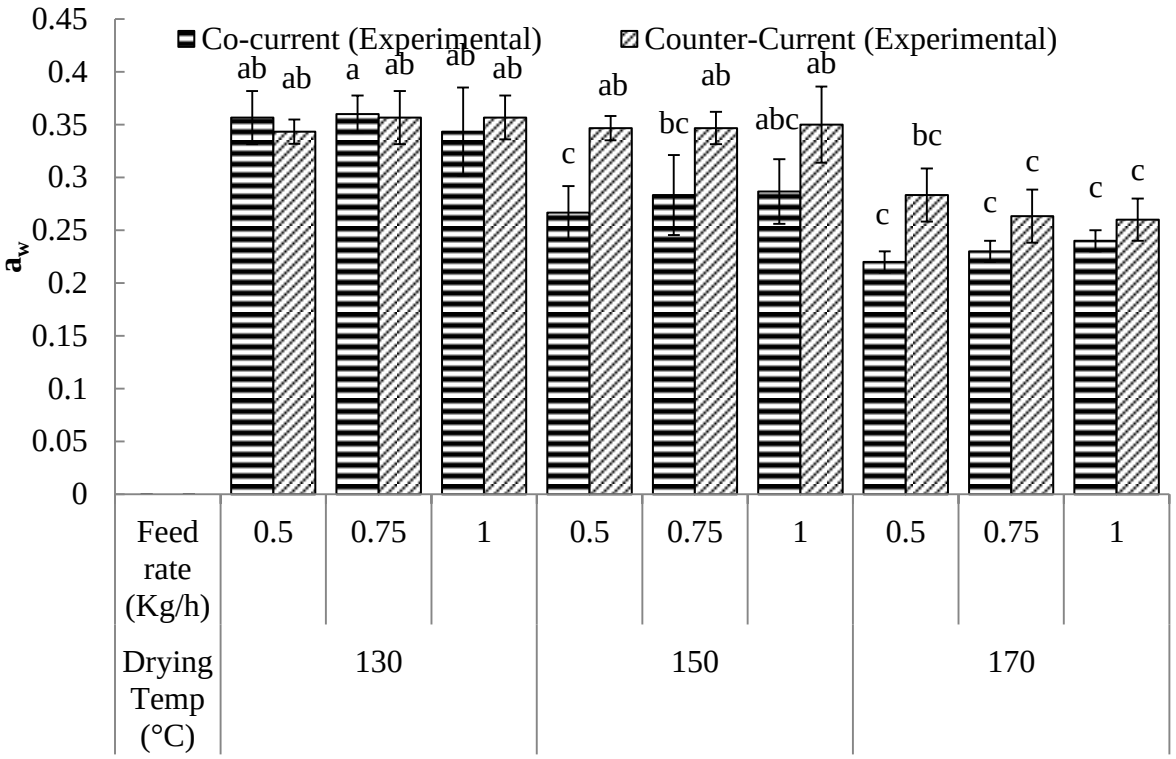

Fig. 4.16 - Experimental water activity (a_w) of powders dried at different inlet air temperatures in co-current and counter-current spray drying configurations. [abc]Means with same letters are not significantly ($P<0.05$) different between experimental values

4.3.1.3.3 Microencapsulation efficiency (ME)

ME is a relationship between the encapsulated oil and the total lipid content of the food powder. It has been previously reported that non-encapsulated oil is prone to oxidation and developing off-flavors that may affect the product acceptance (Drusch & Berg, 2008). In this study, the spray drying conditions did not affect the ME of the spray-dried powders (Table 4.4). According to Wan et al., (2011), ME is highly affected by the emulsification procedure before spray drying. They have reported ME (g/100g) values of 53.3 for the spray-dried menhaden oil powders; meanwhile, greater ME values (84.5 to 86.9) are reported by Klinkesorn, Sophanodora, Chinachoti, Decker and McClements (2006).

High oil/wall material ratios in the emulsion may lower the ME; while increasing the concentration of encapsulation agents in the emulsions can increase ME due to the formation of

surface core before crust formation around the drying droplets (Young, Sarda & Rosenberg, 1993). According to Gharsallaoui, Roudaut, Chambin, Voilley and Saurel (2007), proteins are good coating material for microencapsulation of bioactives by spray drying. This study is first attempt to use egg white hydrolysates as coating material for microencapsulation of fish oil.

Table 4.4 - Microencapsulation efficiency of spray-dried powders produced at different inlet air temperatures, feed rates, and spray drying configurations. **

	Inlet air Temp. (°C)	Feed rate (Kg/h)	ME (g/100 g)		Inlet air Temp. (°C)	Feed rate (Kg/h)	ME (g/100g)
Co-current (Predicted)	130	0.5	71.50±0.76[a]	Counter-Current (Predicted)	130	0.5	71.55±0.95[a]
		0.75	71.78±1.23[a]			0.75	71.38±0.86[a]
		1	71.89±1.55[a]			1	71.20±0.97[a]
	150	0.5	71.20±0.55[a]		150	0.5	70.61±0.56[a]
		0.75	70.95±0.70[a]			0.75	71.34±0.74[a]
		1	71.25±0.40[a]			1	70.85±0.73[a]
	170	0.5	71.30±1.13[a]		170	0.5	70.97±0.69[a]
		0.75	71.58±1.21[a]			0.75	71.31±0.69[a]
		1	70.73±0.88[a]			1	70.94±0.50[a]

**Values are means ±SD of triplicate determinations.

4.3.1.3.4 Lipid Oxidation

Microencapsulation by spray drying is a widely used technology to protect bioactives against light and oxygen (Serfert, Drusch & Schwarz, 2009). However, degradation of bioactives can occur during the microencapsulation process during emulsification and drying steps (Gharsallaoui, Roudaut, Chambin, Voilley & Saurel, 2007). According to Baik, Suhendro, Nawar, McClements, Decker and Chinachoti (2004), lipid oxidation in microencapsulated oils can be quantified by determining their peroxide value (PV) and thiobarbituric acid reactive substances (TBARS).

a. Peroxide value (PV)

The PV (meq/Kg) of the E-MO-LEWH was 7.8. Spray-dried powders had a PV that ranged from 12.5 to 32.18 (Fig. 4.16). The PV of the spray-dried powders was significantly ($P<0.05$)

affected by the inlet air temperature, spray dying configuration, feed rate, and the interaction between the spray drying configuration and feed rate. Hence, spray-dried powders with lower PV were obtained at 130°C inlet air temperatures in CNT conditions, at a feed rate of 1 Kg/h. These results may be due to lower thermal degradation of the powders produced in CNT spray drying because of their shorter RT. According to Drusch, Serfert, Scampicchio, Schmidt-Hansberg and Schwarz (2007), during spray drying, fish oil is exposed to hot air at high pressures which may increase lipid oxidation. Higher amounts of non-encapsulated oil and drying temperatures increase lipid oxidation during spray drying (Drusch, Serfert, Scampicchio, Schmidt-Hansberg & Schwarz, 2007; Kolanowski, Ziolkowski, Weißbrodt, Kunz & Laufenberg, 2006). Although an accurate prediction of lipid oxidation of microencapsulated fish oil powders during spray drying is not possible yet using computational models, CFD simulations are excellent tools that can be used to estimate thermal degradation of bioactives during spray-dried powders by estimating RT.

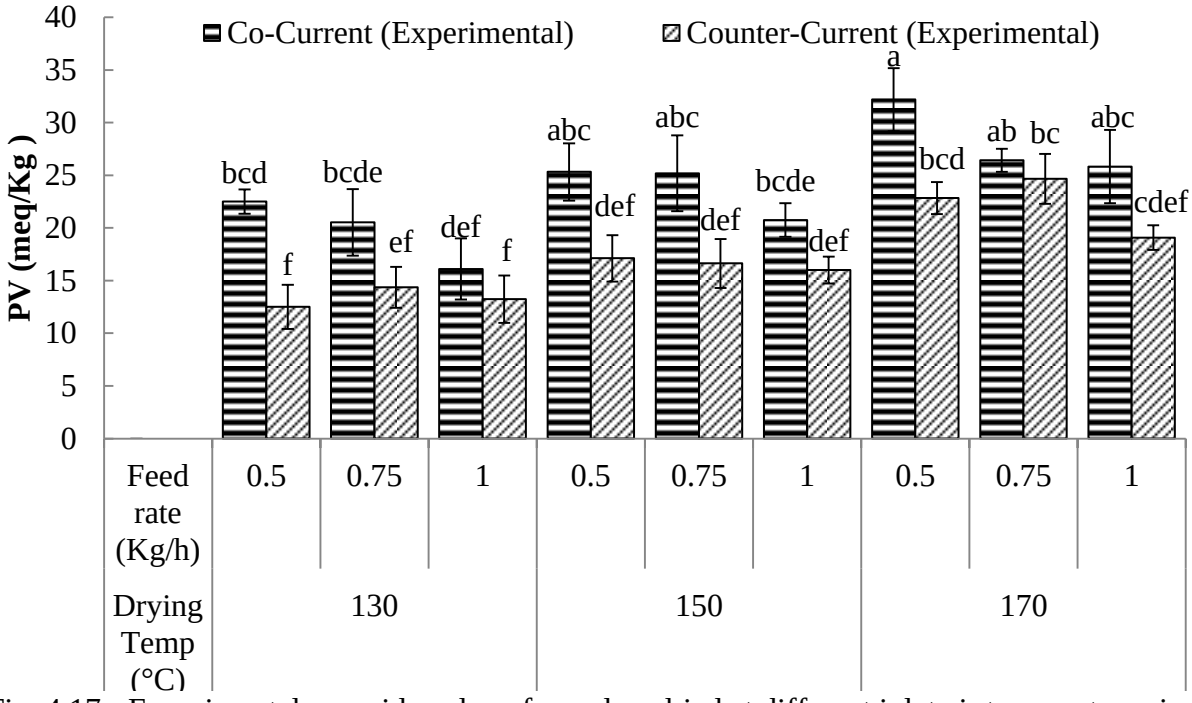

Fig. 4.17 - Experimental peroxide value of powders dried at different inlet air temperatures in co-current and counter-current spray drying configurations. [a-f]Means with same letters are not significantly ($P<0.05$) different between experimental values

b. TBARS

TBARS indicate secondary lipid oxidation compounds that arise from the decomposition of fatty acid hydro peroxides during processing (Damodaran, Parkin & Fennema, 2008). The TBARS (mmol MDA/Kg oil) result for E-MO-LEWH was 0.12.

Experimental results demonstrated that TBARS of the spray-dried powders were significantly ($P<0.05$) affected by the inlet air temperature and spray drying configuration. Hence, spray-dried powders produced in CO conditions had significantly ($P<0.05$) greater TBARS values compared to those of the powders produced in CNT conditions.

Furthermore, powders produced a 170°C inlet air temperatures had significantly ($p<0.05$) higher values of TBARS compared to those produced at 130°C (Fig. 4.17).

According to Klinkesorn, Sophanodora, Chinachoti, Decker and McClements (2006) TBARS in microencapsulated oils increases with time and higher temperatures. TBARS values of microencapsulated powder ranged from 0.13 to 0.23 mmol MDA/Kg oil. Jónsdóttir, Bragadóttir and Arnarson (2005) reported that TBARS is a good indicator to measure oxidative stability of microencapsulated fish oil. They also have reported TBARS values from 0.08 to 0.11 mmol MDA/kg oil for microencapsulated fish oil using different antioxidants and after 20 weeks of storage.

4.3.1.3.5 Particle size

Predicted and experimental mean particles sizes of the spray-dried powder are shown in Fig. 4.18. It was seen that 3D-CFD model predicted the final sizes of the powder particles with good accuracy. However, the 3D-CFD model was not able to predict any differences in particle sizes between the powders produced in CO and CNT spray drying configurations.

Predicted mean particle sizes ranged from 23 to 25 μm for all of the spray-dried powders. Meanwhile, experimental results revealed that powders produced in CO spray drying conditions had mean particle sizes ranged from 13 to 27 μm; and powders produced in CNT spray drying conditions had mean particle sizes ranged from 14 to 29 μm.

These results are in agreement with those obtained by Kagami, Sugimura, Fujishima, Matsuda, Kometani and Matsumura (2003) for the microencapsulation of fish oil using proteins and dextrin as wall materials.

Experimental results also demonstrated that higher inlet air temperatures in CNT spray drying produced smaller powder particles. However, this effect was not observed in CO spray drying.

Feed rate did not have a significant effect on the mean particle size of the spray-dried powders.

According to Pinto, Kemp, Bermingham, Hartwig and Bisten (2014), feed atomization tremendously impacts the final particle size of spray dried powders.

Shear forces on the feed in the atomizer defines the sizes of the feed droplets; therefore, higher shear forces result in smaller feed droplets which eventually will result in smaller powder particles.

Particle size of spray-dried powders also depends on feed temperature, inlet air temperature, and outlet air temperature (AlChE, 2003).

Also, Hogan, McNamee, O'Riordan and O'Sullivan (2001) have reported that the particle size of spray-dried powders increases with the increase of total solids content and/or apparent viscosity of the feed.

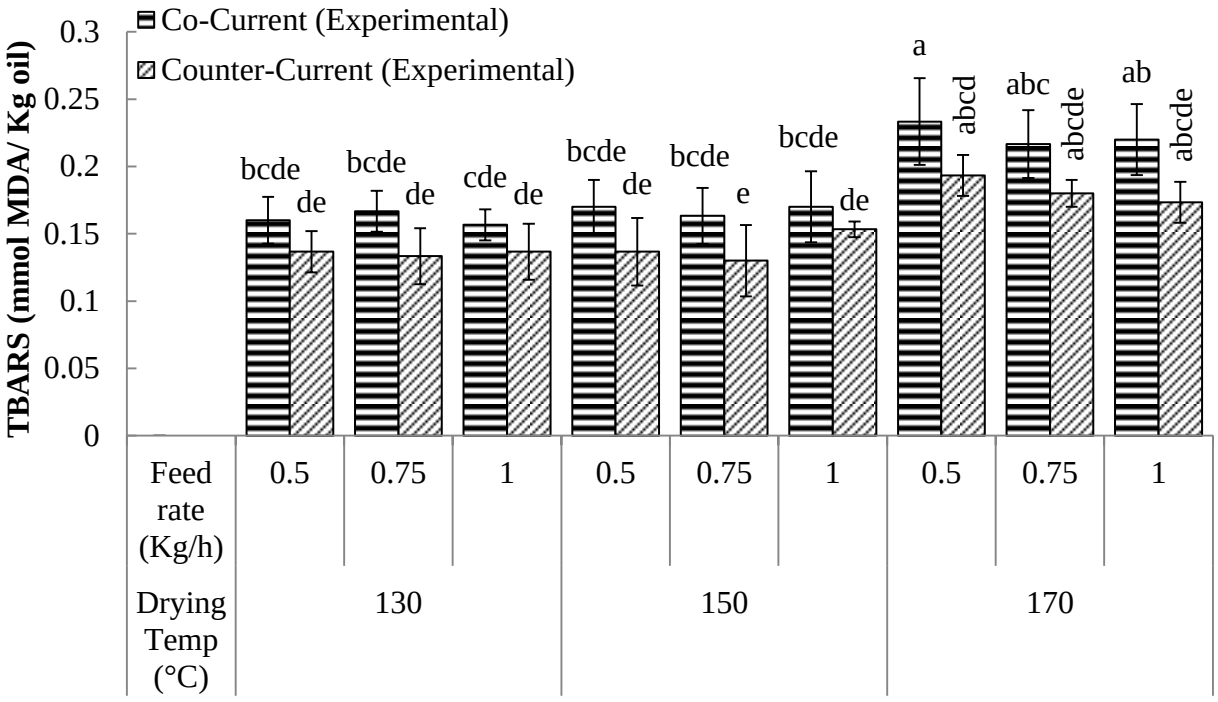

Fig. 4.18 - Experimental TBARS value of powders dried at different inlet air temperatures in co-current and counter-current spray drying configurations. [a-e]Means with same letters are not significantly ($P<0.05$) different between experimental values

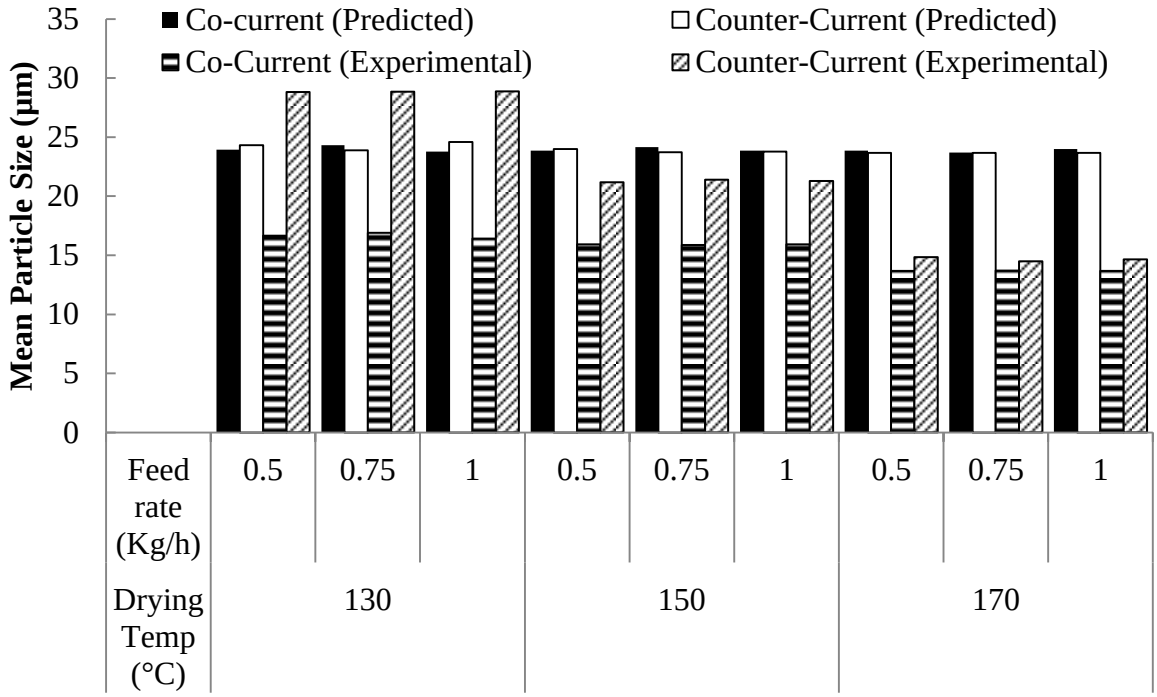

Fig. 4. 19 - Predicted and experimental particles sizes of powders dried at different inlet air temperatures in co-current and counter-current spray drying configurations.

4.3.1.3.6 Microstructure

A 3D characterization of the powder particles was carried out through SEM to evaluate particle microstructure. Higher shrinkage was observed in powder particles produced at 170°C inlet air temperatures (Figs. 4.19 and 4.20). This may the result of moisture transport during the falling rate period (Walton, 2000). According to Gharsallaoui, Roudaut, Chambin, Voilley and Saurel (2007), during the constant drying rate period, the rate of water diffusion from the inside of a particle to its surface is equal to the surface evaporation rate; once the droplet reaches a critical moisture content, a dry crust is formed at the feed droplet surface and the drying rate quickly decreases. Powder particles tend to contain voids, inflate and break when evaporation occurs at higher temperatures during this phase.

More particle agglomeration was observed in powders dried at 130°C inlet air temperatures. Huang, Kumar and Mujumdar (2006) have reported that low inlet air temperatures produce agglomerated powders with high moisture contents; meanwhile, high air inlet temperature causes excessive evaporation and produce low quality powders. It was also observed that the feeding rates did not affect the microstructure of the powder particles.

The SEM micrographs also revealed that powders dried in CO spray drying conditions had higher shrinkage and particle breakage compared to those dried in CNT conditions. This may be due to the shorter RT in CNT spray drying compared to CO spray drying. These results are in agreement with those of lipid oxidation (previously discussed).

In this study, CNT spray drying produced more spherical powder particles with few signs of shrinkage and disruption. These results are not in agreement with those described by (Gharsallaoui, Roudaut, Chambin, Voilley & Saurel, 2007), who reported that better quality particles are obtained with CO spray drying.

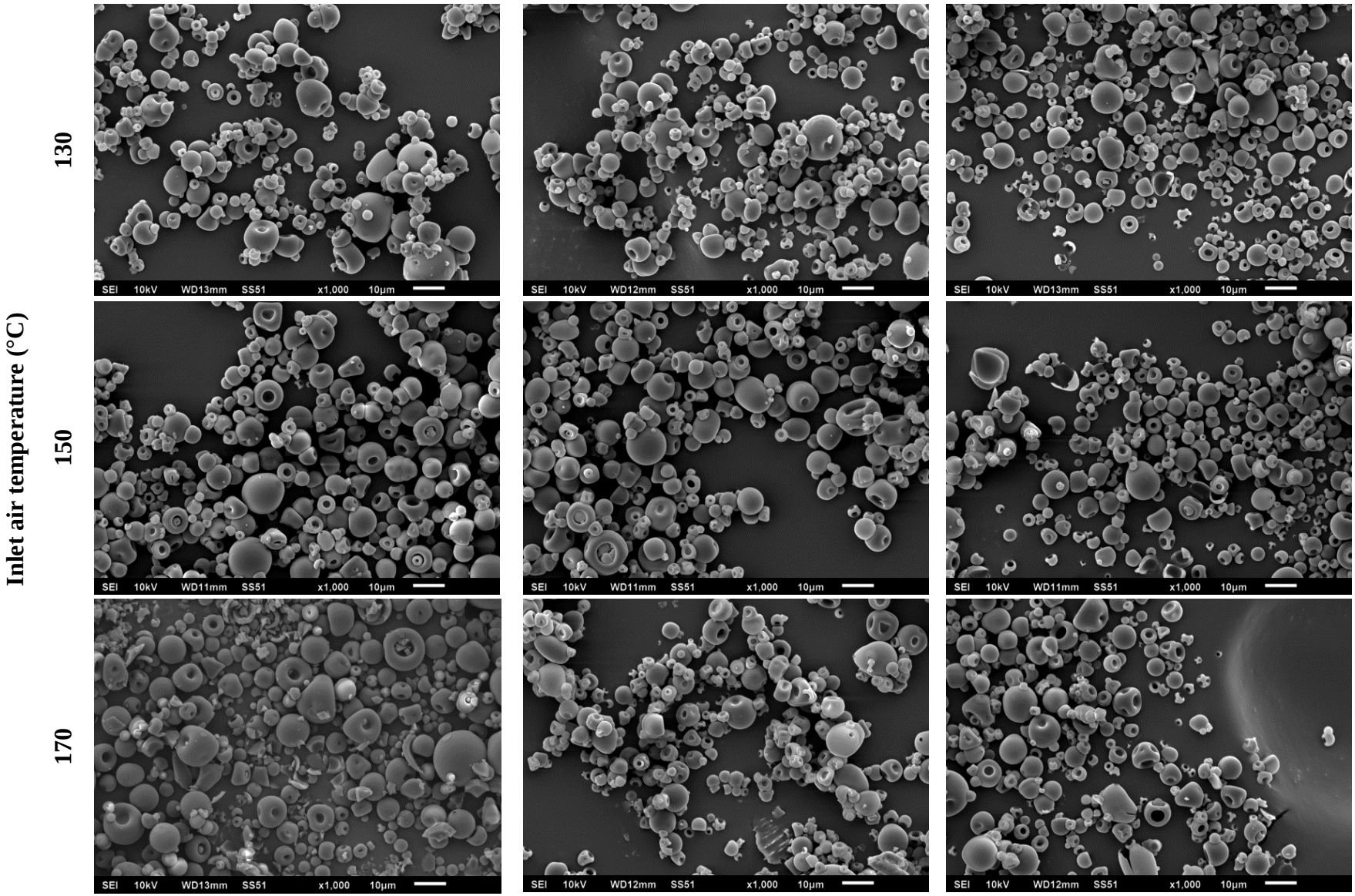

Fig. 4.20 - Scanning Electron Micrographs of microencapsulated powder dried at different inlet air temperatures and feed rates in co-current spray drying configurations.

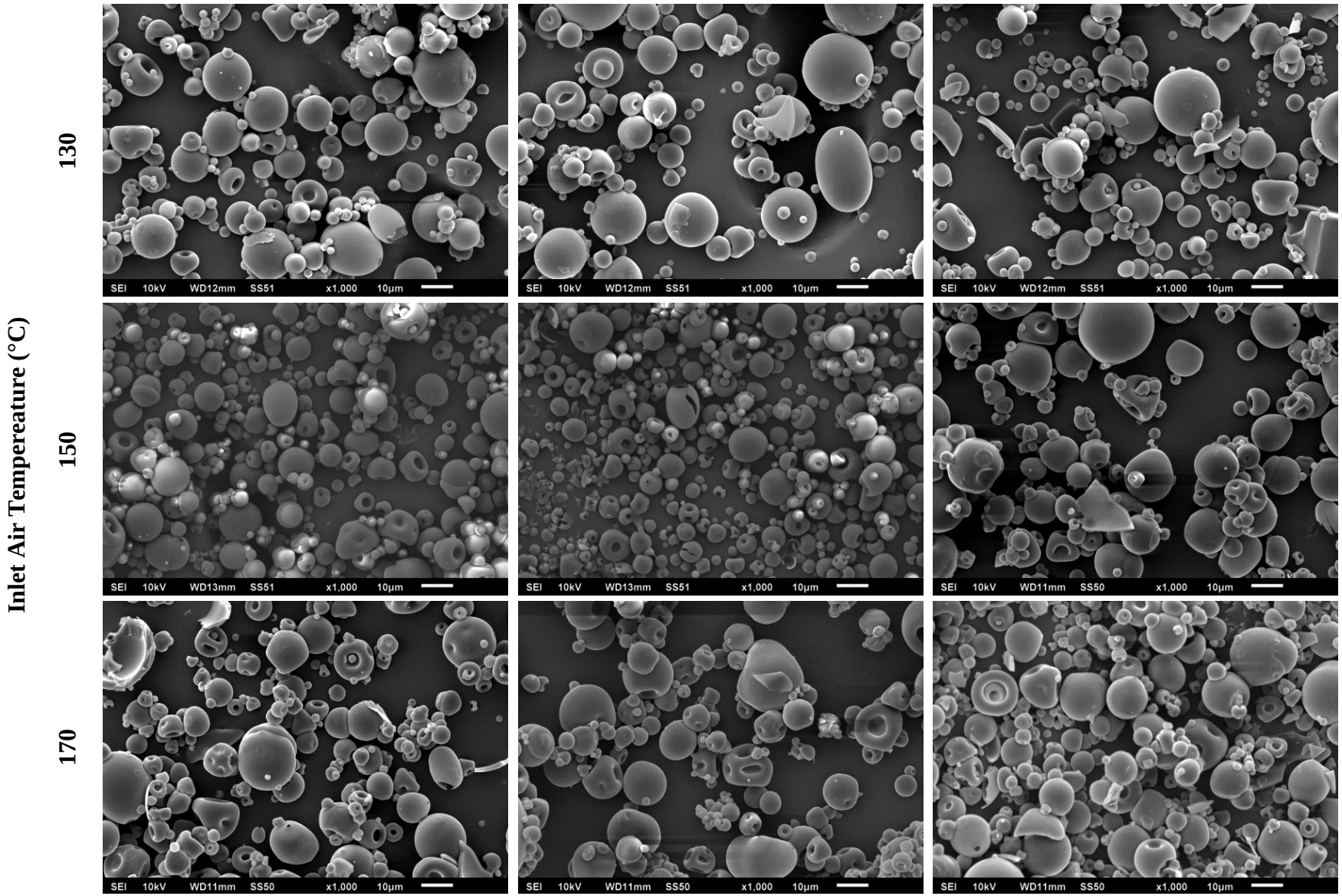

Fig. 4.21 - Scanning Electron Micrographs of microencapsulated powder dried at different inlet air temperatures and feed rates in counter-current spray drying configurations.

4.3.2 Case 2

According to Gimbun, Chuah, Fakhru'l-Razi and Choong (2005), cyclone separators use centrifugal forces produced by the spinning drying air stream to separate particles from the carrier air. Due to their design, cyclones separators are highly suitable for high temperature and pressure conditions and can reach collection efficiencies up to 99% for particles larger than 5 μm (Da Silva, Briens & Bernis, 2003). Collection efficiencies and pressure drops are the two important parameters identified in the study of the performance of cyclones separators. In this work, a numerical study of the pilot-scale spray dryer's cyclone separator was conducted by 3D-CFD simulations. A finite volume method was used to solve the set of partial differential equations of a two-way couple Euler-Lagrange approach for the continuous (drying air) and discrete phase (dried particles).

4.3.2.1 Simulation results

4.3.2.1.1 Drying air flow pattern

The drying air flow pattern is shown in Fig. 4.21. It can be observed that the drying air flow forms descending and ascending streams which flow parallel to one another before leaving the cyclone through the outlet. Also, the ascending flow is not symmetrical and has a twisted cylinder shape. Similar observations are previously reported (Da Silva, Briens & Bernis, 2003; Griffiths & Boysan, 1996). According to Griffiths and Boysan (1996), after entering the cyclone, the drying air flow creates a stream that flows and accelerates along the outer wall towards the bottom of the cyclone; once it reaches the bottom, it changes direction and ascends through the core towards the outlet. Identifying the air flow pattern inside the cyclone is important because it can help to detect leakages which decrease collection efficiencies. In this study, no leakage flows were identified inside the cyclone at any operating conditions.

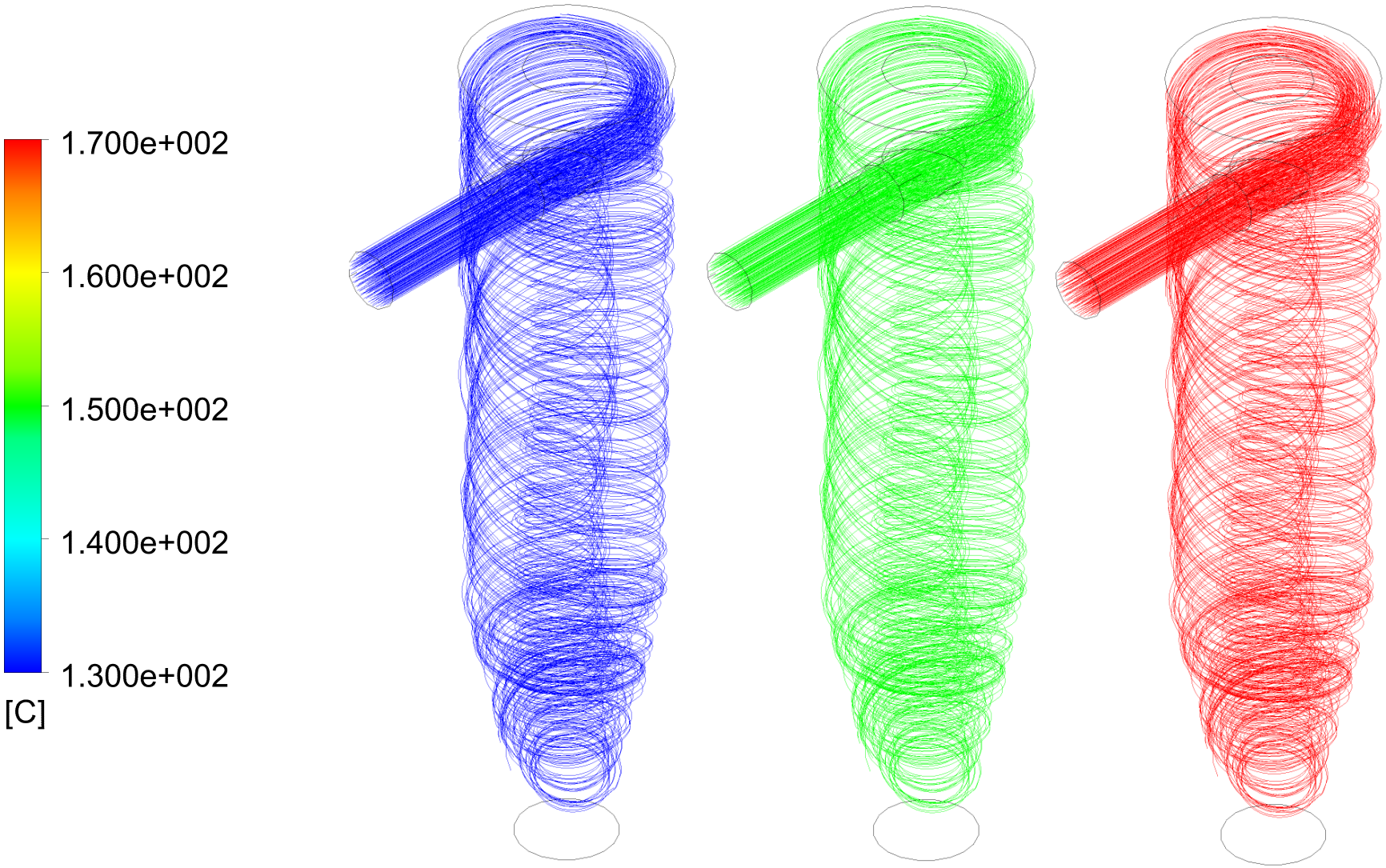

Inlet temperature (°C) **130** **150** **170**

Fig. 4.22 - Drying air flow patterns inside the spray dryer's cyclone separator at different inlet air temperatures.

4.3.2.1.2 Drying air velocity

To successfully model the drying air flow inside the cyclone separator using CFD, it is necessary to effectively describe the turbulent behavior of the flow. Several studies have reported that the Reynolds stress model (RSM) shows a high accuracy in describing the swirl flow pattern, axial velocity, tangential velocity and pressure drop inside cyclone separators (Chu, Wang, Xu, Chen & Yu, 2011; Gimbun, Chuah, Fakhru'l-Razi & Choong, 2005).

In this study, the average initial velocity of the drying air at the inlet was set to 25 m/s, this velocity was selected from the results obtained in CFD –case 1. The velocity magnitude of the drying air is shown in Fig. 4.22-A. Higher drying air velocities are observed at the radial center of the inlet; meanwhile, lower values are seen near the wall of the inlet. Furthermore, asymmetric velocity values are seen inside the cyclone separator; which may be due to the interaction with the dried particles.

The results for radial, axial and tangential velocities are inside the cyclone is shown in Figs. 4.22-B, C and D; respectively. Negative values indicate the direction of the velocity vector in the x-y-z axis. At the cylindrical region of the cyclone, higher radial and tangential velocities are observed. Also, the magnitude of tangential velocities is higher than those of radial and axial velocities. According to Chu, Wang, Xu, Chen and Yu (2011), radial, tangential, and axial velocities inside cyclone separators are highly affected by the presence of dried particles. This effect may be due to the density differences of the drying air and the dried particles that affects rotational and centrifugal forces of the drying air (Griffiths & Boysan, 1996). These results are in agreement with those reported by Chu, Wang, Xu, Chen and Yu (2011). Up to date, there is limited literature about velocity profiles inside a spray dryer's cyclone separator when dried particles are loaded. Nevertheless, this information can be readily obtained by CFD simulations.

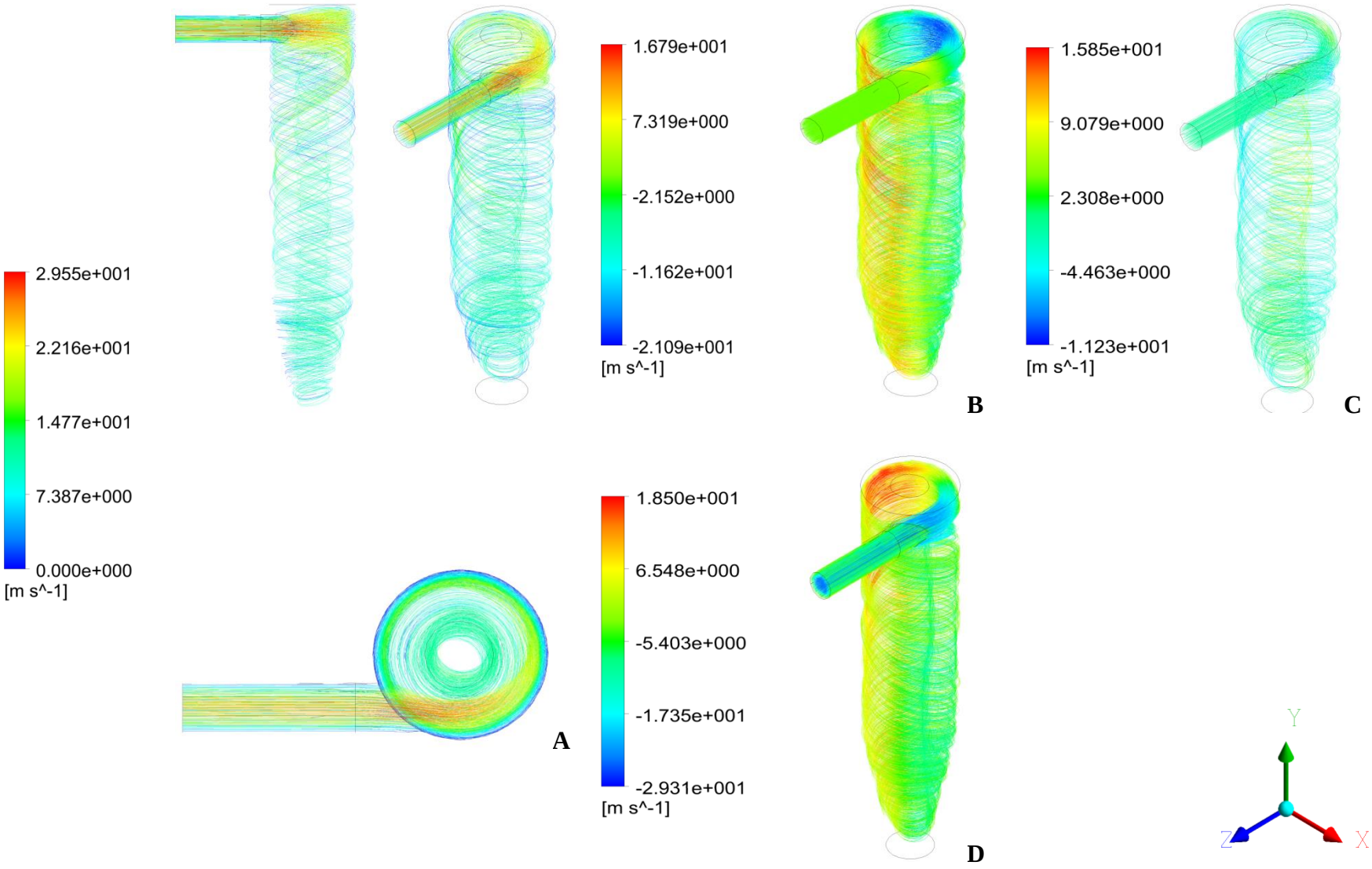

Fig. 4.23 –Drying air velocity inside the spray dryer's cyclone separator. Numerical magnitude (A), x-axis velocity (radial)(B), y-axis velocity (axial) (C), and z-axis velocity (tangential) (D).

4.3.2.1.3 Pressure

Pressure drop is an important parameter in designing and evaluating the performance of the cyclone separators because it defines the requirements for energy. In this study, the asymmetric pressure drop inside the cyclone separator is observed in Fig. 4.23. It can be seen that the time-averaged static pressure decreases radially from the wall to the core of the cyclone. Even more, a low pressure zone is identified at the core (central region) of the cyclone separator due to high swirling velocity.

The average predicted pressure drop was 470.3 Pa which was not affected by the drying air temperatures. The pressure drop was experimentally measured by the digital manometers installed at the outlets of the spray chamber and cyclone separator. Experimental results demonstrated that pressure drop (Pa) was 635.15, 616.78 and 605.17 for spray drying operations at inlet air temperatures of 130, 150, and 170°C. So, the CFD model underestimated the pressure drops in the cyclone separator for approximately less than 165 Pa which is considered accepted for this type of simulations. It has been reported that higher drying air velocities at the inlet increases pressure drops; meanwhile, higher drying air temperatures decrease pressures drops inside cyclone separators (Gimbun, Chuah, Fakhru'l-Razi & Choong, 2005). Even more, the same authors reported that 80% of pressure drop in cyclone separators is due to the energy dissipation by the viscous stress of the turbulent rotational fluid; meanwhile, the rest of the pressure drop are due to the contraction of the drying air at the outlet, expansion at the inlet and friction on the cyclone wall surface.

Chu, Wang, Xu, Chen and Yu (2011) reported that increasing dried particles load decreases pressure drops in cyclone separators. In this study, one dried particle load was studied (0.081144 Kg/h), so, this effect was not observed.

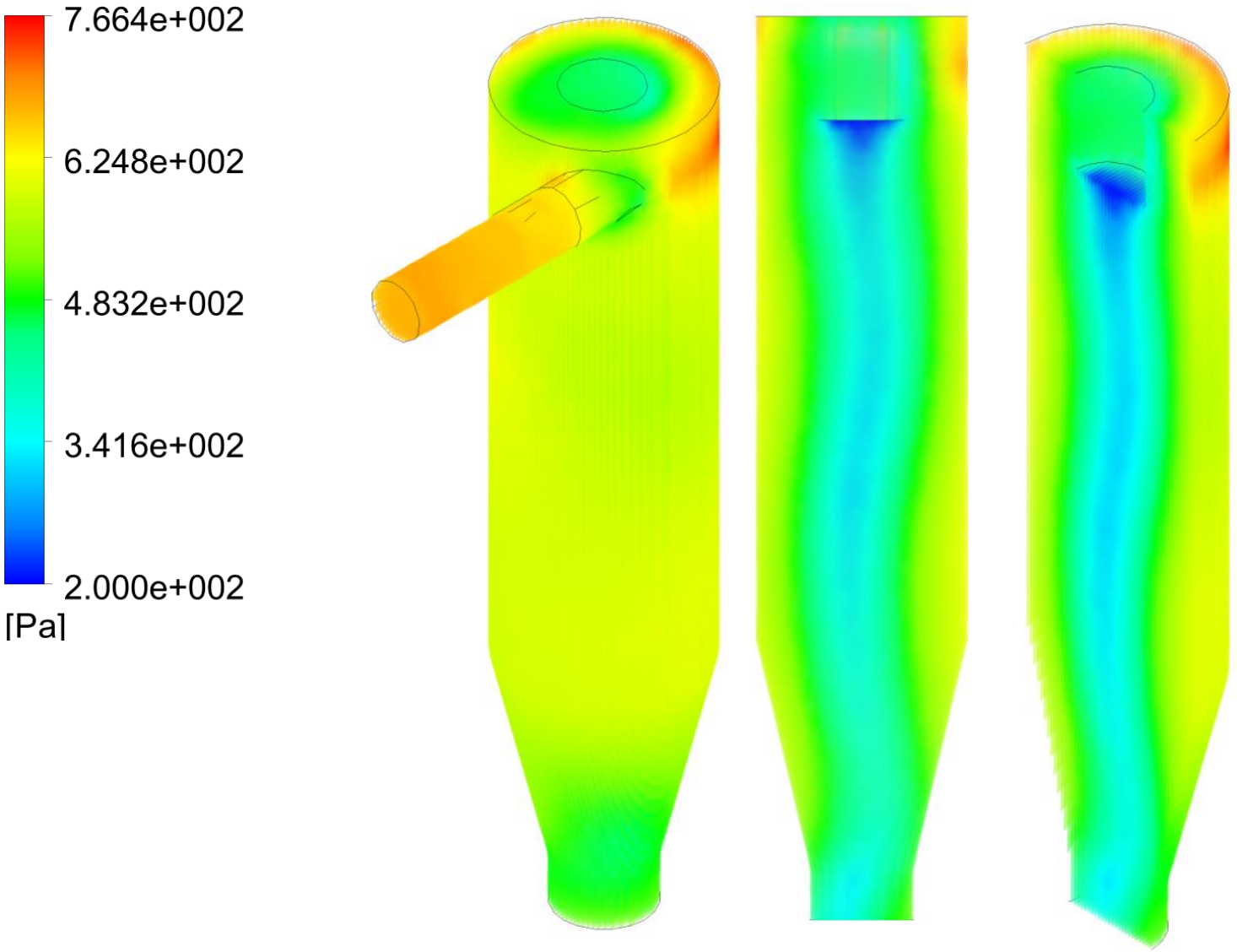

Fig. 4.24 – Predicted pressure inside the spray dryer's cyclone separator

4.3.2.1.4 Flow of dried particles

The flow pattern of dried particle inside the cyclone separator is presented in Fig. 4.24. It can be seen that the dried particles follow the drying air flow pattern and congregate at the wall immediately after entering the inlet and subsequently descend in bands.

These predicted results are in agreement with those experimentally observed in this study and those reported by (Chu, Wang, Xu, Chen & Yu, 2011). Due to the high air velocities inside the cyclone, dried particles reached the bottom very quickly (less than 1 s) where they reach their steady state.

According to the results of the CFD simulations, no dried particles leave the cyclone at the outlet; therefore, it is assumed that the collection efficiency was close to 100%.

However, experimental results have demonstrated that a small amounts of dried particles normally scape by the outlet; especially those particles with small diameter (<5 μm) which are referred as dust.

Even more, it was seen that dried particles of different sizes are homogenously distributed along particle flow pattern inside the cyclone.

The CFD simulations also revealed a particle flow trapped at the top of the cyclone that never reaches the bottom. Hence, this effect may change the quality of these dried particles.

The CFD simulations also demonstrated that drying air temperatures did not affect the flow patterns of the dried particles; since the flow pattern of dried particles is given by the flow pattern of the drying air, these results are in agreement with the results obtained for flow patterns of drying air which were not affected by the drying air temperatures.

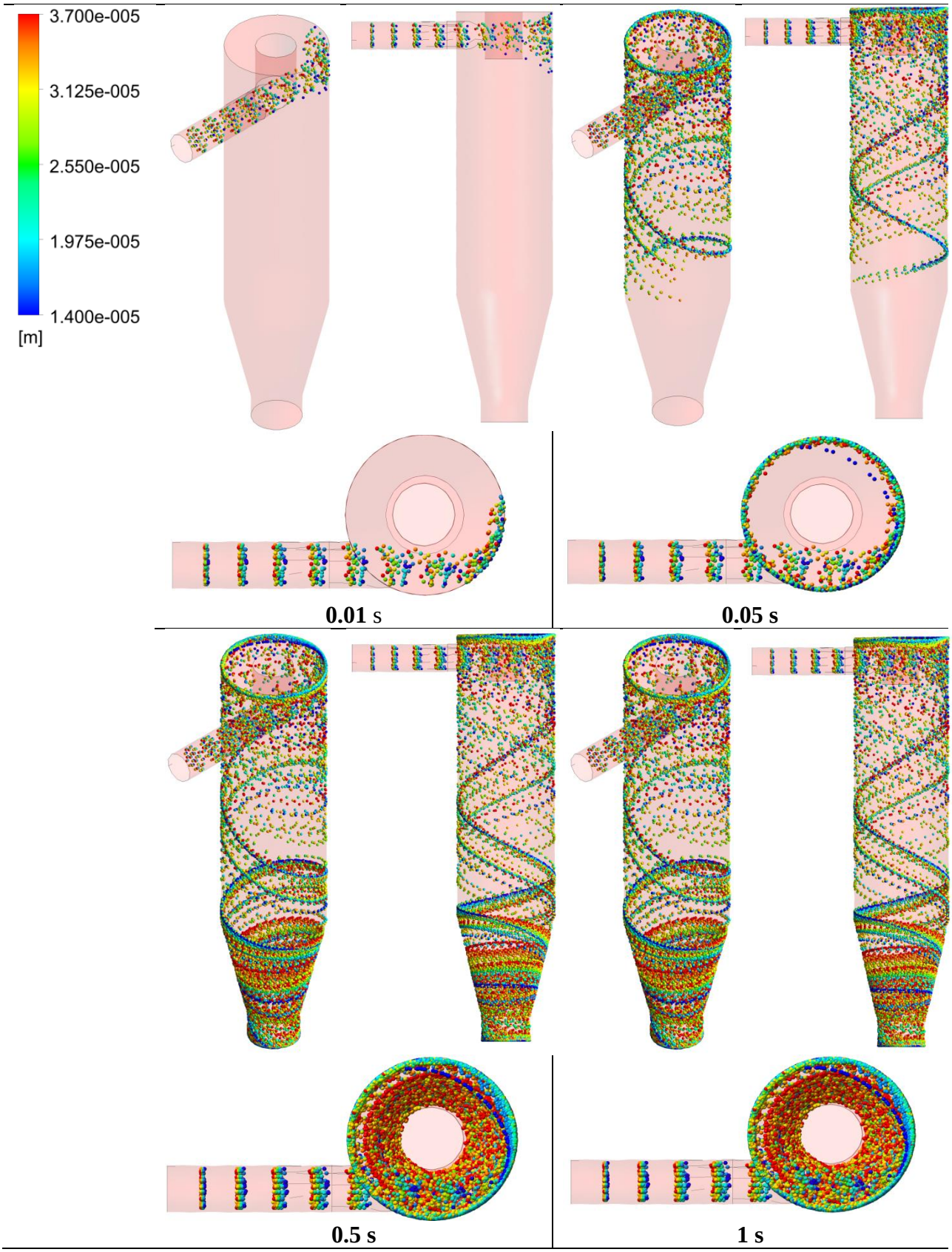

Fig. 4.25 - Time - Particle size distribution profile inside the spray dryer's cyclone

4.4 Conclusion

Microencapsulated menhaden oil with egg white hydrolysates powders were effectively produced by spray drying. This study is the first attempt to compare the performance of co-current and counter-current spray drying configurations in the production of microencapsulated fish oil powders using CFD simulations and experimental tools. The complex transport phenomena occurring during spray drying was effectively modeled using 3D-CFD simulations. The drying air flow inside the drying chamber and the cyclone separator was successfully modeled by the realizable k-ε and Reynolds stress model (RSM) turbulent models, respectively.

Predicted results for moisture content and particle size distribution of microencapsulated powders was comparable to those experimentally obtained. Lower lipid oxidation and thermal degradation was observed in powders produced at 130°C inlet air temperatures under counter-current spray drying configurations. Counter-current spray drying produced better quality microencapsulated powder than co-current spray drying due to lower predicted particle residence times.

Particle separation inside the spray dryer's cyclone separator was successfully modeled by 3D-CFD. Also, predicted results for pressure drop inside the spray dryer's cyclone separator was comparable with those experimentally obtained.

Prediction of particle agglomeration, lipid oxidation and microstructure of spray dried powders using CFD simulations is still limited. Nevertheless, it is a powerful tool to study the spray drying process. The numerical results generated in this study provide valuable information to pilot-scale testing and to engineer new powder products using spray drying technology.

The study demonstrated that the 3D-CFD spray drying modeling can be effectively used to study the drying phenomena and to predict the final quality of spray dried powders.

4.5 References

AlChE. (2003). Spray dryers: a guide to performance evaluation: Equipment Testing Procedures Committee - American Institute of Chemical Engineers

Anandharamakrishnan, C., Gimbun, J., Stapley, A., & Rielly, C. D. (2009). Application of computational fluid dynamics (CFD) simulations to spray-freezing operations. *Drying Technology*, 28(1), 94-102.

AOAC. (1999). Official methods of analysis. Arlington, VA: Association of Official Analytical Chemists.

Baik, M.-Y., Suhendro, E., Nawar, W., McClements, D., Decker, E., & Chinachoti, P. (2004). Effects of antioxidants and humidity on the oxidative stability of microencapsulated fish oil. *Journal of the American Oil Chemists' Society*, 81(4), 355-360.

Bimbenet, J., Bonazzi, C., & Dumoulin, E. (2002). Drying of foodstuffs. *Drying 2002*, 64-80.

Birchal, V., Huang, L., Mujumdar, A., & Passos, M. (2006). Spray dryers: modeling and simulation. *Drying Technology*, 24(3), 359-371.

Chu, K. W., Wang, B., Xu, D. L., Chen, Y. X., & Yu, A. B. (2011). CFD–DEM simulation of the gas–solid flow in a cyclone separator. *Chemical Engineering Science*, 66(5), 834-847.

Da Silva, P., Briens, C., & Bernis, A. (2003). Development of a new rapid method to measure erosion rates in laboratory and pilot plant cyclones. *Powder technology*, 131(2), 111-119.

Damodaran, S., Parkin, K., & Fennema, O. (2008). Fennema's Food Chemistry: CRC PRESS.

Drusch, S., & Berg, S. (2008). Extractable oil in microcapsules prepared by spray-drying: Localisation, determination and impact on oxidative stability. *Food Chemistry*, 109(1), 17-24.

Drusch, S., Serfert, Y., Scampicchio, M., Schmidt-Hansberg, B., & Schwarz, K. (2007). Impact of Physicochemical Characteristics on the Oxidative Stability of Fish Oil Microencapsulated by Spray-Drying. *Journal of Agricultural and Food Chemistry*, 55(26), 11044-11051.

Ducept, F., Sionneau, M., & Vasseur, J. (2002). Superheated steam dryer: simulations and experiments on product drying. *Chemical Engineering Journal*, 86(1), 75-83.

Fletcher, D., Guo, B., Harvie, D., Langrish, T., Nijdam, J., & Williams, J. (2006). What is important in the simulation of spray dryer performance and how do current CFD models perform? *Applied mathematical modelling*, 30(11), 1281-1292.

Gharsallaoui, A., Roudaut, G., Chambin, O., Voilley, A., & Saurel, R. (2007). Applications of spray-drying in microencapsulation of food ingredients: An overview. *Food Research International*, 40(9), 1107-1121.

Gimbun, J., Chuah, T. G., Fakhru'l-Razi, A., & Choong, T. S. Y. (2005). The influence of temperature and inlet velocity on cyclone pressure drop: a CFD study. *Chemical Engineering and Processing: Process Intensification*, 44(1), 7-12.

Griffiths, W. D., & Boysan, F. (1996). Computational fluid dynamics (CFD) and empirical modelling of the performance of a number of cyclone samplers. *Journal of Aerosol Science*, 27(2), 281-304.

Hogan, S. A., McNamee, B. F., O'Riordan, E. D., & O'Sullivan, M. (2001). Emulsification and microencapsulation properties of sodium caseinate/carbohydrate blends. *International Dairy Journal*, 11(3), 137-144.

Huang, L., Kumar, K., & Mujumdar, A. (2003a). A parametric study of the gas flow patterns and drying performance of co-current spray dryer: Results of a computational fluid dynamics study. *Drying Technology*, 21(6), 957-978.

Huang, L., Kumar, K., & Mujumdar, A. (2003b). Use of computational fluid dynamics to evaluate alternative spray dryer chamber configurations. *Drying Technology*, 21(3), 385-412.

Huang, L., Kumar, K., & Mujumdar, A. (2004). Simulation of a spray dryer fitted with a rotary disk atomizer using a three-dimensional computional fluid dynamic model. *Drying Technology*, 22(6), 1489-1515.

Huang, L. X., Kumar, K., & Mujumdar, A. S. (2006). A comparative study of a spray dryer with rotary disc atomizer and pressure nozzle using computational fluid dynamic simulations. *Chemical Engineering and Processing: Process Intensification*, 45(6), 461-470.

Jimenez, M., García, H. S., & Beristain, C. I. (2004). Spray-drying microencapsulation and oxidative stability of conjugated linoleic acid. *European Food Research and Technology*, 219(6), 588-592.

Jónsdóttir, R., Bragadóttir, M., & Arnarson, G. (2005). Oxidatively Derived Volatile Compounds in Microencapsulated Fish Oil Monitored by Solid-phase Microextraction (SPME). *Journal of Food Science*, 70(7), c433-c440.

Kagami, Y., Sugimura, S., Fujishima, N., Matsuda, K., Kometani, T., & Matsumura, Y. (2003). Oxidative Stability, Structure, and Physical Characteristics of Microcapsules Formed by Spray Drying of Fish Oil with Protein and Dextrin Wall Materials. *Journal of Food Science*, 68(7), 2248-2255.

Kieviet, F., & Kerkhof, P. J. (1995). Measurements of particle residence time distributions in a co-current spray dryer. *Drying Technology*, 13(5-7), 1241-1248.

Kieviet, F. G. (1997). Modelling quality in spray drying: Laboratory of Separation Processes and Transport Phenomena, Department of Chemical Engineering, Eindhoven University of Technology.

Klinkesorn, U., Sophanodora, P., Chinachoti, P., Decker, E. A., & McClements, D. J. (2006). Characterization of spray-dried tuna oil emulsified in two-layered interfacial membranes prepared using electrostatic layer-by-layer deposition. *Food Research International*, 39(4), 449-457.

Kolanowski, W., Ziolkowski, M., Weißbrodt, J., Kunz, B., & Laufenberg, G. (2006). Microencapsulation of fish oil by spray drying--impact on oxidative stability. Part 1. *European Food Research and Technology*, 222(3-4), 336-342.

Kuriakose, R., & Anandharamakrishnan, C. (2010). Computational fluid dynamics (CFD) applications in spray drying of food products. *Trends in Food Science & Technology*, 21(8), 383-398.

Langrish, T., Williams, J., & Fletcher, D. (2004). Simulation of the effects of inlet swirl on gas flow patterns in a pilot-scale spray dryer. *Chemical Engineering Research and Design*, 82(7), 821-833.

Langrish, T., & Zbicinski, I. (1994). The effects of air inlet geometry and spray cone angle on the wall deposition rate in spray dryers. *Chemical engineering research & design*, 72(A3), 420-430.

Mei, L., McClements, D. J., Wu, J., & Decker, E. A. (1998). Iron-catalyzed lipid oxidation in emulsion as affected by surfactant, pH and NaCl. *Food Chemistry*, 61(3), 307-312.

Mezhericher, M., Levy, A., & Borde, I. (2009). Modeling of droplet drying in spray chambers using 2D and 3D computational fluid dynamics. *Drying Technology*, 27(3), 359-370.

Mezhericher, M., Levy, A., & Borde, I. (2012). Three-dimensional spray-drying model based on comprehensive formulation of drying kinetics. *Drying Technology*, 30(11-12), 1256-1273.

Oakley, D., & Bahu, R. (1993). Computational modelling of spray dryers. *Computers & chemical engineering*, 17, S493-S498.

Paris, J. R., Ross Jr, P. N., Dastur, S. P., & Morris, R. L. (1971). Modeling of the air flow pattern in a countercurrent spray-drying tower. *Industrial & Engineering Chemistry Process Design and Development*, 10(2), 157-164.

Pinto, M., Kemp, I., Bermingham, S., Hartwig, T., & Bisten, A. (2014). Development of an axisymmetric population balance model for spray drying and validation against experimental data and CFD simulations. *Chemical Engineering Research and Design*, 92(4), 619-634.

Quek, S. Y., Chok, N. K., & Swedlund, P. (2007). The physicochemical properties of spray-dried watermelon powders. *Chemical Engineering and Processing: Process Intensification*, 46(5), 386-392.

Scott, G., & Richardson, P. (1997). The application of computational fluid dynamics in the food industry. *Trends in Food Science & Technology*, 8(4), 119-124.

Serfert, Y., Drusch, S., & Schwarz, K. (2009). Chemical stabilisation of oils rich in long-chain polyunsaturated fatty acids during homogenisation, microencapsulation and storage. *Food Chemistry*, 113(4), 1106-1112.

Shantha, N. C., & Decker, E. A. (1993). Rapid, sensitive, iron-based spectrophotometric methods for determination of peroxide values of food lipids. *Journal of AOAC International*, 77(2), 421-424.

Tonon, R. V., Grosso, C. R. F., & Hubinger, M. D. (2011). Influence of emulsion composition and inlet air temperature on the microencapsulation of flaxseed oil by spray drying. *Food Research International*, 44(1), 282-289.

Walton, D. E. (2000). The Morphology of Spray-dried Particles a Qualitative View. *Drying Technology*, 18(9), 1943-1986.

Wan, Y., Bankston Jr, J. D., Bechtel, P. J., & Sathivel, S. (2011). Microencapsulation of menhaden fish oil containing soluble rice bran fiber using spray drying technology. *Journal of Food Science*, 76(4), E348-E356.

Wanasundara, U. N., & Shahidi, F. (1995). Storage Stability of Microencapsulated Seal Blubber Oil. *Journal of Food Lipids*, 2(2), 73-86.

Woo, M. W., Daud, W. R. W., Mujumdar, A. S., Wu, Z., Meor Talib, M. Z., & Tasirin, S. M. (2008). CFD evaluation of droplet drying models in a spray dryer fitted with a rotary atomizer. *Drying Technology*, 26(10), 1180-1198.

Xia, B., & Sun, D.-W. (2002). Applications of computational fluid dynamics (CFD) in the food industry: a review. *Computers and electronics in agriculture*, 34(1), 5-24.

Yin, H., Pu, J., Wan, Y., Xiang, B., Bechtel, P. J., & Sathivel, S. (2010). Rheological and Functional Properties of Catfish Skin Protein Hydrolysates. *Journal of Food Science*, 75(1), E11-E17.

Young, S., Sarda, X., & Rosenberg, M. (1993). Microencapsulating properties of whey proteins. 1. Microencapsulation of anhydrous milk fat. *Journal of Dairy Science*, 76(10), 2868-2877.

CHAPTER 5 - CONCLUSIONS

The study demonstrated that egg white hydrolysates powders containing (1) all of the essential amino acids including leucine, valine and lysine, (2) high amount of free amino acids and (3) antioxidant properties can be effectively produced using food-grade proteases obtained from *Aspergillus oryzae* and spray drying. Maximum degree of protein hydrolysis in the egg white hydrolysates was achieved by optimizing the reaction temperature, pH, enzyme:substrate ratio, and reaction time of the hydrolysis procedure using a surface response methodology (RSM).

Also, the study demonstrated that egg white hydrolysates can be effectively use in media that supports the growth of starter cultures of lactic acid bacteria (LAB) including *L. plantarum, L. acidophilus*, and *L. reuteri* as a nitrogen source. Therefore, egg white hydrolysates may have a potential application for the production of *halal* and *kosher* foods.

Furthermore, microencapsulated menhaden oil with egg white hydrolysates powders were effectively produced by spray drying. The first attempt to compare the performance of co-current and counter-current spray drying configurations in the production of microencapsulated fish oil powders using computational fluid dynamics (CFD) simulations and experimental tools was presented in this study. CFD simulations effectively described the complex transport phenomena occurring during spray drying by modeling the drying air flow inside the drying chamber and the cyclone separator using the realizable k-ε and the Reynolds stress model (RSM) turbulent models. Also, CFD simulations predicted moisture contents and particle size distributions of the microencapsulated powders with high accuracy. The results of this study also demonstrated that lower spray drying temperatures (130°C) and counter-current spray drying configurations produced better quality microencapsulated powders with lower lipid oxidation and thermal degradation.

It was also possible to model particle separation inside the spray dryer's cyclone separator using CFD simulations; this allowed estimating pressure drops in the cyclone separator which were comparable with those experimentally obtained.

CFD simulations can be used as a simulation tool in the food processing area; however, prediction of particle agglomeration, lipid oxidation and microstructure of spray dried powders is still limited using this technology. Nevertheless, it is a powerful tool to study the spray drying process.

The valuable information obtained in this study can be used to scale-up the process to effectively produce egg white hydrolysates powders that can be use in media for LAB growth and to engineer new food powder products using spray drying technology.

VITA

Kevin Estuardo Mis Solval is originally from Guatemala. In December 2008 he obtained his B.S. in Food Science and Technology from Escuela Agricola Panamericana, El Zamorano, Honduras. Afterwards, he joined the LSU Department of Food Science as a graduate student in the spring of 2009 under the supervision of Dr. Subramaniam Sathivel. He successfully completed his master's degree in Food Science in May 2011. Then, he joined the LSU-Biological and Agricultural Engineering department as a Ph.D. student in June 2011. He has visited many countries including the USA, Mexico, Guatemala, El Salvador, Honduras, Nicaragua, Costa Rica, Panama and Brazil. He speaks Spanish, English and Portuguese. Kevin happily got married with Deborah Xavier in December 2014. He is deeply thankful to the LSU community for making his time at graduate school more fun, enjoyable and unforgettable. He is set to obtain his Ph.D.'s degree in Engineering Science in May 2015. Kevin enjoys attending sport events, swimming, and cooking.